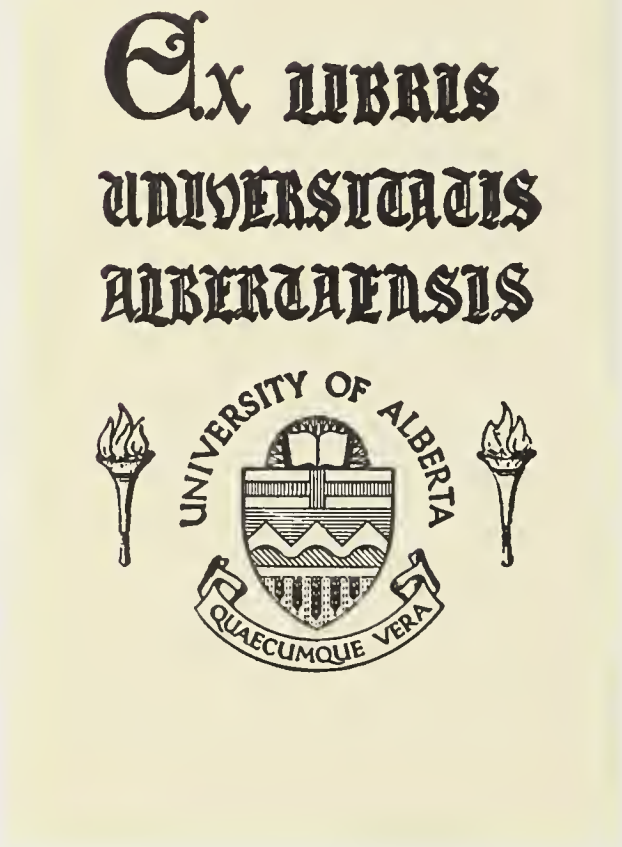

University of Alberta
Printing Department

THE UNIVERSITY OF ALBERTA

THE HORIZONTAL PIPELINE FLOW OF AIR-WATER MIXTURES

A THESIS

SUBMITTED TO THE FACULTY OF GRADUATE STUDIES

IN PARTIAL FULFILMENT OF THE REQUIREMENTS FOR THE DEGREE

OF MASTER OF SCIENCE IN CHEMICAL ENGINEERING

DEPARTMENT OF CHEMICAL AND PETROLEUM ENGINEERING

BY

MIR. M. OMER, B. Sc., B. Sc. (Tech.)

EDMONTON, ALBERTA

ABSTRACT

A detailed literature survey on two-phase flow of gas-liquid mixtures in horizontal pipes is presented.

Flow characteristics of air-water mixtures were studied in a 1.026 inch inside diameter transparent plastic pipe. The input air-water volume ratios were varied from 0.1 to 200 in some and up to 700 in other cases, for 10 superficial velocities of the reference phase (water) ranging from 0.01 ft. per sec. to 5.03 ft. per sec.

A correlation of the experimental pressure drop for the flow rates and ratios investigated is presented in terms of a superficial friction factor based on the properties of the reference phase and reference phase Reynolds number. The data showed good agreement with the Lockhart and Martinelli correlation, though in the viscous-turbulent and viscous-viscous mechanisms of flow, the present data fell below the Lockhart and Martinelli line.

Some photographic and mostly visual observations were made of the flow patterns that existed during the experiments. A tentative chart is presented that enables the prediction of the flow pattern that would exist in air-water systems at given mass velocities of the two phases.

The hold-up ratio is presented as a function of the superficial velocity of the second phase at different superficial velocities of the reference phase.

Slip velocity is presented as a function of the input air-water volume ratio. At zero input volume ratio, that is all liquid flow, the hold-up ratio approaches unity, while the slip velocity approaches zero.

ACKNOWLEDGEMENTS

The author is indebted to Dr. G. W. Govier whose assistance, guidance and creative criticism have been invaluable throughout the present investigation.

Sincere thanks are extended to Mr. R. Kirby and Mr. H. Tebelmann for the construction of the equipment and to Mr. R. A. S. Brown for his help in the preparation of the photographs.

Acknowledgements are also extended to the Government of Canada, Economic and Technical Assistance Branch, for the award of a Scholarship and the Government of Pakistan for the financial assistance received during the course of the study.

TABLE OF CONTENTS

LIST OF TABLES

LIST OF FIGURES

LIST OF PLATES

INTRODUCTION

In the last decade, there has been a decided trend towards the transport of liquids and gases simultaneously through pipe line systems, more particularly in the case of oil and natural gas. In areas like swamps, offshore locations and hilly regions where transportation is generally a problem, this method of transportation is more favourable.

Two-phase flow is not confined to the pipe line systems alone but is encountered in many engineering processes. Horizontal tube evaporators, chemical reactors, heat exchangers, dry return of a vapour heating system, oil-gas wells, boiling water reactors and the injection of a liquid drying agent in natural gas lines to reduce hydrate formation are some examples that involve two-phase flow. In some cases as in chemical reactors it is often a question of necessity rather than choice.

The design of a pipe line or any other equipment for two-phase flow depends in large measure upon an ability to predict the energy losses that can be expected. This is possible only if the mechanism of two-phase flow is well understood. The energy losses for the flow of single-phase fluids can easily be determined by the use of the well known friction factor - Reynolds number - relative roughness relationships and the Fanning equation. In the case of two-phase flow, the presence of the second phase increases the number of variables and changes the geometry of the system. Consequently the problem of analysis is more complicated. As yet, no complete and satisfactory correlation is available for the prediction of the pressure drop resulting under a given set of conditions. Moreover the relationship of the flow types

or patterns to the relative flow rates of the two phases and their physical properties is not well understood. This much is certain however - the energy losses encountered in two-phase flow are ordinarily greater than those for single-phase flow (3, 29, 34, 41). The increase in energy losses is generally attributed to two factors. One, the irreversible work done by the gas on the liquid as it is dragged along the pipe, and two, the smaller areas of flow available to each phase as a result of the presence of the other phase. Since in turbulent flow the pressure drop is known to be inversely proportional to about the fifth power of the effective diameter, even a small decrease in the flow areas causes a substantial increase in the pressure drop.

Previous Investigators:

One of the earliest experimental investigations on two-phase flow was reported by Boelter and Kepner (8)* in 1939. They measured the pressure drop for the horizontal flow of air-water and air-oil mixtures in a study of a fuel distribution system for heaters in California citrus orchards. The test sections consisted of 50 feet long 1/2 inch and 3/4 inch steel pipes. They suggested that the pressure gradients were functions of several dimensionless groups but no correlation was presented.

Martinelli, Boelter, Taylor, Thomsen and Morrin (29) presented the first more or less general correlation in 1944, for gas turbulent-liquid turbulent and gas turbulent-liquid viscous flow mechanism. A further analysis was made by Martinelli et al (30) covering the viscous flow region. These tests were conducted in tubes of 2 to 50 feet in

* Figures in parentheses refer to the bibliography at the end. (Page 86)

length ranging in size from capillary tubing to 1 inch pipe. A year later in 1947, Bergelin and Gazley (6) at the University of Delaware investigated the effect of the hydraulic gradient in stratified flow. These tests were carried out in 1 inch pyrex tube, the pressure taps being 10.48 feet apart.

Lockhart and Martinelli (28) presented a final and revised correlation in 1949, covering all the flow mechanisms. This correlation was based not only on the data from their previous work but also one some new data covering a wider range of flow rates and liquid properties. Air was the only gas used though eight different liquids including water, benzene, kerosene, etc. were employed. Martinelli and coworkers (28, 29, 30) basing their correlation upon an analogy to single phase flow, suggested the possibility of the following mechanisms existing in two-phase flow:

i) Both the liquid and gas in turbulent motion

ii) The liquid in viscous and gas in turbulent motion

iii) Both the liquid and gas in viscous motion

iv) The liquid in turbulent and gas in viscous motion

The transitional Reynolds number from viscous to turbulent flow, calculated as if each phase was flowing alone, was arbitrarily chosen as 2000 for the gas and 1000 for the liquid phase. The correlation is also based on the following two basic assumptions which are quoted:

i) "that the static pressure drop for the liquid phase must equal the static pressure drop for the gas phase, regardless of the details of flow as along as appreciable static pressure differences do not exist along any pipe diameter.

ii) that the volume occupied by the liquid plus the volume occupied by the gas at any instant must equal the total volume of the pipe".

Gazley (6) in his experiments on stratified flow, found that the profile of the liquid surface varied along the tube, thereby showing that the pressure drops experienced by each phase were not the same when the flow was stratified. Gazley measured the pressure drops in the gas phase. Jenkins (22) who measured the pressure drops in the liquid phase found that these were as much as 100% higher than those in the gas phase for stratified flow. This was due to the hydrostatic head difference in the liquid.

There is a general agreement among various investigators (3, 2, 21, 22, 25) that six or seven patterns of flow can exist depending upon the flow rates and a given set of fluids. Thus Martinelli's distinction of viscous and turbulent flow in each of the phases does not in itself describe the flow pattern. The flow patterns that are developed when increasing amounts of gas are introduced into a pipe flowing full of liquid are:

i) Bubble Flow: Flow in which bubbles of gas move along the upper part of the pipe at approximately the same velocity as the liquid.

ii) Plug Flow: in which alternate plugs of liquid and gas move along the upper part of the pipe. The plugs of gas are in effect elongated bubbles.

iii) Stratified Flow: in which the liquid flows along the bottom of the pipe and the gas flows above it over a relatively smooth gas-liquid interface.

iv) Wave or Ripple Flow: which is similar to stratified flow except that the gas moves at a higher velocity causing wave formation at the interface.

v) Slug Flow: Flow in which waves are broken up by the more rapidly moving gas to form a frothy slug which occupies the whole cross-section of the pipe and moves at a much greater velocity than the average liquid velocity. Violent fluctuations result due to the acceleration experienced by the slug.

vi) Film, Semi-annular or Annular Flow: a type in which the liquid flows in a film around the inside wall of the pipe and the gas flows at a higher velocity as a central core.

vii) Spray or Mist-annular Flow: a flow resembling annular flow, occurs at much higher liquid rates, in which most or all of the liquid is entrained as a spray by the gas. Schneider (34) has called this type 'Cresting' flow.

The Martinelli correlation (28) does not cover slug flow because of its unsteady nature and, as pointed out by Gazley (18) excludes stratified flow due to the effect of the hydraulic gradient.

The correlation of Martinelli et al (28) involves the use of an experimentally determined variable ϕ_{lorg} which is defined as:

$$\phi_{lorg} = \left[\frac{(\Delta P/\Delta L)tp}{(\Delta P/\Delta L)_{lorg}}\right]^{1/2} \qquad \text{Eqn. (1)*}$$

* Please refer to the nomenclature at the end. (Page 84)

The function $\phi_{l \text{ or } g}$ is assumed to be dependent on one other variable, X, which is defined as:

$$X = \left[\frac{(\Delta P/\Delta L)_l}{(\Delta P/\Delta L)_g}\right]^{1/2} \qquad \text{Eqn. (2)}$$

where the pressure gradients expressed are for the liquid and gas phase calculated as if each phase were flowing alone in the pipe.

Four different relationships between ϕ and X were obtained for each of the four mechanisms possible depending upon whether the two phases were in viscous or turbulent motion as determined by their superficial Reynolds numbers. Another variable, R_l , defined as the fraction of pipe volume occupied by the liquid phase, was measured and was also found to be a function of X.

The Martinelli correlation (28) represents their data with an accuracy of plus or minus thirty percent. Later investigators (18, 34) suggested that since it was $\phi^2_{l \text{ or } g}$ that entered directly into the calculations of two-phase pressure drop, a plot of ϕ^2 versus X or X^2 was more appropriate than that of ϕ versus X as the latter reduced the spread of the data. Jenkins (22) found an accuracy of plus or minus 40% while comparing his data with the Martinelli correlation. He also noticed that definite changes in slope occurred when his data were plotted on the ϕ versus X plot, with constant liquid flow rates as parameters. This he concluded, showed that ϕ was not a function of X alone. His argument was supported by the fact that the changes in slope coincided with the visually observed changes in the flow pattern in all cases.

Some determinations of interfacial shear have been reported

by Gazley (17), who studied the stratified flow of air-water mixtures in 2.065 inch diameter, horizontal tube. Mechanical energy balances were written for the liquid and gas phases separately. It was assumed that the wall friction factors for both the gas and liquid could be defined in the usual fashion as a function of the Reynolds number provided the appropriate equivalent diameters were used. The interfacial shears, then, could be calculated from the mechanical energy balances using the measurements of the mass flow rates, fluid temperatures, gas phase pressure drop, liquid level and the interfacial gradient. The two interfacial shears are defined as:

$$\tau_{il} = \frac{f_{il}\, \rho_g\, (V_g - V_l)^2}{2\, g_c} \quad \text{and} \quad \tau_{ig} = \frac{f_{ig}\, \rho_g\, (V_g - V_l)^2}{2\, g_c}$$

where τ_{il} and τ_{ig} are the shear stresses, lbs. per sq. ft. at the interface for the liquid and the gas and f_{il} and f_{ig} are the friction factors at the interface for the liquid and the gas. Gazley (17) concluded that the energies lost by the gas phase and gained by the liquid at the interface were equal if the interface was smooth but if it was wavy, more energy was lost by the gas phase than appeared as work transmitted to the liquid phase.

Van Wingen (40) compared the pressure drops for flow of oil and gas mixtures in a 3 inch flow line with the Martinelli correlation (28). He found that at lower gas rates the observed pressure drops were higher than those predicted by the Martinelli correlation but such a difference was less than 1 psi per 1000 foot, which was quite insignificant from the practical point of view. At higher gas rates, however, the divergence was in the direction of conservatism in that the analytically

computed pressure drops were higher than the actually observed.

The work of Johnson and Abou-Sabe (23) on two-phase flow of air-water mixtures involved heat transfer also. However, some of their data from isothermal tests in a 0.87 inch inside diameter pipe indicated that more accurate correlation was obtained if curves similar to those of Lockhart and Martinelli were drawn through points having the same liquid flow rates.

Schueler (35) applied Martinelli's correlation to liquid-liquid flow. He studied the isothermal flow of different mixtures of carbon tetrachloride and water and calculated the parameters ϕ and X. ϕ_l and ϕ_g were found to be 53% lower than the Martinelli curves. (Here the subscript g refers to water and l to carbon tetrachloride)

Levy (27) presented an analytical treatment of annular flow in horizontal pipe which confirmed Martinelli's (28) choice of parameters. He concluded, however, that for a system in which the ratio $\left(\frac{\mu_g}{\mu_l}\right)$ exceeded the limit $0.005 > \frac{\mu_g}{\mu_l} > 0.001$, additional parameters should be introduced. His basic assumptions were:

i) an annular flow pattern with no effect of gravity

ii) the liquid velocity at the pipe was zero and the gas and liquid velocities were equal at the interface i.e. equal shear stresses at the gas-liquid interface.

iii) the application of reduced Navier-Stokes equations for laminar and the one-seventh power law for trubulent flow.

The theoretical predictions of pressure drop were lower than the empirically determined by Martinelli by a maximum deviation of 20%. Predicted values of R_l, the fraction of pipe volume occupied by the

liquid however, were considerably higher than the empirical values and depended upon the flow pattern. He also noted that the discrepancies between his analysis and the experimental data might be attributed to the idealized geometry, the assumption of equal shear stresses at the gas liquid interface, the use of constant properties, the unsteady state effects at the interface and the effect of flow pattern.

An investigation of annular liquid flow with cocurrent air flow in horizontal tubes was made by Abramson (1). Water containing various quantities of detergent and water-ethylene glycol solutions were injected radially into horizontal tubes of pyrex or lucite and visual and photographic observations made upon the appearance of the film surface as a function of a number of variables. A transition region of liquid flow from a relatively smooth to a definitely disturbed condition was observed for the various liquids used. The limits of this transition region in terms of liquid flow rates were determined. An optical device developed to measure the film thicknesses was found to be insensitive in the flow range studied indicating that liquid film thicknesses were less than 0.005 inch. The velocities of the film surface disturbances were measured by means of a high speed camera. Variations in air-mass velocity between 30 and 108 per sec.-sq. ft. for 4 inch pyrex and lucite and 2 inch lucite tube resulted in appreciable change in the water flow defining the transition region which was of the order of 0.04-0.07 lbs. per sec.-ft. However, the disturbances appeared smaller and more numerous with increasing air velocity. The effect of increasing viscosity and decreasing surface tension was to increase the flow rate range over which the transition occurred. The Reynolds number for water corresponding to the transition range is

from 200-400. He also applied the Universal Velocity profile analysis of Von Karman (13) and on this basis the transition occurred for values of Y^+ between 12 and 21 corresponding to a region of the buffer layer $5 < Y^+ < 30$. Y^+ is one of two parameters of a relationship that expresses the Universal Velocity Profile for turbulant flow.

$$Y^+ = \frac{U^* \rho_l y}{\mu_l} \quad \text{where}$$

y = distance from the pipe wall, ft.

$$U^* = \sqrt{\frac{\tau_w g_c}{\rho_l}}$$

τ_w = shear force at the wall per unit area lbs. (F) per sq.ft.

Schneider's (34) work for his thesis (M.Sc. in Pet. Eng.) is important in the sense that he was the first person to use a long transparent test section for his studies which covered mainly wave or ripple, film or semi-annular and annular flow. Twenty foot sections of 'Kraloy' plastic tubing of 1, 1 1/2 and 2 inch diameter, with an average overall length of 100 feet and an average test section length of 70 feet were employed. Natural gas in combination with water, kerosene and SAE 40 lubricating oil were used. His correlation is a plot on logarithmic co-ordinates of a pseudo friction factor f_{tpg} and the ratio $\frac{G_l \mu_l}{G_g \mu_g}$.

f_{tpg} is defined by the equation:

$$f_{tpg} = \frac{(\Delta P/\Delta L)_{tp.} g_c D \rho_g}{2 G_g^2} \qquad \text{Eqn. (3)}$$

This correlation represents his data with an accuracy of +32% to -24%. It, however, applies to those flow types which exhibit steady

state conditions and where evaporation and kinetic energy losses are small. It does not include slug and stratified flow.

Alves (2) in his work with air-water mixtures in a 1 inch pipe line contactor found fairly good agreement with the Lockhart and Martinelli (28) correlation. In general the experimental values were higher than the predicted for annular flow and lower than the predicted for the slug and wavy flow.

Baker (3, 4) presented data collected at Magnolia Petroleum Company field research laboratory, for the flow of gas-oil mixtures, through 4 to 10 inch diameter lines. The length of the lines varied from 2 to 8 miles. He found that the Martinelli (28) correlation was inadequate for the larger diameter lines and concluded that the flow pattern had a marked effect on the pressure drop. Separate equations for different flow types were proposed including one for the case of a hilly terrain. These equations are modified forms of the Martinelli equations involving ϕ , X , and G_1 , the mass velocity of the liquid phase lbs. per hr. - sq. ft. of total pipe cross-section.

Fried (16) reported that the parameter ϕ_{ltt} for non-isothermal flow of air-water mixtures was about equal to the Martinelli (28) curve provided the pressure drop measurements were corrected for momentum pressure drop. In making the momentum corrections, Fried considered the mixture flow at the inlet and exit as being homogeneous. The data of Fried were obtained in a 0.737 inch inside diameter pipe 15.7 ft. long, at pressures up to 40 psig.

White and Huntington (41) presented an empirical correlation as a result of experiments on three liquids and two gases in 1, 1 1/2 and 2 inch diameter lines, with an overall length of 100 ft. and test

section length of 70 ft. The correlation represents their data with a maximum deviation of + or -17%. It is a plot on logarithmic co-ordinates of the two variables e and R defined as:

$$e = \frac{2g_c D^6 \Delta P_{tp} \rho_l}{L\left(\frac{W_l^{3.6}}{W_l + W_g}\right)} \qquad \text{Eqn. (4)}$$

$$\text{and} \quad R = \left(\frac{W_l}{W_g}\right)^{1.8}\left(\frac{\rho_g}{\rho_l}\right)^{0.9}\left(\frac{1}{\mu_g^{0.1}}\right)\left(\frac{1}{\mu_l^{0.1}}\right) \qquad \text{Eqn. (5)}$$

This correlation, however, is limited to low gas phase densities, and to liquids with viscosities of less than 120 centipoises. It also does not include slug and stratified flow.

Another correlation that has found favour with later investigators is the one presented by Chenoweth and Martin (11). Their data werecollected using air-water mixtures in 35 ft. test sections of 1 1/2 inch and 3 inch diameter galvanized steel pipes at pressures from atmospheric to 100 psia. They found that the Martinelli correlation (28) was reasonably suitable for the data collected with the 1 1/2 inch line but predicted high pressure drops for the 3 inch line. In some cases the predicted pressure drop was 2.5 times as great as the actually observed. Their correlation is a plot on logarithmic co-ordinates of the superficial liquid volume fraction, L.V.F., as abscissa, the ratio $\frac{\Delta P_{tp}}{\Delta P_l^*}$, as ordinate with the ratio $\frac{\Delta P_g^*}{\Delta P_l^*}$ as the parameter. The parameter is a ratio of a fictitious all gas pressure drop calculated from total flow rate but using the properties of the gas to a pressure drop calculated in the similar way but using the properties of the liquid.

The superficial liquid volume fraction is calculated from the flow rates and the densities of the two phases as:

$$\text{L.V.F.} = \frac{W_l/\rho_l}{W_l/\rho_l + W_g/\rho_g} = \frac{Q_l}{Q_l + Q_g} = C_l$$

It is claimed that this correlation can be used for any liquid-vapor mixture as long as the Reynolds number calculated from the total flow rates and the properties of the liquid is greater than 2000. However it does not specifically include the concept of flow pattern.

Bertuzzi et al (7) presented another correlation developed from data then available in literature. A friction factor f_{tpm} is defined as:

$$f_{tpm} = \frac{(\Delta P)_{tp}\ g_c\ D\ \rho_m}{2\ L\ G_m^{\ 2}} \qquad \text{Eqn. (6)}$$

In the correlation, f_{tpm} is plotted as a function of the product $(N_{Re})_g^{\ a}\ (N_{Re})_l^{\ b}$ on logarithmic co-ordinates.

The exponents a and b are defined as $a = \frac{R_M}{R_M+1}$ and $b = \frac{1}{e^{0.1R_M}}$

Where R_M is the gas-liquid mass ratio.

The selection of the exponents a and b was arbitrary except that they met requirements at the limiting conditions of all liquid and all gas. The plot was divided into four groups with a range of values of gas-liquid mass ratio as parameter i.e. R_M values of 0-0.2, 0.2-0.4, 0.4-0.6 and 0.6-1.0. Furthermore, the individual correlation for a particular range of R_M values consisted of two distinct curves which gave two values of f_{tpm} for a single value of $(N_{Re})_g^{\ a}\ (N_{Re})_l^{\ b}$. One curve was stated to apply to stratified, wave and semi-annular flow and the other to other

types. The transition from one curve to the other appeared to be associated with liquid Reynolds numbers in the region of 500 to 10,000.

Reid et al (32) conducted tests in 4 inch and 6 inch commercial steel pipes with an overall length of 76 ft. and with the pressure taps 56 ft. apart to determine the validity of Chenoweth and Martin (11) and Lockhart-Martinelli (28) correlations for low pressure air-water flow in large diameter pipes. It is noted that the data from the 4 inch line were well represented by the Lockhart-Martinelli correlation while the 6 inch data fell about 20% below but on a smooth parallel curve. Comparison of experimental data with Chenoweth and Martin (11) correlation showed excellent agreement and no noticeable effects of pipe diameter. They concluded that above a superficial liquid volume fraction of 0.1 i.e. 10% to 100%, two-phase pressure drop may be estimated from the equation:

$$\Delta P_{tp} = \Delta P_l^* \ (LVF)^{-0.86} \qquad \text{Eqn. (7)}$$

since at high values of superficial LVF (> 0.1) all parameteric curves converge to a single line.

Chisholm and Laird (12) presented two-phase air-water flow data in one inch diameter rough tubes. Besides a smooth brass tube, five other tubes were employed with the ε/D value ranging from 0.0025 to 0.068. The test section was 8 feet long with the pressure taps located at 2 feet intervals. The tubes were in the horizontal plane and the pressures were close to atmospheric throughout. According to these investigators the general form of Lockhart and Martinelli (28) parameter:

$$X = \left(\frac{G_l}{G_g}\right)^{\frac{2-n}{2}} \left(\frac{\mu_l}{\mu_g}\right)^{n/2} \left(\frac{\rho_g}{\rho_l}\right)^{0.5} \qquad \text{Eqn. (8)}$$

n, being the power of the Reynolds number in the friction factor relationship $f' = C' N_{Re}^{-n}$ Eqn. (9) was not very appropriate. They argued that though for smooth tubes, for which the Blasius Equation gave n = 0.25; Eqn. 8 was reduced to:

$$X = \left(\frac{G_l}{G_g}\right)^{0.875} \left(\frac{\mu_l}{\mu_g}\right)^{0.125} \left(\frac{\rho_g}{\rho_l}\right)^{0.5} \qquad \text{Eqn. (10)}$$

and provided a satisfactory parameter for the correlation of two-phase flow data, it did not provide a satisfactory parameter for the correlation of two-phase flow data in rough tubes for which the value of n approaches zero. Moreover, they found that the most satisfactory correlation for rough tubes data was obtained using X calculated, regardless of the value of n, by Eqn. (10). Hence they redefined the parameter as:

$$\bar{X} = \left(\frac{G_l}{G_g}\right)^{0.875} \left(\frac{\mu_l}{\mu_g}\right)^{0.125} \left(\frac{\rho_g}{\rho_l}\right)^{0.5} \qquad \text{Eqn. (11)}$$

In the special case of n = 0.25, $\bar{X}$ is identical to X, the Martinelli parameter.

They recommended logarithmic plots of $\frac{\Delta P_{tp}}{\Delta P_l} - 1$, as a function of parameter $\bar{X}$ in preference to the plot of $\frac{\Delta P_{tp}}{\Delta P_l}$ as a function of the parameter X as recommended by Lockhart and Martinelli. For rough tubes the following equation is recommended:

$$\frac{\Delta P_{tp}}{\Delta P_l} = 1 + \frac{C}{\bar{X}^m} \qquad \text{Eqn. (12)}$$

Where C and m are constants. Approximate correlations for the estimation of C and m were given in the form of arithmetic plots, wherein C was

plotted as a function of $\sqrt{(N_{Re})_l}\ \frac{f_{RT}}{f_s}$ and 'm' as a function of $\frac{f_{RT}}{f_s}$,

where $(N_{Re})_l$ = Reynolds number for the liquid flowing alone dimensionless.

f_{RT} = friction factor for rough tubes, dimensionless.

f_s = friction factor for smooth tubes, dimensionless.

This correlation gave pressure drop predictions within plus or minus 15% of the experimental values for the majority of their tests.

They presented another equation that correlated the two-phase pressure drops and 'saturations'. Saturation was defined as the fraction of the pipe volume occupied by each phase.

$$\Delta P_{tp} = \frac{1.6\ f\ L\ (V_l')^2\ \rho_l}{g_c\ D} \qquad \text{Eqn. (13)}$$

Where V_l' = Actual lineal velocity of the liquid during two-phase flow ft./sec. and is equal to $\frac{V_l}{R_l}$ where V_l is the superficial velocity of the liquid phase based on the total pipe cross section and R_l is the liquid saturation, the volume fraction of pipe occupied by the liquid. The correlation in the form of equation (13), however, is limited to commercial tubes with ε/D values up to 0.0025. No satisfactory correlation of this form could be obtained with the rougher tubes since in these cases the data no longer fell on a single line. They also developed equations for the prediction of liquid saturation having the general form:

$$\frac{a}{R_l^{\,b}} = 1 + \frac{c}{\overline{X}} + \frac{d}{\overline{X}^2} \qquad \text{where}$$

a, b, c and d are all constants.

Besides the North American continent, considerable work is being done in this field in other parts of the world, particularly in Europe and the U.S.S.R.

Kosterin (24) showed that the friction factor (hydraulic resistance) in the flow of gas-liquid mixtures through horizontal pipes, was a variable quantity depending on the concentration of the gas phase (vapor content) the Reynolds number calculated for the liquid phase, the diameter and roughness of the pipe, the pressure at small Reynolds numbers for the liquid. Comparison with experiments performed on water-vapor mixtures at high pressures showed the analogy with the hydrodynamic relationship obtained from experiments on air-water mixtures.

The same investigator (25) reported the results of experiments with air-water mixtures in 1, 2, 3 and 4 inch diameter tubes with 49 foot test sections. He found that the friction factor was a function of the volumetric flow concentration of the gas and the Froude number. He defined the friction factor f_{tpm} for two-phase flow as:

$$f_{tpm} = \frac{\Delta P_{tp} \; g_c \; D \; \rho_m \; A^2}{2 \; \Delta L \; W_m^{\,2}} \qquad \text{Eqn. (14)}$$

Where ρ_m = density of the mixture, $\frac{\text{lbs.}}{\text{cu. ft.}}$ and is calculated as:

$$\rho_m = \rho_g \; C_g + (1-C_g) \; \rho_l \quad \text{where} \qquad \text{Eqn. (15)}$$

C_g = Volume flow concentration of the gas and is given by:

$$C_g = \frac{Q_g}{Q_g + Q_l}$$

where the Qs are the volumetric flow rate of each component, $\frac{\text{cu. ft.}}{\text{sec.}}$

The coefficient $\Psi = f_{tpm} / f_{(N_{Re})_{tpl}}$, representing the deviation of the two-phase friction factor f_{tpm} from the law of resistance was defined as the ratio of f_{tpm} to the friction factor of a homogeneous liquid taken for the Reynolds number $(N_{Re})_{tpl} = \frac{4 W_m}{\pi D \mu_l}$.

The Froude number was defined as:

$$Fr_m = \frac{W_m^2}{g_c A^2 D \rho_m^2} \qquad \text{Eqn. (16)}$$

An arithmetic plot of the coefficient Ψ against C_g with Fr_m as parameter is given. The range of Fr_m is from 0.1 to 1,000.

Kosterin and Rubanovich (26) carried out tests to determine the effects of surface tension on pressure losses in two-phase flow. It was reported that a decrease in the surface tension of the liquid phase did not exert an influence on the magnitude of pressure losses under conditions of unstable foam formation over a considerable range (0.164 to 11.481 ft. per sec.) of velocity of the liquid phase. A decrease in surface tension however, increased the degree of dispersion of gas in the liquid in certain types of flow. The formation of an intense and stable foam in pipe could lead to a considerable increase in the 'hydraulic resistance' during the flow of the gas-liquid mixtures.

Hoogendoorn (21) employed both smooth pipes with the inside diameter ranging from 0.945 inch to 5.51 inch and rough pipe of 1.97 inch inside diameter with the ϵ/D value ranging from 0.0012 - 0.03, in his experiments. Water, spindle oil, and gas oil in combination with air were used in a horizontal 82 foot long test section of transparent perspex pipe. He found that the Lockhart-Martinelli (28) correlation cannot

be used for the following three flow patterns:

a) Plug, slug and froth flow, if gas densities differ from that of air at atmospheric pressure.

b) Stratified and wave flow.

c) Mist-annular flow.

Separate correlations for each of these patterns were suggested. For plug, slug and froth flow, an experimental correlation which included the influence of gas density and pipe roughness gave:

$$\Delta P_{tp} = \Delta P_l^* \left[1 + 230 \left(\frac{G_g}{G_m}\right)^{0.84}\right] \left[0.00138 \frac{\rho_l}{\rho_g}\right]^{\alpha} \qquad \text{Eqn. (17)}$$

and $$\alpha = 9.5\left(\frac{G_g}{G_m}\right)^{0.5} - 62.6 \left(\frac{G_g}{G_m}\right)^{1.3} \qquad \text{Eqn. (18)}$$

the limiting conditions being $\left(\frac{G_g}{G_m}\right) < 0.05$ and $(N_{Re})_{tpl} > 3000$, where

ΔP_l^* = Pressure drop over distane ΔL, calculated for the total mass $(W_g + W_l)$ of gas and liquid, flowing in the liquid phase.

$(N_{Re})_{tpl} = \frac{G_m D}{\mu_l}$ where μ_l is the viscosity of the liquid in $\frac{\text{lb.}}{\text{ft. sec.}}$

For wave flow a new correlation gave:

$$\frac{\Delta P_{tp}}{1/2 \frac{\Delta L}{D} \frac{G_m^2}{\rho_g}} = C \left(\frac{G_g}{G_m}\right)^{1.45} \text{ for } \left(\frac{G_g}{G_m}\right) < 0.8 \qquad \text{Eqn. (19)}$$

Where C is a constant, whose value depends mainly on pipe diameter and pipe roughness. Some values of C were given. For mist-annular flow, he found that the pressure drop was independent of the

liquid mass velocity if it was greater than $\frac{6.14 \text{ lb.}}{\text{sq. ft. - sec.}}$, $\left(\frac{30 \text{ kg.}}{\text{sq. m. - sec.}}\right)$.

A new correlation based on data from air-gas oil runs gave:

$$\frac{\Delta P_{tp}}{1/2 \; \frac{\Delta L}{D} \; \frac{G_g^2}{\rho_g}} = 0.12 \; (G_g)^{-1/4} \qquad \text{Eqn. (20)}$$

The following correlation was given between the slip velocity, V_{sl}, and the gas hold-up, R_g:

$$\frac{R_g}{1-R_g} = 0.6 \left[R_g \, V_{sl}\right]^{0.85} \qquad \text{Eqn. (21)}$$

$$\text{and since } V_{sl} = \frac{V_g}{R_g} - \frac{V_l}{(1-R_g)} \qquad \text{Eqn. (22)}$$

Eqn. (21) can be written as:

$$\frac{R_g}{1-R_g} = 0.6 \left[V_g \left(1 - \frac{R_g}{(1-R_g)} \cdot \frac{V_l}{V_g}\right)\right]^{0.85} \qquad \text{Eqn. (23)}$$

This correlation, however, is based only on the air-oil flow data.

Widell (41) conducted tests with air-water mixtures in 0.984 inch, 1.416 inch and 3.36 inch inside diameter brass pipes and with steam and water in 1.008 inch copper pipe. The distance between the pressure taps was very small being 3.395 ft., 4.92 ft., 5.9 ft. and 3.34 ft. respectively. The Martinelli correlation (28) was found to be unsuitable for his data especially at lower water velocities. No correlation in the real sense was presented although logarithmic plots of $\frac{\Delta P_{tp}}{\Delta P_g}$ vs $\frac{G_l}{G_g}$ $(G_l + G_g)$ were given for the 0.984 inch and 1.416 inch diameter pipes.

Baxendell (5) has derived an empirical relationship linking density, velocity and pipe diameter to predict pressure losses in two-phase pipe line flow. The final equation was the result of an analysis of each term involved in the integrated form of the mechanical energy balance for flow of a compressible fluid in a circular pipe of constant diameter as applied to two-phase flow, particularly oil and gas. It is assumed that the density of the mixture might be expressed in terms of pressure through the gas law.

The final equation is:

$$-2\int_1^2 PdP = P_1^2 - P_2^2 = \frac{9.187\ F\ Q'^2\ L'}{m\ K^2\ D^5} \qquad \text{Eqn. (24)}$$

where Q' = rate of flow of tank oil $\frac{\text{cu.m.}}{\text{day}}$

L' = length of pipe line in kilometers

D = diameter of pipe, ft.

m = slope of the density-pressure curves at various gas-oil ratios, $\frac{\text{sq.in.}}{\text{cu.ft.}}$

$K = \frac{(24)\ (3600)}{(Y + X'\ \rho'_g)}$ where

Y = mass of one cu.m. tank oil + soln. gas, lbs.

X' = excess gas-oil ratio cu.m./cu.m.

ρ'_g = density of gas at standard conditions, $\frac{\text{lbs.}}{\text{cu.m.}}$

F = friction factor

Another relationship that is necessary for the calculations is:

$$W_T = \frac{Q'}{K} \quad \text{or} \quad K = \frac{Q'}{W_T} \quad \text{where}$$

W_T is the total mass rate of flow - sum of the mass rate of flow of tank oil plus the mass rate of flow of gas, $\frac{\text{lb.}}{\text{sec.}}$.

Since the terms, 'm' and 'K' are characteristics of a particular field, it is necessary that these be evaluated before equation (24) can be used to calculate the pressure drop. For field calculations, the first step is to construct from the PVT data of a representative well a set of pressure-density curves to cover the range of gas-oil ratios encountered in the area. From these curves, plots of gas-oil ratios against m and K are drawn. A plot of friction factor F against $DV\rho$, which in terms of field units can be written as equivalent to $1.2733 \frac{Q'}{KD}$ or $\frac{1.2733\ W_T}{D}$, is also necessary. This plot is constructed from the field data. At the high rates of flow generally encountered in pipe lines, the degree of turbulence is of such magnitude that of the total energy loss, the portion due to viscous shear is negligible. Consequently, in the turbulent zone, a plot of friction factor against $DV\rho$ can be expected to give a definite trend equivalent to the curves of Reynolds number versus friction factor for single phase fluid flow.

Freeman (15) has also developed an empirical relationship for two-phase flow, from the data obtained at the Kirkuk oil field in Iraq.

$$P_1^{2.43} - P_2^{2.43} = 1.11 \times 10^6 \frac{(Q+1)^{2.43}}{D^{5.51}} \qquad \text{Eqn. (25)}$$

where P = Pressure, in $\frac{\text{lb.}}{\text{in.}^2}$ abs.

L = Length 1000 ft.

Q = Flow rate $\frac{1000 \text{ bbl.}}{\text{day}}$

D = Diameter inches.

Teletov (39) defined a friction factor similar to the one employed by Kosterin (25) i.e.

$$f_{tpm} = \psi \, f_{(N_{Re})_{tpm}} ,$$

where the function ψ representing the deviation of the two-phase friction factor, f_{tpm}, from the law of resistance was defined as the ratio of f_{tpm} to the friction factor of homogeneous liquid taken for the Reynolds number $(N_{Re})_{tpm} = \frac{4 W_m}{\pi D \mu_m}$, where

μ_m = Effective viscosity of the mixture, $\frac{lb.}{ft.sec.}$

The effective viscosity of the mixture was defined using the corresponding kinematic viscosities as follows:

$$\frac{1}{\nu_m} = \frac{C_g}{\nu_g} + \frac{C_l}{\nu_l} \qquad \text{Eqn. (26)}$$

Two arithmetic plots of ψ and C_g with the viscosity ratio $\frac{\mu_g}{\mu_l}$ as the parameter, for viscous and turbulent flow were given.

A considerable amount of work has been done at the University of Alberta, on two-phase flow both in vertical and horizontal pipes. Studies of vertical gas-liquid flow at this university, by Govier and his associates have led to a separation of the hydrostatic head component from the irreversibility component. This was accomplished by Radford (31) who investigated the effect of air and water flow rates on the flow pattern. By the application of a mechanical energy balance to each of the two flowing fluids, he was able to develop a general equation which permitted the separation of the pressure drop into its two components. The equation is as follows:

$$-v_l \frac{\Delta P_{tp}}{\Delta X} = \frac{1 + R_M}{1 + R_v} + \frac{1}{1 + R_v} \left(\frac{\Delta F}{\Delta X}\right)_L \qquad \text{Eqn. (27)}$$

where $\left(\frac{\Delta F}{\Delta X}\right)_L$ = Sum of the irreversibility effects attributable to both the gas and liquid phases in height ΔX, $\frac{\text{ft. liquid}}{\text{ft.}}$

It can be seen from the equation (27) that the term $\frac{1 + R_M}{1 + R_v}$ represents the hydrostatic head component and the term $\frac{1}{1 + R_v} \left(\frac{\Delta F}{\Delta X}\right)_L$ represents the irreversibility component. Moreover, in the limiting conditions of all liquid flow, equation (27) reduces to:

$$-v_l \frac{\Delta P}{\Delta X} = 1 + \frac{\Delta F}{\Delta X} \qquad \text{Eqn. (28)}$$

where $\frac{\Delta F}{\Delta X} = \frac{2 f V^2}{g_c D}$, since then $R_M = R_v = 0$ and where f is the common single phase friction factor and V, the fluid velocity, in feet per sec.

Dunn (14) continued this work and was able to determine the effect of the air and water flow rates on the pressure drop, flow pattern and hold-up. He proposed a correlation based on the flowing gas phase, using a superficial friction factor and Reynolds number. Results of the work of Radford and Dunn were published by Govier, Radford and Dunn (19). Their correlation is a logarithmic plot of the friction factor f'_{tpl}, based on the liquid properties and superficial liquid velocity V_l, with the gas-liquid input volume ratio R_v as the parameter. The friction factor f'_{tpl} is defined by the following equation:

$$-v_l \frac{\Delta P_{tp}}{\Delta X} = \frac{1 + R_M}{1 + R_v} + \frac{1}{1 + R_v} \frac{2 f'_{tpl} V_l^2}{g_c D} \qquad \text{Eqn. (29)}$$

Another correlation represents the hold-up ratio H_R as a function of the superficial liquid velocity V_L, with R_v again being the parameter. The hold-up ratio H_R, is defined as the ratio of (a) the gas-liquid volume ratio in the supply mixture to (b) the gas-liquid volume ratio in the flow section, all volumes calculated at average flow conditions.

They also observed that a plot on arithmetic co-ordinates of unit pressure drop, $v_l \frac{\Delta P_{tp}}{\Delta X}$, and gas-liquid volume ratio R_v at a constant liquid rate, could, at low liquid velocities be divided into four sections, which they called the "Pressure drop Regimes". The following flow patters were observed both visually and photographically.

1) Bubble 2) Slug 3) Froth 4) Ripple 5) Film or annular and 6) Mist.

A closer look at a typical pressure drop relationship at low liquid rates shows that the bubble flow pattern extends to the first half of Regime I, the slug pattern occurs during the second half of Regime I and extends midway into Regime II. The second half of Regime II and most of Regime III is occupied by froth flow. Ripple, film or annular and mist flow occur in the last Regime. The above flow patterns, however, do not occur for all water rates. As the water rate is increased Regime II and III become progressively narrower and finally disappear.

In 1957, Short (36) expanded the experimental facilities used by Radford (31) and Dunn (14) and was able to determine the effect of tube diameter on the pressure drop, flow patterns and hold-up. Data collected by Short (36) together with the applicable data from the work of Radford (31) and Dunn (14) was published by Govier and Short (20).

New correlations are presented which enable the prediction for any diameter between 0.5 and 3.0 inch, of the pressure drop, the hold-up and the flow pattern, as a function of the diameter and the gas and liquid rates for the upward vertical flow of air-water mixtures at an average pressure and temperature of 36.0 psia and 70-85°F respectively.

The friction factor f'_{tpl}, is correlated as a function of a reduced form of the superficial Reynolds number for the liquid phase DV_l, with $(V_g D^{3.5})$ as the parameter.

Three different correlations for the hold-up ratio, H_R, one each for Regimes I and II, III and IV are presented. The hold-up ratio, H_R , and the superficial water velocity, V_l, are the ordinates and abscissae respectively in each case, the parameter being $R_v D^{1/3}$, R_v and $R_v D^{-1/3}$ respectively.

Further studies of two-phase vertical flow were made by Sullivan (38). The two-phase systems studied were composed of water as the reference phase with air or oil as the second phase. His work was an investigation of the effect of the second phase (non-water) density on the pressure drop, flow patterns and the hold-up. Three second phase densities were studied by varying the average pressure in the air-water system and a fourth was obtained with oil as the second phase.

The friction factor, f'_R, correlation is a logarithmic plot of f'_R and DV_R with $D^{3.85} V_s^{1.1} (\nu_s - \nu_R)^{0.33}$ as the parameter, where f'_R is the friction factor, dimensionless, calculated from the equation (29) developed by Govier, Radford and Dunn (19). The subscript 'R' refers to the reference phase, defined as the phase having the lower kinematic viscosity (water here) and 's' to the second phase (air or oil).

The correlation for the hold-up ratio H_R, is a semi-log plot of $H_R\ V_R^{0.0022\ (\rho_R-\rho_s)}$ and $\rho_R - \rho_s$ with $R_v D^{1/3}$ as the parameter.

Data collected by Sullivan with the air-water system together with applicable data from previous investigators in this field are being published by Brown, Sullivan and Govier (9).

Studies of two-phase flow in horizontal pipes at the University of Alberta and the Research Council of Alberta, have been centered around only liquid-liquid flow. Russell (33) studied the flow characteristics of a white mineral oil 'Kremol 70' (having a specific gravity of 0.834 and viscosity of 22 c.p. at 20°C) in the presence of water in a smooth one inch pipe. The pressure drop data are presented as a modified Fanning friction factor, f_{tpl}, (based upon water properties) versus a superficial velocity of water, V_l, with the input volume ratio of oil to water as the parameter. The friction factor f_{tpl} is defined as:

$$f_{tpl} = \frac{\Delta P_{tp}\ g_c\ D}{2\ L\ V_l^2\ \rho_l} \qquad \text{Eqn. (30)}$$

(The subscript 'l' refers to the water phase)

Three flow patterns were observed which were designated as bubble flow, stratified flow and mixed flow. Hold-up measurements indicated that in the laminar region of flow, the hold-up ratio, H_R, was a function of the input volume ratio and the viscosities of the two liquids, while in the turbulent region, H_R was also a function of the superficial water velocity.

Charles (10) studied the flow of three oils of viscosities 6.29, 16.8 and 65.0 cp in the presence of water in a horizontal pipe line of 1.04 inch internal diameter. The densities of the oils were

equalized to that of water by adding carbon tetrachloride. It was noticeable that the oil viscosity had little or no effect on the flow pattern, although the most viscous oil showed dissimilar behaviour at higher input oil-water ratios. A similar trend was observed with regard to the pipe line pressure gradients especially at low oil-water ratios. At high oil-water ratios, however, the most viscous oil gave relatively high pressure gradients in those regions of flow in which oil was the continuous phase in contact with the pipe wall.

The hold-up relationships at constant superficial water velocities, exhibited a maximum at input volume ratios corresponding to 'oil in water concentric' flow regime.

Theory

1. Pressure Drop and Friction Factor:

The pressure drop and the friction factor for the flow of a fluid in one phase through a horizontal pipe line are interrelated by the well known Fanning Equation through which the friction factor is defined:

$$\frac{\Delta P}{\Delta L} = \frac{2 f V^2 \rho}{g_c D} \qquad \text{Eqn. 31)}$$

where ΔP = pressure drop, lbs. per sq. ft.

ΔL = distance across which the pressure drop occurs, ft.

f = single phase friction factor, dimensionless

V = fluid velocity at average flow conditions, ft. per sec.

ρ = fluid density at average flow conditions, lbs. per cu.ft.

g_c = dimensional conversion constant, $\frac{\text{lb. mass}}{\text{lb. force}} \frac{\text{ft.}}{\text{sec.}^2}$

D = pipe diameter, ft.

Extensive theoretical and experimental work has shown that the friction factor is a function of the Reynolds number, $\frac{DV\rho}{\mu}$, and the relative roughness, $\frac{\epsilon}{D}$, of the pipe wall.

The Fanning equation may be applied in any of several ways to the flow of two phases and serves to define "two-phase friction factors" as follows:

Based on the superficial velocity and density of liquid phase

$$\frac{\Delta P_{tp}}{\Delta L} = \frac{2 f_{tpl} V_l^2 \rho_l}{g_c D} = \frac{2 f_{tpl} G_l^2}{g_c D \rho_l} \qquad \text{Eqn. (32)}$$

Based on the superficial velocity and density of gas phase

$$\frac{\Delta P_{tp}}{\Delta L} = \frac{2 f_{tpg} V_g^2 \rho_g}{g_c D} = \frac{2 f_{tpg} G_g^2}{g_c D \rho_g} \qquad \text{Eqn. (33)}$$

Based on the superficial velocity and density of the mixture

$$\frac{\Delta P_{tp}}{\Delta L} = \frac{2 f_{tpm} V_m^2 \rho_m}{g_c D} = \frac{2 f_{tpm} G_m^2}{g_c D \rho_m} \qquad \text{Eqn. (34)}$$

where $\frac{\Delta P_{tp}}{\Delta L}$ = Two-phase pressure drop over a distance ΔL ft. $\frac{\text{lb.}}{\text{sq. ft.-ft.}}$

f_{tpl} = Two-phase friction factor based on the liquid phase properties, dimensionless.

f_{tpg} = Two-phase friction factor based on the gas phase properties, dimensionless.

f_{tpm} = Two-phase friction factor based on the properties of the mixture, dimensionless.

V_l, superficial velocity of the liquid at average flow conditions and based on the total cross-section, ft. per sec.

V_g, superficial velocity of the gas at average flow conditions and based on the total cross-section, ft. per sec.

V_m, superficial velocity of the mixture at average flow conditions and based on the total cross-section, ft. per sec.

ρ_l, density of the liquid at average flow conditions, lb. per cu. ft.

ρ_g, density of the gas at average flow conditions, lb. per cu. ft.

ρ_m, density of the mixture at average flow conditions, lb. per cu. ft.

G_l, mass velocity of the liquid phase $\frac{\text{lbs.}}{\text{sec. square ft.}}$ based on the total cross-section

G_g, mass velocity of the gas phase based on total cross-section $\frac{\text{lbs.}}{\text{sec. sq. ft.}}$

G_m, mass velocity of the mixture based on total cross-section $\frac{\text{lbs.}}{\text{sec. sq. ft.}}$

g_c, dimensional conversion constant $\frac{\text{lb. mass}}{\text{lb.force}} \quad \frac{\text{ft.}}{\text{sec.}^2}$

D, diameter of the pipe ft.

The three two-phase friction factors so defined are mathematically interrelated and the choice among them can only be arbitrary.

Russell (33) and Charles (10) have used the friction factor, f_{tpl}, defined by Eqn. (32) in their work on oil-water flow in horizontal pipe. Schneider (34) has used, f_{tpg}, defined by Eqn. (33). Lockhart and Martinelli (28) have introduced a parameter, ϕ^2, which is the ratio of the two-phase pressure drop to the single phase pressure drop of either the gas or liquid i.e.

$$\frac{\Delta P_{tp}}{\Delta L} = \phi_g^2 \frac{\Delta P_g}{\Delta L} = \phi_l^2 \frac{\Delta P_l}{\Delta L}$$

$$= \phi_g^2 \frac{2 f_g G_g^2}{g_c D \rho_g} = \phi_l^2 \frac{2 f_l G_l^2}{g_c D \rho_l} \qquad \text{Eqn. (35)}$$

where f_g and f_l are the single phase Fanning friction factors for gas and liquid respectively.

Comparison of Eqn. (35) with Eqn. (32) and Eqn. (33) shows that $f_{tpg} = \phi_g^2 f_g$ and $f_{tpl} = \phi_l^2 f_l$. Another parameter introduced by Lockhart and Martinelli (28) is X^2 which is defined as the ratio of the single phase liquid pressure drop to the single phase gas pressure drop i.e.

$$X^2 = \frac{\Delta P_l / \Delta L}{\Delta P_g / \Delta L} = \frac{2 f_l G_l^2 / g_c D \rho_l}{2 f_g G_g^2 / g_c D \rho_g} \qquad \text{Eqn. (36)}$$

$$= \left(\frac{G_l}{G_g}\right)^2 \frac{f_l}{f_g} \frac{\rho_g}{\rho_l} \qquad \text{Eqn. (36)}$$

$$X = \frac{G_l}{G_g} \left(\frac{f_l}{f_g}\right)^{0.5} \left(\frac{\rho_g}{\rho_l}\right)^{0.5} \qquad \text{Eqn. (37)}$$

and ϕ is plotted as a function of X in the general correlation.

Chenoweth and Martin (11) have used the ratio $\frac{\Delta P_{tp}}{\Delta L} \Big/ \left(\frac{\Delta P}{\Delta L}\right)_l^*$ as the ordinate in their correlation where $\left(\frac{\Delta P}{\Delta L}\right)_l^*$ is a fictitious all liquid pressure drop per unit length calculated for the total mass flow

rate of both liquid and gas but using the properties of the liquid. This again can be written in terms of a modified Fanning equation as:

$$C_m = \frac{\Delta P_{tp}/\Delta L}{(\Delta P/\Delta L)_l^*} = \frac{2 f_{tpg} G_g^2/g_c D \rho_g}{2 f_l' G_m^2/g_c D \rho_l}$$

$$= \frac{2 f_{tpl} G_l^2/g_c D \rho_l}{2 f_l' G_m/g_c D \rho_l} \qquad \text{Eqn. (38)}$$

$$C_m = \frac{f_{tpg}}{f_l'} \left(\frac{G_g}{G_m}\right)^2 \frac{\rho_l}{\rho_g} = \frac{f_{tpl}}{f_l'} \left(\frac{G_l}{G_m}\right)^2$$

or $$f_{tpg} = C_m f_l' \left(\frac{G_m}{G_g}\right)^2 \frac{\rho_g}{\rho_l} \qquad \text{Eqn. (39)}$$

where C_m is the ratio of the two-phase pressure drop to the all liquid pressure drop and f_l' is the single phase friction factor calculated from the total mass flow of both the liquid and gas and using the liquid properties.

Bertuzi et al (7) and Kosterin (25) have based the two-phase friction factor on the total mass velocity of the mixture and the mixture density i.e.

$$\frac{\Delta P_{tp}}{\Delta L} = \frac{2 f_{tpm} G_m^2}{g_c D \rho_m} \qquad \text{Eqn. (34)}$$

and the mixture density, ρ_m is defined as $\rho_m = C_g \rho_g + (1-C_g) \rho_l$ where C_g is the volume fraction of the gas in the mixture. Comparing Eqn. (34) with Eqn. (32) and Eqn. (33) we have:

$$\frac{f_{tpm} G_m^2}{\rho_m} = \frac{f_{tpl} G_l^2}{\rho_l} = \frac{f_{tpg} G_g^2}{\rho_g} \qquad \text{Eqn. (40)}$$

and $$f_{tpg} = f_{tpm}\left(\frac{G_m}{G_g}\right)^2 \frac{\rho_g}{\rho_m} = f_{tpl}\left(\frac{G_l}{G_g}\right)^2 \frac{\rho_g}{\rho_l}$$ Eqn. (41)

In the present and several previous investigations at the University of Alberta the following approach has been adopted. The well known mechanical energy balance (37) may be written for each phase in the following way:

$$W_l\, dt\, (v_l\, dP + \frac{V_l' dV_l'}{g_c} + dF_l) = 0$$ Eqn. (42)

and $$W_g\, dt\, (v_g\, dP + \frac{V_g' dV_g'}{g_c} + dF_g) = 0$$ Eqn. (43)

where W_l = mass rate of flow of the liquid, lbs. per sec.

W_g = mass rate of flow of the gas, lbs. per sec.

v_l = specific volume of the liquid at average flow conditions, cu. ft. per lb.

v_g = specific volume of the gas at average flow conditions, cu. ft. per lb.

P = pressure, lb. per sq. ft., absolute

V_l = actual linear velocity of liquid, ft. per sec., at average flow conditions

V_g = actual linear velocity of gas, ft. per sec., at average flow conditions

dF_l = irreversibilities attributable to liquid ft. of liquid

dF_g = irreversibilities attributable to gas ft. of gas

dt = differential element of time, sec.

Adding Eqns. (42) and (43) yields:

$$v_l\,dP + \frac{V'_l\,dV'_l}{g_c} + dF_l + \frac{W_g}{W_l}\,v_g\,dP + \frac{W_g}{W_l}\,\frac{V'_g\,dV'_g}{g_c} + \frac{W_g}{W_l}\,dF_g = o \qquad \text{Eqn. (44)}$$

If the kinetic energy effects are neglected or considered to be included within the terms dF_l and dF_g we have:

$$dP\left(v_l + \frac{W_g}{W_l}\,v_g\right) + (dF)_l = o \qquad \text{Eqn. (45)}$$

where $(dF)_l = dF_l + \frac{W_g}{W_l}\,dF_g$

$$v_l\,dP\left(1 + \frac{W_g}{W_l}\,\frac{v_g}{v_l}\right) + (dF)_l = o$$

$$-\,v_l\,dP\,(1 + R_v) = (dF)_l \qquad \text{Eqn. (46)}$$

where $R_v = \frac{W_g}{W_l}\,\frac{v_g}{v_l} = \frac{Q_g}{Q_l}$, air-water volume ratio.

If the right hand side of Eqn. (46) is equated to the Fanning equation we have:

$$-\,v_l\,dP\,(1 + R_v) = \frac{2\,f\,V^2\,dL}{g_c D}$$

$$-\,v_l\,\frac{dP}{dL} = \frac{2\,f\,V^2}{g_c D\,(1 + R_v)} \qquad \text{Eqn. (47)}$$

and a modified "two-phase friction factor" is defined.

Eqn. (47) is integrated, assuming that the variations in R_v are small enough to justify the use of average values based upon an average system pressure and temperature. Under these conditions:

$$- v_1 \frac{\Delta P}{\Delta L} = \frac{1}{(1 + R_v)} \frac{2 f V^2}{g_c D} \qquad \text{Eqn. (48)}$$

$$\frac{\Delta P_{tp}}{\Delta L} = \frac{1}{(1 + R_v)} \frac{2 f_R V_R^2 \rho_R}{g_c D} \qquad \text{Eqn. (49)}$$

The subscript 'R' refers to the reference phase which in the present investigation is the liquid phase. Later on, subscript 's' is used to signify the gas or second phase which is air.

In terms of the mass velocities of each phase Eqn. (49) can be written as:

$$\frac{\Delta P_{tp}}{\Delta L} = \frac{1}{(1 + R_v)} \frac{2 f_R G_R^2}{g_c D \rho_R} = \frac{R_v}{(1 + R_v)} \frac{2 f_s G_s^2}{g_c D \rho_s} \qquad \text{Eqn. (50)}$$

Comparison of Eqn. (50) with Eqn. (32) and Eqn. (33) shows that:

$$f_{tpg} = \frac{R_v}{(1 + R_v)} \quad f_s = \frac{1}{(1 + R_v)} \left(\frac{G_R}{G_g}\right)^2 \frac{\rho_g}{\rho_R} f_R \qquad \text{Eqn. (51)}$$

A review of the various equations used so far, shows that the following relationship exist between the two-phase friction factor f_{tpg}, based on the gas phase properties, used by Schneider (34) and those used by other investigators.

$$f_{tpg} = \phi_g^2 f_g = \frac{1}{(1 + R_v)} \left(\frac{G_R}{G_g}\right)^2 \frac{\rho_g}{\rho_R} f_R = C_m f_1' \left(\frac{G_m}{G_g}\right)^2 \frac{\rho_g}{\rho_1} = f_{tpm} \left(\frac{G_m}{G_g}\right)^2 \frac{\rho_g}{\rho_m}$$

Schneider | Martinelli | Present Investigation U. of A. | Chenoweth and Martin | Kosterin, Bertuzzi et al

Similar relationships can be written for the friction factor based on the liquid phase properties:

$$f_{tpl} = \phi_1^2 f_1 = \frac{1}{(1 + R_v)} f_R = C_m f_1' \left(\frac{G_m}{G_1}\right)^2 = f_{tpm} \left(\frac{G_m}{G_1}\right)^2 \frac{\rho_1}{\rho_m}$$

Hold-up and Slip Velocity

One of the distinguishing characteristics of two-phase flow is the development, within the test section of a concentration of one of the phases greater than that in the supply mixture. The term "Hold-up ratio" is used in the present investigation as a quantitative measure of the liquid accumulation. Hold-up ratio is defined as the ratio of a) the volume ratio in the supply mixture to b) the volume ratio in the flow section. Both volume ratios are expressed in cubic feet of gas per cubic feet of liquid at average flow pressure and temperature. This phenomenon has been observed by many investigators. Martinelli (28, 29, 30) has measured the liquid and gas 'hold-up' and has found it to be a function of the parameter X alone. Alves (2) has also treated it the same way. Chisholm and Laird (12) have given a new terminology to the same phenomenon and have called it 'saturation'. They have presented an equation that correlates the two-phase pressure drop and 'saturation' and have developed equations for the prediction of 'liquid saturation'. Govier, Radford and Dunn (19) and Govier and Short (20) have correlated the hold-up ratio as a function of the superficial liquid velocity and other parameters. Some other workers (19, 20, 21) have referred to the 'slip velocity' of the gas phase. Slip velocity is defined as the difference in the actual average lineal velocity of the gas and the liquid phases both measured at the average flow pressure and temperature. The two quantities, hold-up ratio and slip velocity are two measures of the same phenomenon and are related as follows.

If the volume fraction of the flow section occupied by the

second phase (gas phase) be R_s then $(1-R_s)$ represents the volume fraction occupied by the reference phase (liquid phase).

$$\text{Hold-up ratio} \quad H_R = \frac{W_g}{W_g} \frac{v_g}{v_l} \frac{1-R_s}{R_s} \qquad \text{Eqn. (52)}$$

$$= \frac{Q_g}{Q_l} \frac{1-R_s}{R_s} = \frac{V_s}{V_R} \frac{1-R_s}{R_s} \qquad \text{Eqn. (53)}$$

The average lineal velocities of each phase are:

$$V'_s = \frac{V_s}{R_s} \qquad \text{and} \qquad V'_R = \frac{V_R}{1-R_s}$$

and the slip velocity V_{sl} is:

$$V_{sl} = V'_s - V'_R = \frac{V_s}{R_s} - \frac{V_R}{(1-R_s)}$$

$$= \frac{V_R}{1-R_s} \left[\frac{V_s}{R_s} \frac{(1-R_s)}{V_R} - 1 \right]$$

$$= \frac{V_R}{1-R_s} (H_R - 1) \qquad \text{Eqn. (54)}$$

$$\text{or } V'_s - V'_R = V'_R (H_R - 1) \qquad \text{Eqn. (55)}$$

EXPERIMENTAL EQUIPMENT

The pilot pipe line was designed to obtain pressure drop and hold-up data for the horizontal flow of air and water mixtures.

A schematic flow diagram of the equipment is shown in Figure 1. The main test section of transparent cellulose acetate butyrate pipe of 1.026 inch inside diameter, with an overall length of about 41 feet was supported along its length in a horizontal position by angle iron sections. These sections, in turn, were supported by steel brackets fixed onto the wall. The pipe was secured in position by clamps. For hold-up measurements, two round-port quick closing plug valves, A and B, connected by a mechanical linkage, were installed at the ends of the plastic pipe. Small cocks situated in the valve bodies enabled the trapped water to be drained from the test section. The plastic pipe was attached to the round-port valves by means of adapter couplings. The discharge end of the test section was attached to a separator in such a way that the flow entered the separator tangentially. The separator, Plate 1, was a simple hollow cylindrical vessel, about 6 1/2 inch in diameter and about 6 feet high, having two outlets, one at the bottom for water and the other at the top for air. The outlet for water was provided with a valve D to adjust the discharge of water. A "Belfield parabolic plug valve" was mounted in the air line at the top of the separator, to control the mid point pressure of the test section.

Two, 2 inch galvanized iron pipes served as the water and air lines. Orifice plates were installed in these lines to measure the flow rate of the two components. A pressure regulator on the air line maintained

Fig. 1

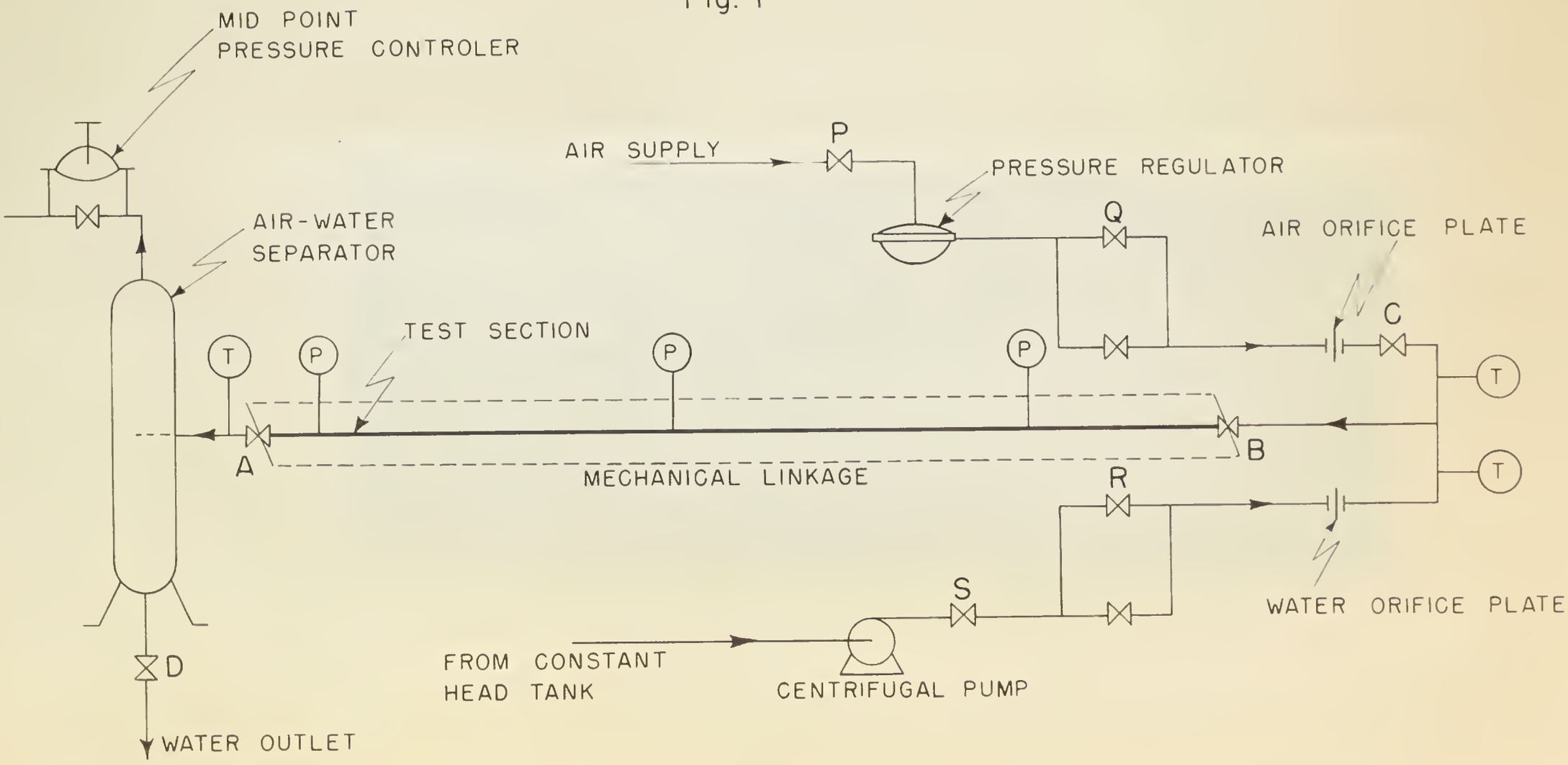

SCHEMATIC FLOW DIAGRAM

PLATE I

SEPARATOR

the pressure of the incoming air between 50-55 psig. Another round-port plug valve C was installed in the air line between the orifice plate and the entrance section, to minimize the fluctuations in the manometers and to give a higher pressure upstream of the air orifice. Govier, Radford and Dunn (19) and Hoogendoorn (21) in their work on two-phase fluid flow concluded that the method of introduction of the two phases did not effect the flow pattern provided the 'calming zone' was of sufficient length. Hence a simple mixing 'tee' was used in this work (Plate 2).

A sufficiently long 'calming zone' was provided by having the upstream pressure tap about 8 feet from the upstream valve B. The downstream pressure tap was about 2 feet from the discharge end providing a test section of 30 feet. A third tap was made halfway along the test section for recording the mid-point pressure. The pressure taps were 1/8 inch holes, drilled through the top of the pipe. Slipped over these taps were sleeves sealed with 'O' rings.

Air and Water Supply

The air was supplied from the University of Alberta power plant compressor at about 80 psig. A pressure regulator on the line maintained the pressure of the air between 50-55 psig.

The water supply was obtained from a constant level overhead tank in conjunction with a 5 H.P. Fairbanks-Morse centrifugal pump, with an intake pressure of 25 psig. and a discharge pressure of about 100 psig.

Control and measurement of the variables were obtained with the aid of orifice plates and rotameters, for the air and water flow

PLATE II ENTRANCE SECTION, SHOWING THE MIXING 'TEE'

rates, differential water and mercury manometers for the pressure drops and simple gravimetric method for the insitu water content of the test section.

Flow Measurements

Orifice plates were used to measure the flow rates of both air and water. In the case of air, one rotameter (Hoke. Meter No. 2102) and six orifices ranging in diameter from 0.082 inch to 0.66 inch and for water one rotameter (Fischer and Porter S.No. M6-1718/1) and five orifices ranging in diameter from 0.101 inch to 0.752 inch were required to cover the range of air and water velocities under investigation. All the orifice plates were fabricated in the Department Work Shop. Flange type pressure taps were used. The calibration curves for the rotameters and the orifice plates are given in Appendix C. A 60 inch differential water manometer and a 60 inch differential mercury manometer recorded the pressure drop across the air and water orifices respectively. Air was the transmitting fluid in the lead lines from the air orifice plate while water was used in the case of the water orifice plate.

Pressure Measurements

The pressure drop across the 30 feet test section was registered on either a 60 inch water or 60 inch mercury manometer. For low pressures an inclined water manometer was used. Since air was the transmitting fluid, 'splash pots' were installed at each of the pressure taps to prevent any water from being carried away into the lead lines. The 'splash pots' (Plate 3) were lucite cylinders about 2 inches in diameter and 6 inches high. A needle valve connected the splash pot

PLATE III

SPLASH POT

to the 'O' ring sleeve. Valves were provided at the bottom of the splash pots to drain away any water that collected. Lead lines of 1/4 inch transparent polythene tubing connected the top of the splash pots to the manometers. The mid-point pressure was registered on a 60 inch mercury manometer and as well as a gauge. A 'Brown Recorder' in connection with the pressure control valve maintained the mid-point pressure at the required level. Plate 4, shows the arrangement on the Panel Board of the different manometers, the two rotameters, the 'Brown Recorder' and the valves controlling the flow rates of air and of water. Figure 1a shows the manometer connections.

Temperature

Two dial thermometers (Bell and Gossett $30^{\circ}F$-$250^{\circ}F$) one each on the air and water lines were installed to record the temperature of the air and water. A third one, similar to those above, in the discharge end recorded the temperature of the mixture as it left the test section.

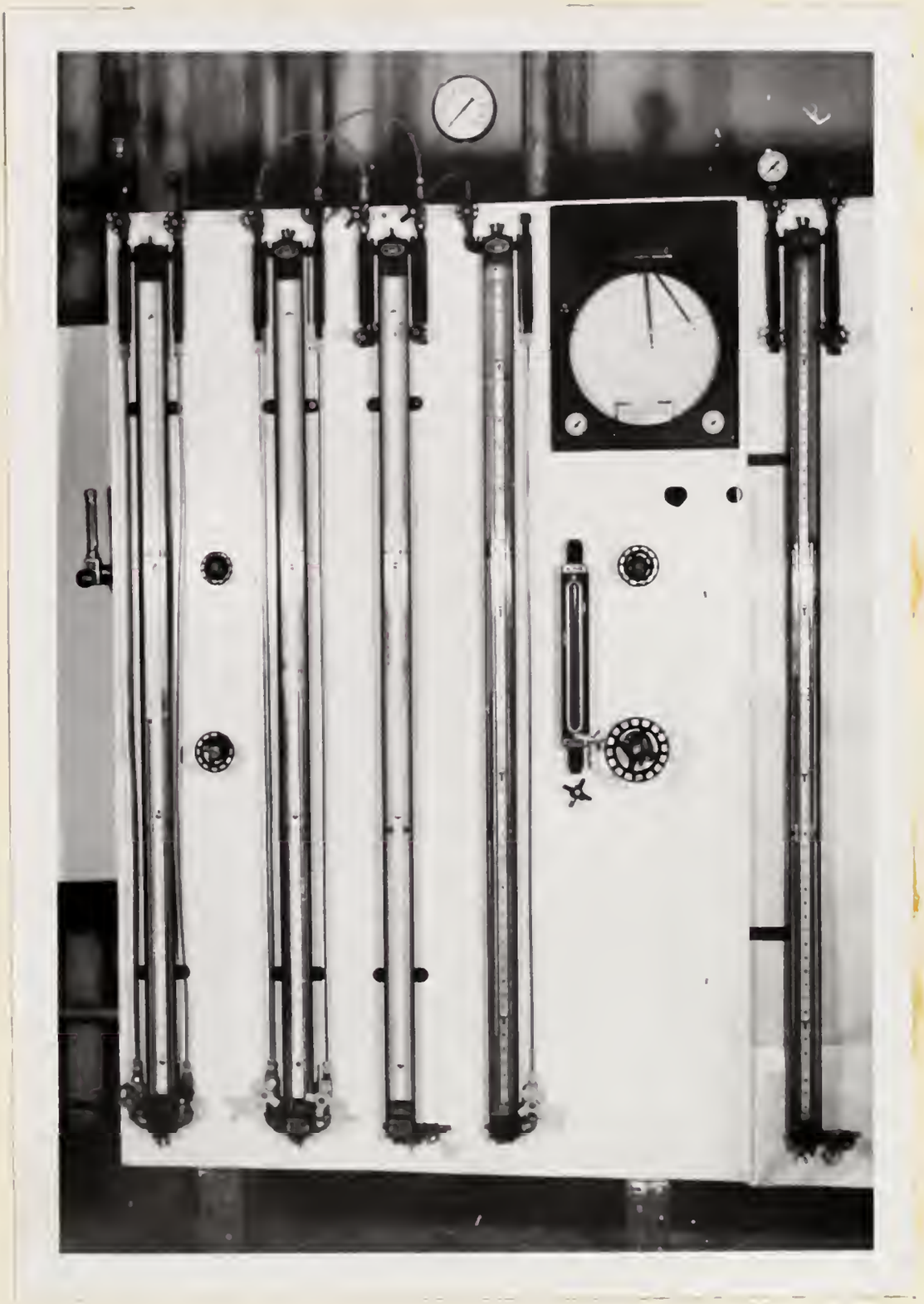

PLATE IV

PANEL BOARD

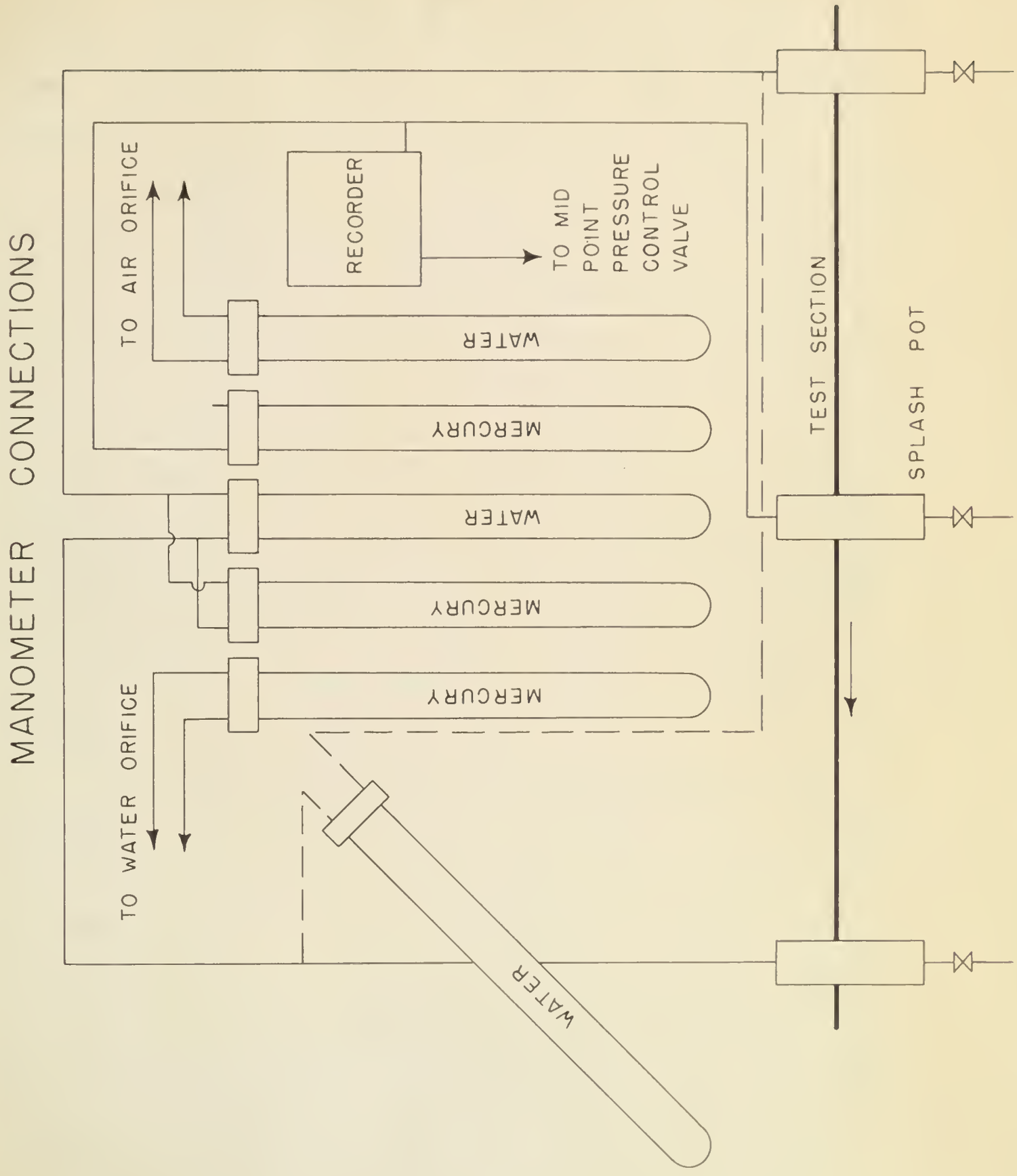
MANOMETER CONNECTIONS
TO AIR ORIFICE
RECORDER
TO MID POINT PRESSURE CONTROL VALVE
WATER
MERCURY
WATER
MERCURY
MERCURY
TO WATER ORIFICE
WATER
TEST SECTION
SPLASH POT

Fig. 1a

EXPERIMENTAL PROCEDURE

Before conducting the two-phase tests, the pressure measuring equipment and the rotameter and orifice plates calibrations were checked by taking pressure drop data for different flow rates of water and air alone. During those test runs when air alone was used, the mid-point pressure in the test section was maintained between 35-36 psia.

Experiments were then conducted to study the two-phase flow of air and water over a range of superficial water velocities from 0.01 ft. per sec. to 5.03 ft. per sec. For each constant superficial water velocity the superficial air velocity varied from 0.1 ft. per sec. to 50 ft. per sec. During all the experiments the average pressure, or the mid-point pressure in the test section was maintained at 35-36 psia. This value was chosen because it was convenient and it was also used by a earlier worker (38). For each test pressure drop across the 30 ft. test section, pressure drop across the air and water orifices, the upstream pressure at the air orifice, the temperature of the air, water and the mixtures and the insitu water content were recorded. A detailed description of one such experiment follows.

Orifices to give the desired superficial velocities of air and water were first selected and installed. Valves A, B, and C (Figure 1) were set in the open position. Valve D was closed. The valves on the manometers recording the pressure drop across the test section were also closed. Air was introduced in the test section by opening the valves P and Q. Valve C was then adjusted to minimize the fluctuations particularly in the manometer across the air orifice, and to give higher pressures upstream of the air orifice. When the mid-point pressure reached the desired level (i.e. 35-36 psia), water was introduced in

the system by turning on the centrifugal pump and opening the valves S and R. Valve D was then opened and adjusted to give a steady discharge of water and to maintain a fairly steady level in the separator. Valves R and Q were adjusted to give the desired flow rates of reference phase (water) and second phase (air). When the conditions inside the test section had reached a steady state as indicated by visual observations, a note of the flow pattern was made. The time interval required to establish steady state conditions varied from a few minutes to almost 10-15 minutes. In general, the slower the flow rates, the longer the time required to reach steady state. In addition to the flow pattern the following data were recorded:

1) Pressure drop across the water and air orifices.

2) The pressure drop across the 30 ft. test section. To obtain this, the valves on the manometers were opened slightly. The pressure differential as registered by the water or mercury manometer was then recorded.

3) Mid-point pressure.

4) Temperature of the air, water and the mixture.

5) Upstream static pressure at the air orifice.

6) Hold-up: After recording the above values, and checking the manometers to ascertain that the correct flow rates were being maintained, valves A and B were closed by using the mechanical linkage and the valves Q and R were closed immediately. The pump was stopped and the air supply turned off by closing the valve P. The small cocks situated in the body of valves A and B were then opened slowly and the trapped water collected in a bucket and weighed. More often, the

pressure inside the test section enabled the water to be discharged easily. When necessary, the clamps were loosened and the pipe was slightly lifted at the center to facilitate draining.

EXPERIMENTAL RESULTS AND DISCUSSION

The results of the preliminary tests of single-phase flow of air and water are presented in the form of the conventional friction factor and Reynolds number charts in Figures 5c and 6c of Appendix C. The calculated data showed good agreement with theoretical curves in the laminar $f = \frac{16}{N_{Re}}$ and in the turbulent region with the Blasius Equation, $f = (0.079)\ N_{Re}^{-0.25}$. Because of the good agreement, it is concluded that the calibrations of the orifice plates and the pressure measuring system were quite accurate.

The flow patterns occurring at various superficial velocities of second phase (air) from 0.1 ft. per sec. to 50 ft. per sec. for constant superficial velocities of reference phase (water) from 0.01 ft. per sec. to 5.03 ft. per sec. were noted. Figures 2 to 11 indicate the type of flow pattern observed during each experiment. In these figures the letter symbols used, represent the following flow patterns:

B = Bubble

PL = Plug

ST = Stratified

W = Wave or Ripple

SL = Slug

F = Film, or Semiannular or Annular

Pressure drops and liquid hole-up data were collected for the range of the velocities mentioned above.

Flow Patterns

Figures 2 to 11 indicate the type of flow pattern occurring at various superficial velocities of second phase (air) for constant

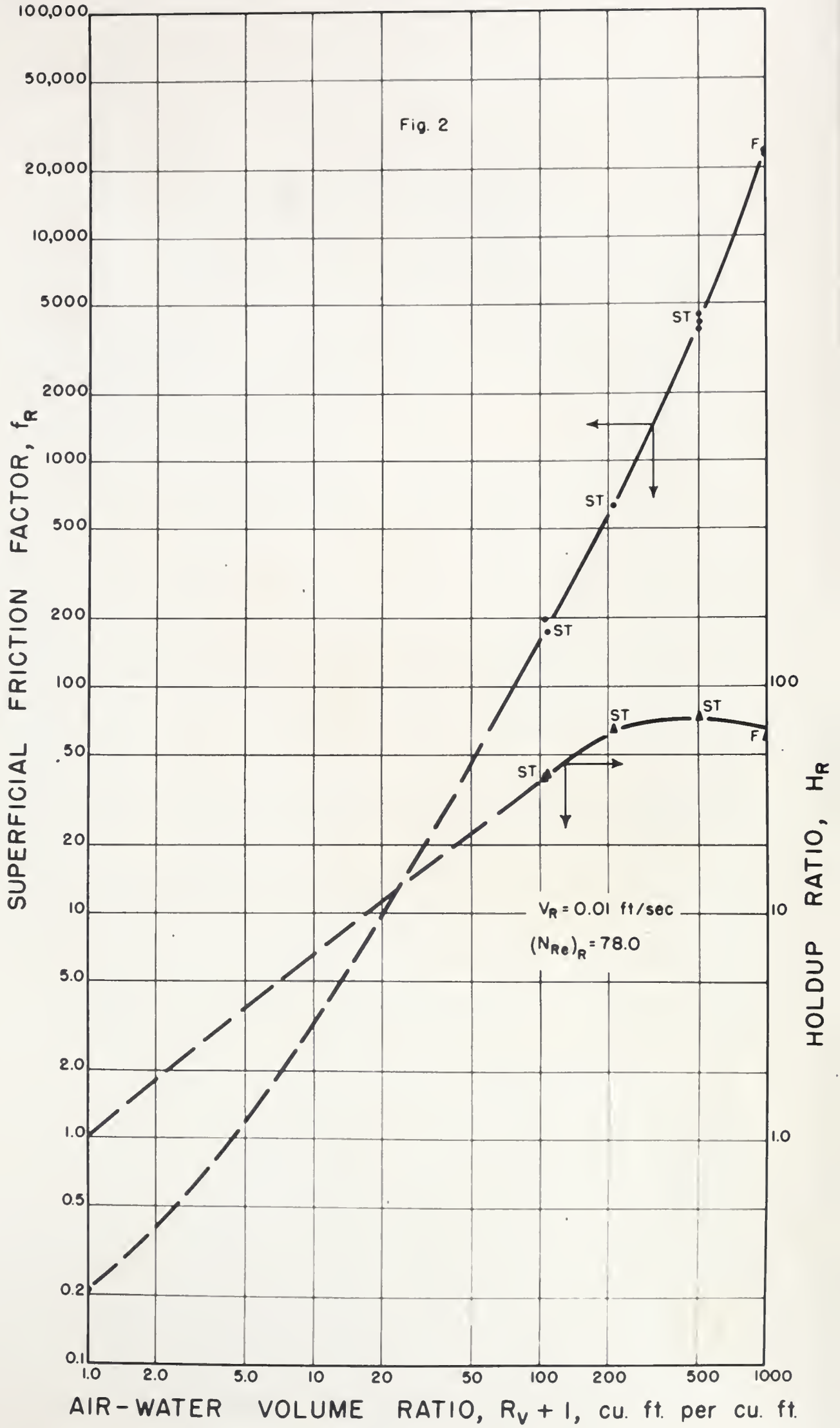
Fig. 2
SUPERFICIAL FRICTION FACTOR, f_R
HOLDUP RATIO, H_R
AIR-WATER VOLUME RATIO, $R_V + 1$, cu. ft. per cu. ft.
100,000
50,000
20,000
10,000
5000
2000
1000
500
200
100
50
20
10
5.0
2.0
1.0
0.5
0.2
0.1
1.0
2.0
5.0
10
20
50
100
200
500
1000
F
ST
ST
ST
ST
ST
ST
F
V_R = 0.01 ft/sec
$(N_{Re})_R$ = 78.0

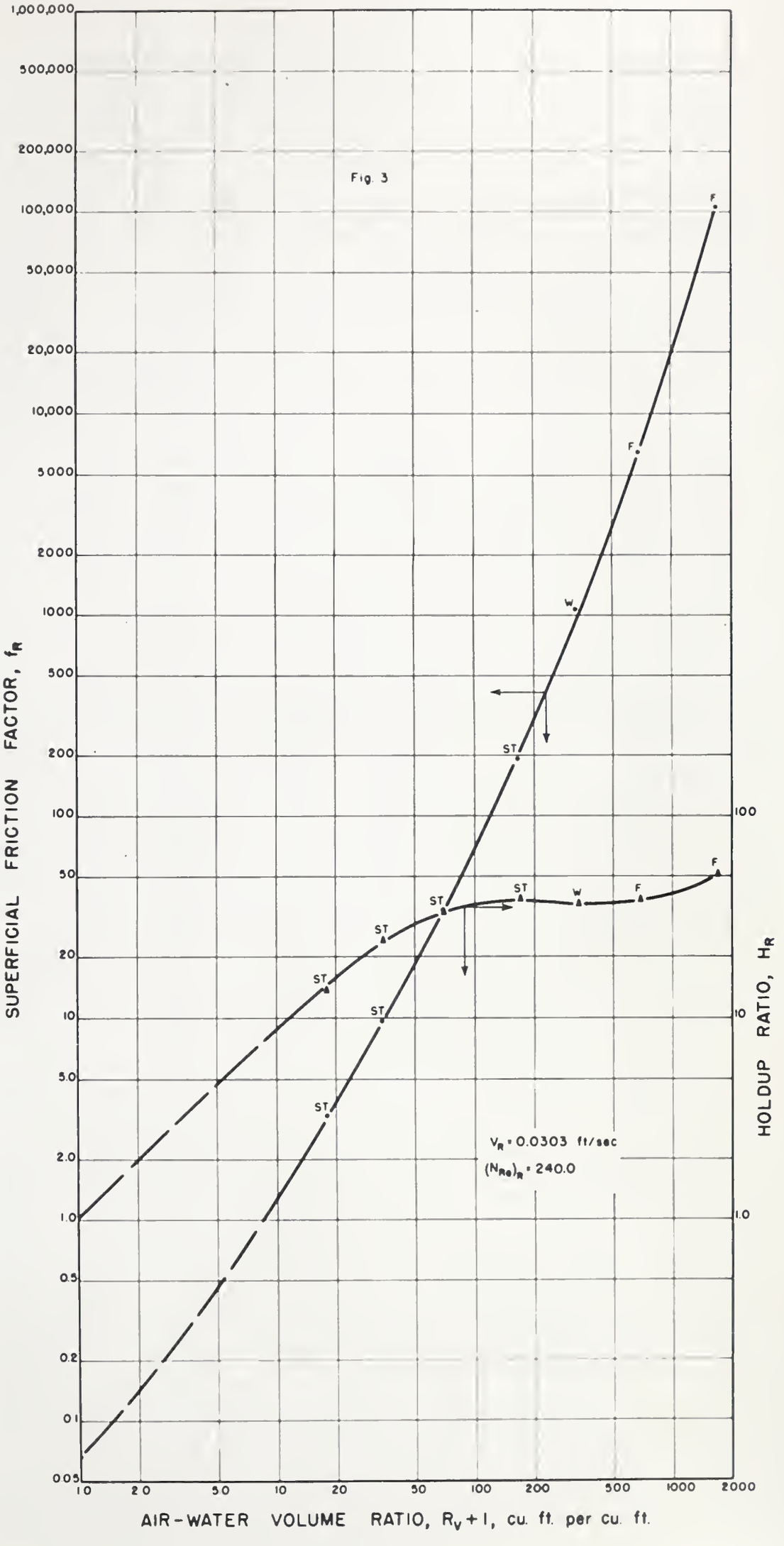
Fig. 3
SUPERFICIAL FRICTION FACTOR, f_R
HOLDUP RATIO, H_R
AIR-WATER VOLUME RATIO, $R_V + 1$, cu. ft. per cu. ft.
1,000,000
500,000
200,000
100,000
50,000
20,000
10,000
5000
2000
1000
500
200
100
50
20
10
5.0
2.0
1.0
0.5
0.2
0.1
0.05
100
10
1.0
10
20
50
10
20
50
100
200
500
1000
2000
ST
W
F
V_R = 0.0303 ft/sec
$(N_{Re})_R$ = 240.0

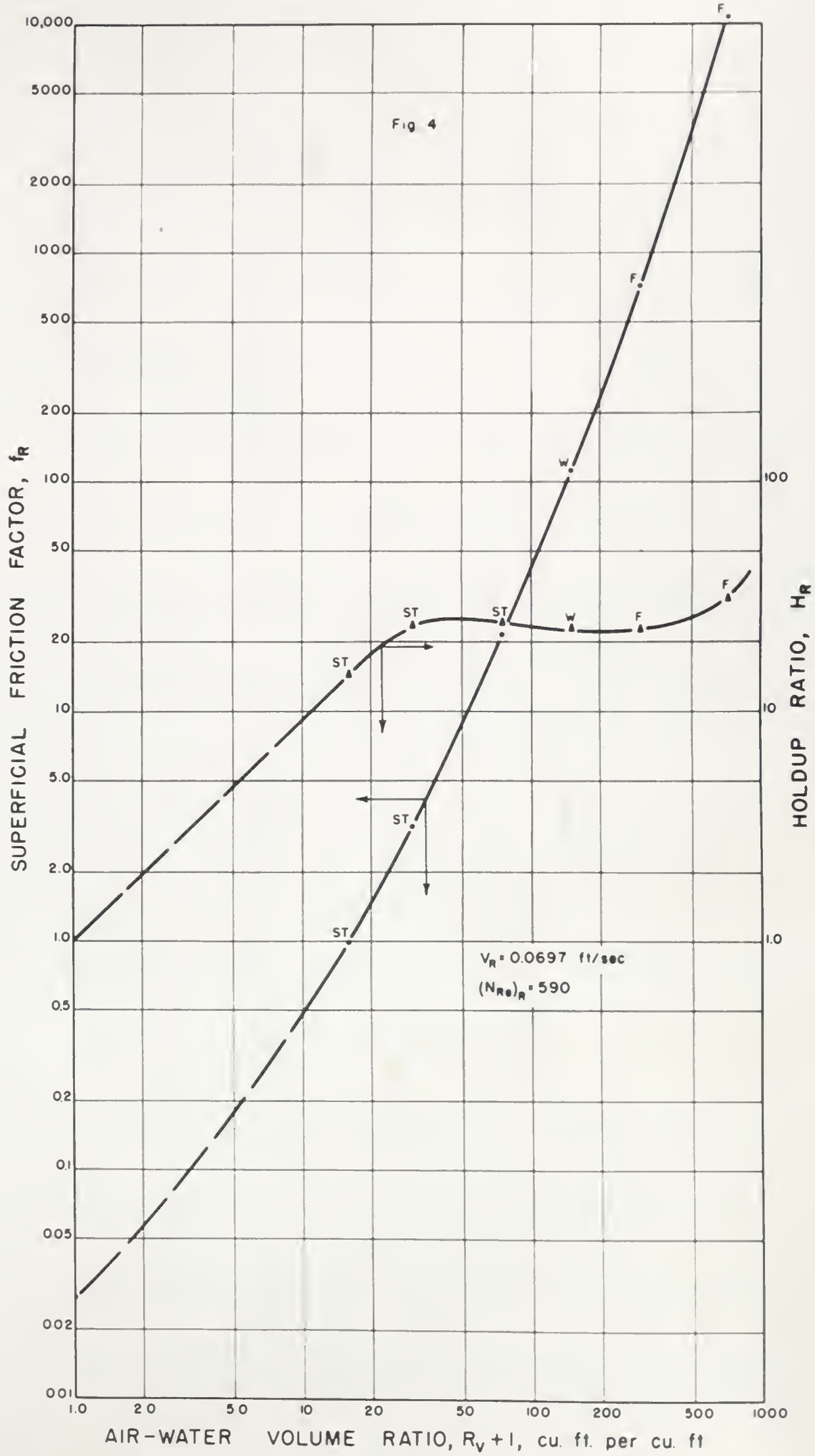
Fig 4
SUPERFICIAL FRICTION FACTOR, f_R
HOLDUP RATIO, H_R
AIR-WATER VOLUME RATIO, $R_V + 1$, cu. ft. per cu. ft
10,000
5000
2000
1000
500
200
100
50
20
10
5.0
2.0
1.0
0.5
0.2
0.1
0.05
0.02
0.01
100
10
1.0
1.0
2.0
5.0
10
20
50
100
200
500
1000
F
W
ST
V_R = 0.0697 ft/sec
$(N_{Re})_R$ = 590

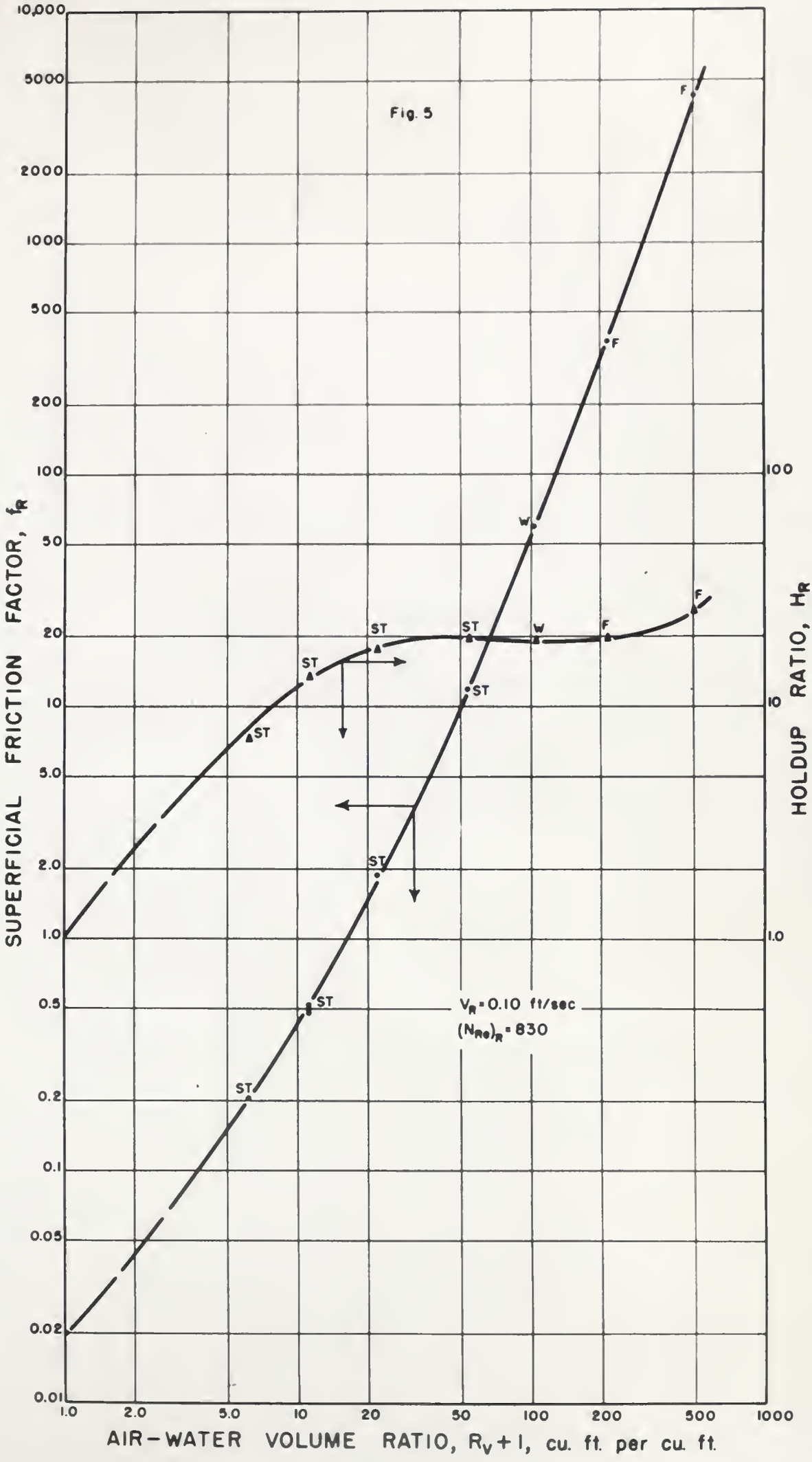
Fig. 5
SUPERFICIAL FRICTION FACTOR, f_R
HOLDUP RATIO, H_R
AIR-WATER VOLUME RATIO, $R_V + 1$, cu. ft. per cu. ft.
$V_R = 0.10$ ft/sec
$(N_{Re})_R = 830$
ST
W
F
10,000
5000
2000
1000
500
200
100
50
20
10
5.0
2.0
1.0
0.5
0.2
0.1
0.05
0.02
0.01
1.0
2.0
5.0
10
20
50
100
200
500
1000

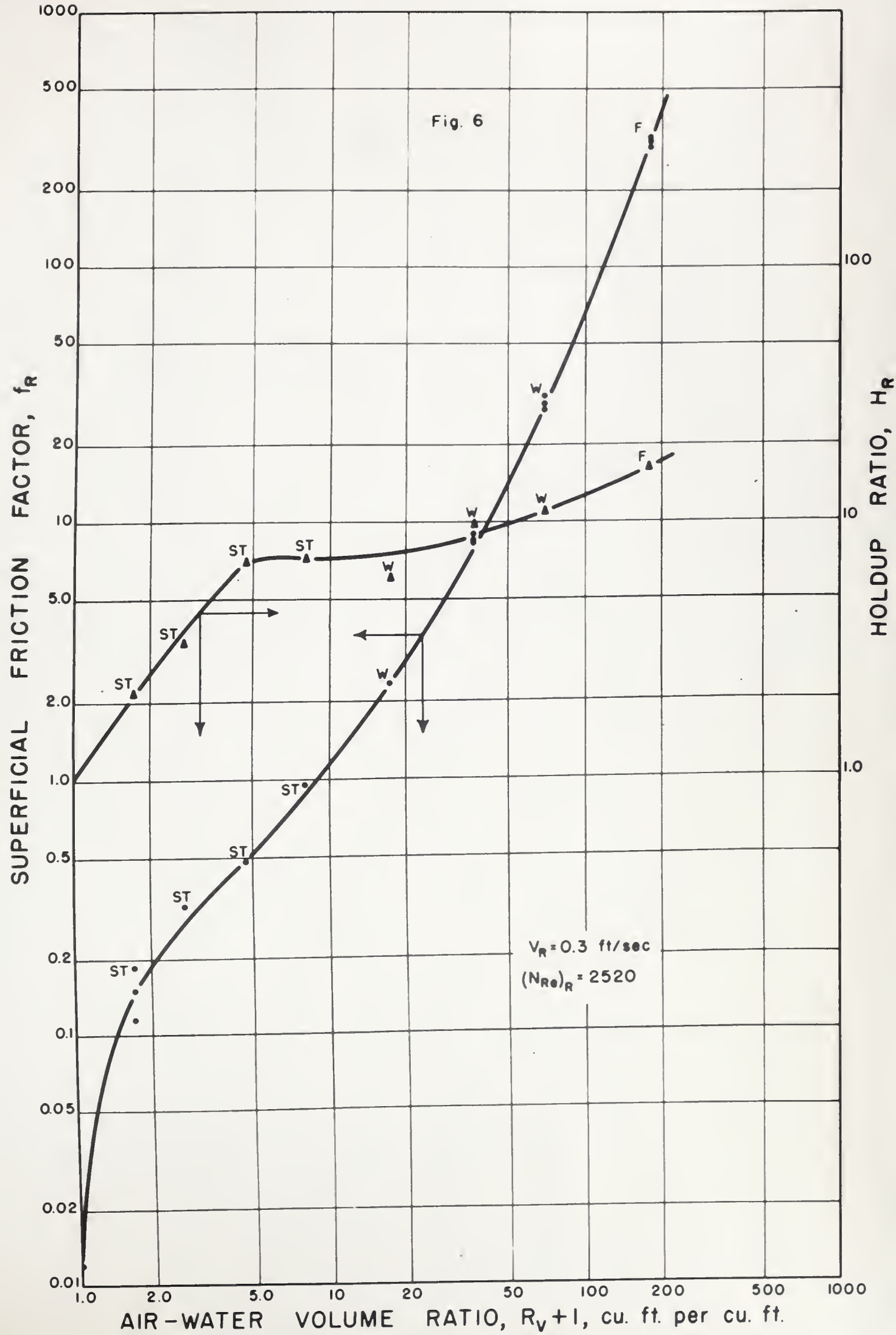
Fig. 6
SUPERFICIAL FRICTION FACTOR, f_R
HOLDUP RATIO, H_R
AIR-WATER VOLUME RATIO, R_V+1, cu. ft. per cu. ft.
1000
500
200
100
50
20
10
5.0
2.0
1.0
0.5
0.2
0.1
0.05
0.02
0.01
100
10
1.0
1.0
2.0
5.0
10
20
50
100
200
500
1000
ST
W
F
V_R = 0.3 ft/sec
$(N_{Re})_R$ = 2520

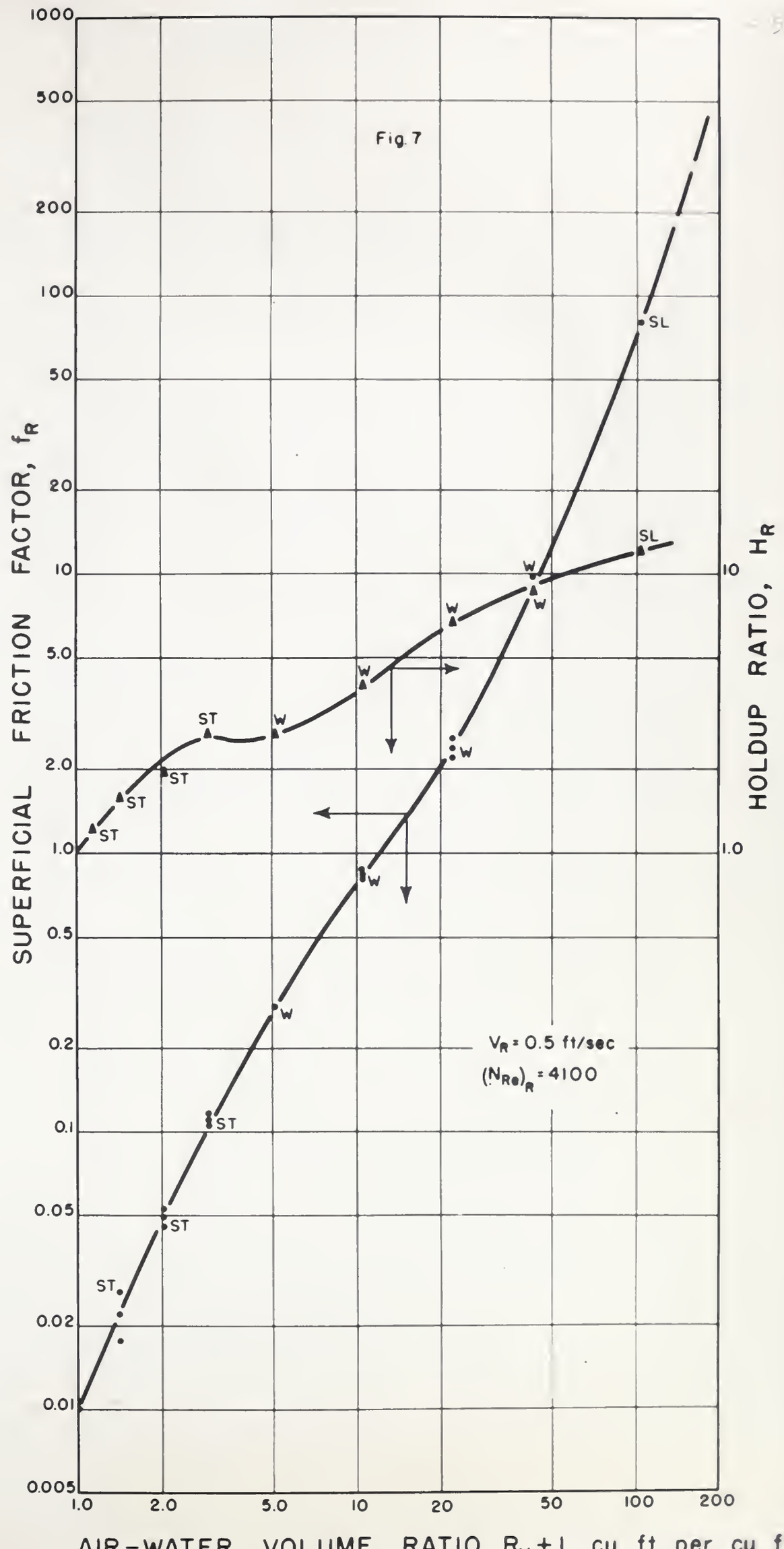
Fig. 7
SUPERFICIAL FRICTION FACTOR, f_R
HOLDUP RATIO, H_R
AIR-WATER VOLUME RATIO, $R_V + 1$, cu. ft. per cu. ft.
1000
500
200
100
50
20
10
5.0
2.0
1.0
0.5
0.2
0.1
0.05
0.02
0.01
0.005
1.0
2.0
5.0
10
20
50
100
200
ST
W
SL
V_R = 0.5 ft/sec
$(N_{Re})_R$ = 4100

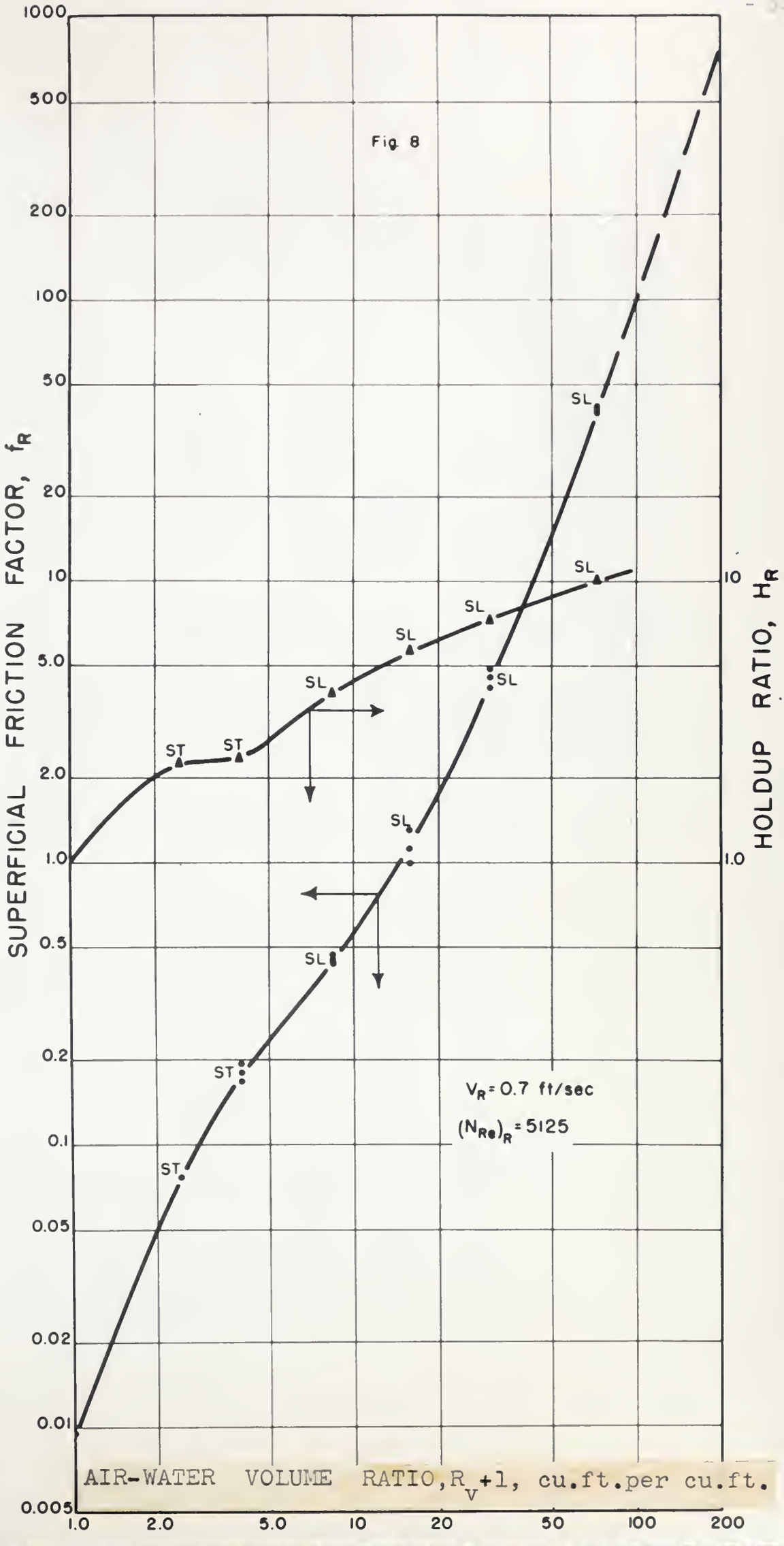
Fig. 8
SUPERFICIAL FRICTION FACTOR, f_R
HOLDUP RATIO, H_R
AIR-WATER VOLUME RATIO, R_V+1, cu.ft.per cu.ft.
$V_R = 0.7$ ft/sec
$(N_{Re})_R = 5125$
ST
SL
1000
500
200
100
50
20
10
5.0
2.0
1.0
0.5
0.2
0.1
0.05
0.02
0.01
0.005
1.0
2.0
5.0
10
20
50
100
200

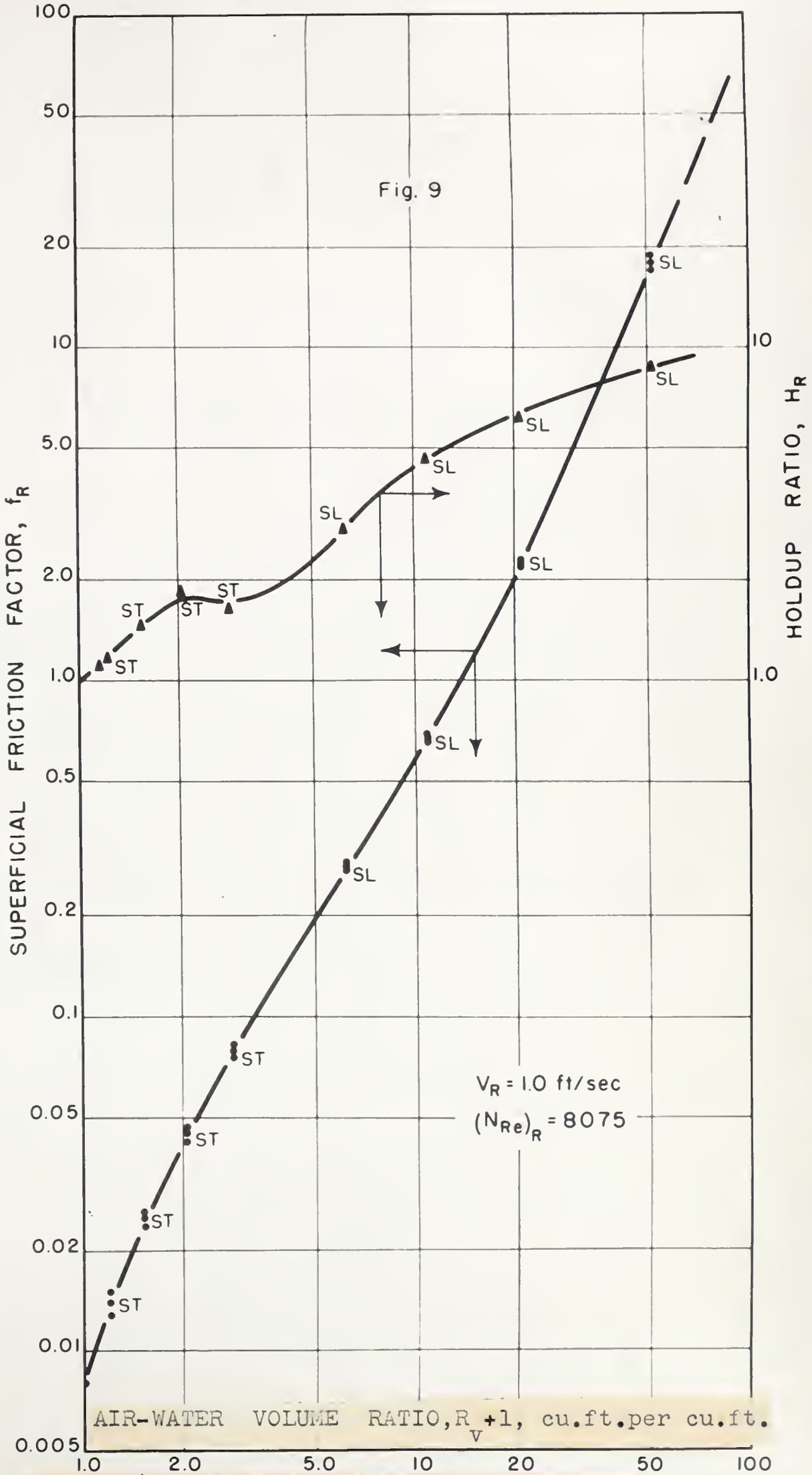
Fig. 9
SUPERFICIAL FRICTION FACTOR, f_R
HOLDUP RATIO, H_R
AIR-WATER VOLUME RATIO, R_V+1, cu.ft.per cu.ft.
100
50
20
10
5.0
2.0
1.0
0.5
0.2
0.1
0.05
0.02
0.01
0.005
1.0
2.0
5.0
10
20
50
100
ST
SL
V_R = 1.0 ft/sec
$(N_{Re})_R$ = 8075

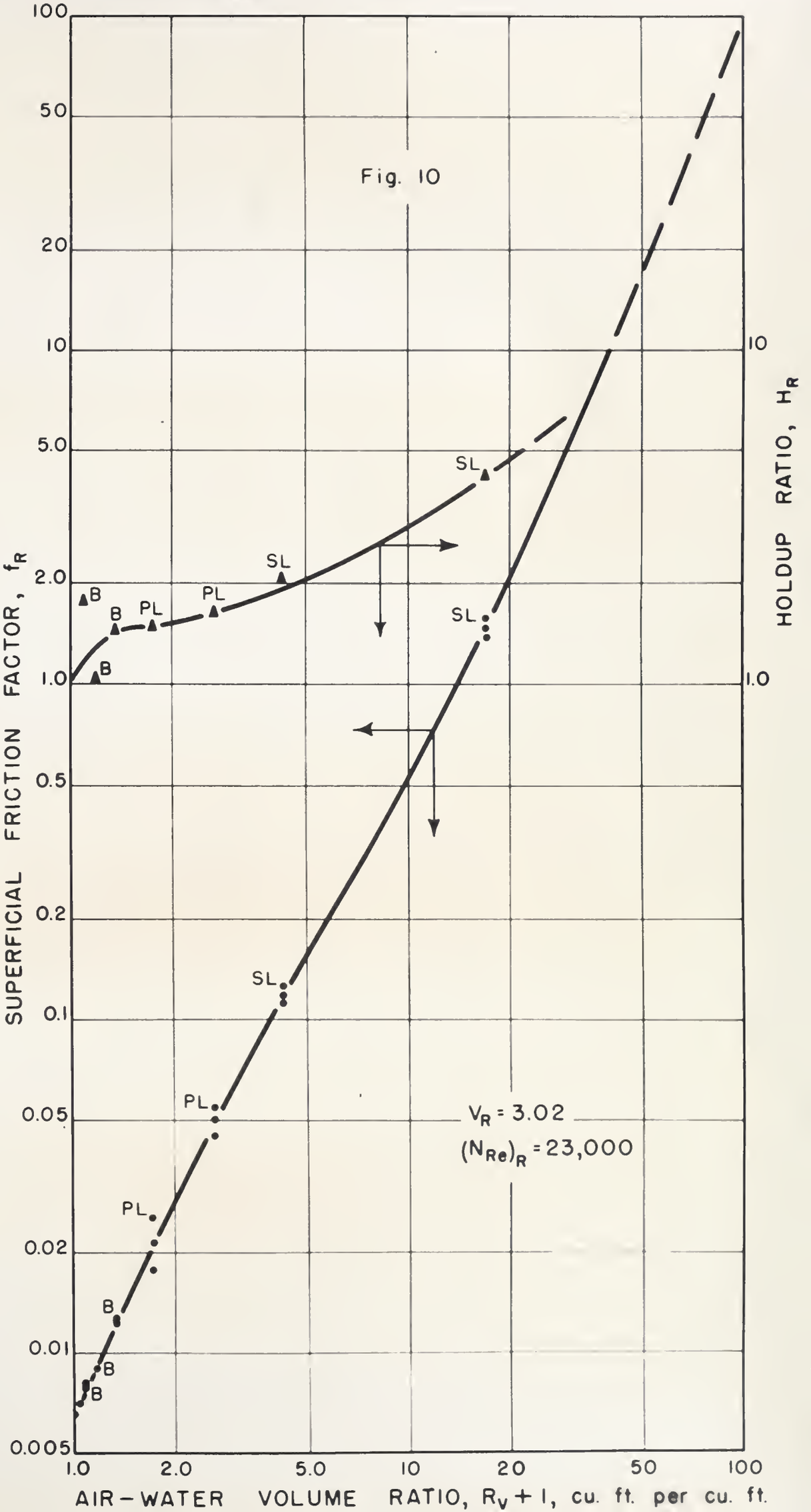
Fig. 10
SUPERFICIAL FRICTION FACTOR, f_R
HOLDUP RATIO, H_R
AIR – WATER VOLUME RATIO, $R_V + 1$, cu. ft. per cu. ft.
100
50
20
10
5.0
2.0
1.0
0.5
0.2
0.1
0.05
0.02
0.01
0.005
1.0
2.0
5.0
10
20
50
100
B
PL
SL
$V_R = 3.02$
$(N_{Re})_R = 23,000$

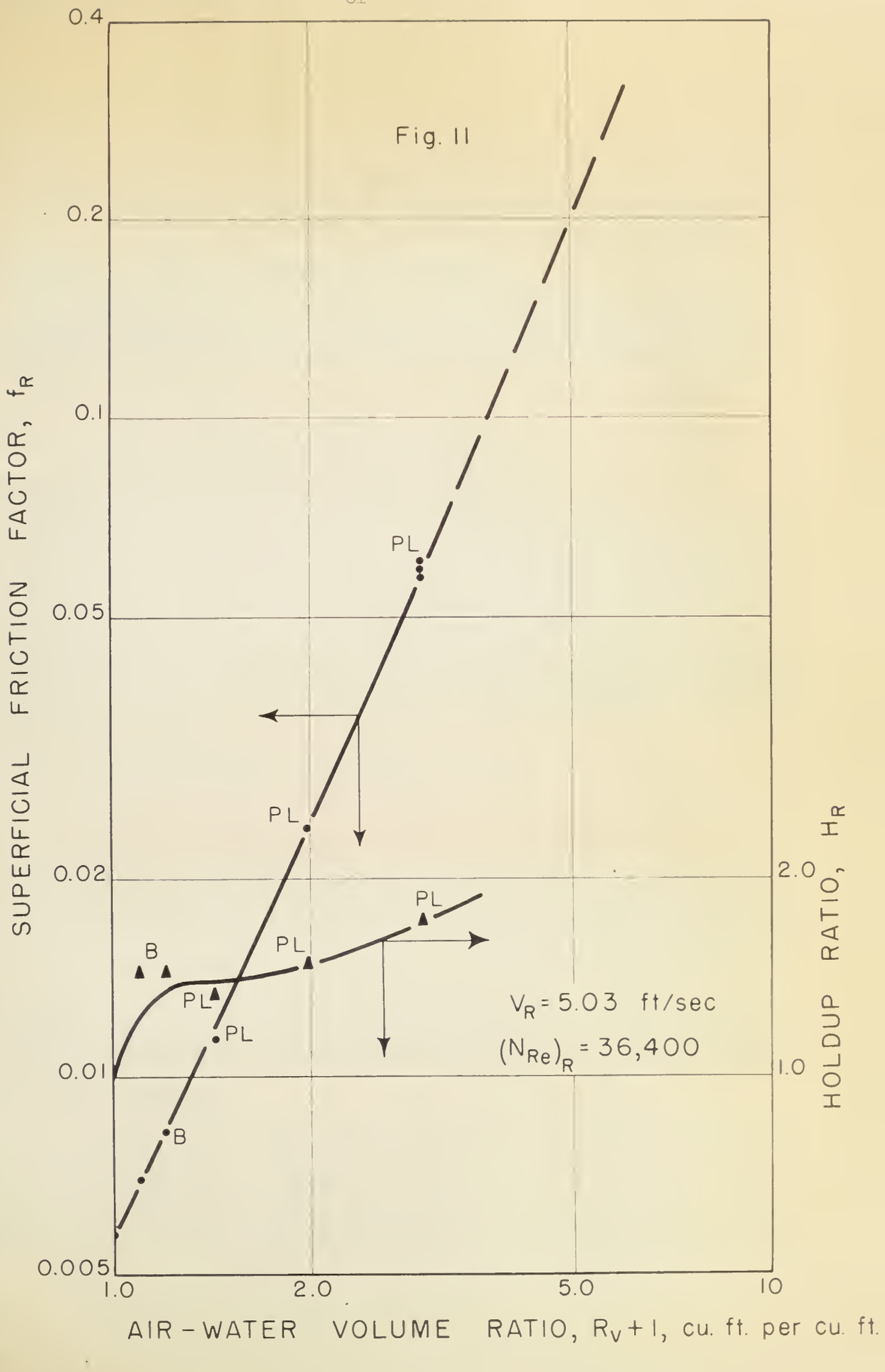
Fig. 11
SUPERFICIAL FRICTION FACTOR, f_R
HOLDUP RATIO, H_R
AIR-WATER VOLUME RATIO, $R_V + 1$, cu. ft. per cu. ft.
0.4
0.2
0.1
0.05
0.02
0.01
0.005
1.0
2.0
5.0
10
2.0
1.0
PL
B
$V_R = 5.03$ ft/sec
$(N_{Re})_R = 36,400$

superficial velocities of reference phase (water) from 0.01 ft. per sec. to 5.03 ft. per sec. In general the following flow patterns were observed:

1) Bubble 2) Plug 3) Stratified 4) Wave or Ripple 5) Slug 6) Film or Semiannular or annular.

The sequence of appearance of the flow patterns at a particular superficial velocity of reference phase and at increasing second phase superficial velocities was not necessarily in the order given above. It was not possible to make photographic studies of the flow pattern during each experiment but some representative patterns are given in Plates 5 and 6.

Plate 5 shows the photographs of flow patterns developed at superficial velocity of reference phase of 0.3 ft. per sec. and superficial velocities of second phase of 52.2 ft. per sec., 21.0 ft. per sec and 1.2 ft. per sec. The flow patterns occurring at these velocities are 'Film', 'Wave or Ripple' and 'Stratified' respectively. Plate 6 shows the flow patterns developed at superficial velocity of reference phase of 3.02 ft. per sec. and superficial velocities of second phase of 10.0 ft. per sec., 2.00 ft. per sec and 0.14 ft. per sec. The flow patterns that developed at these velocities are 'Slug', 'plug' and 'Bubble' respectively. The 'Slugs' were moving at such high velocities that it was not possible to get a good photograph with the equipment available. No other flow pattern was developed at second phase superficial velocities other than those mentioned above.

Bubble Flow: Bubble flow occurred at high superficial velocites of reference phase and low superficial velocities of second phase. This type of flow occurred at superficial velocities of reference phase of more

Film Flow V_s = 52.2 ft. per sec.

Wave or Ripple Flow V_s = 21.0 ft. per sec.

Stratified Flow V_s = 1.2 ft. per sec.

PLATE V

FLOW PATTERNS AT V_R = 0.3 ft. per sec.

Slug Flow V_s = 10.0 ft. per sec.

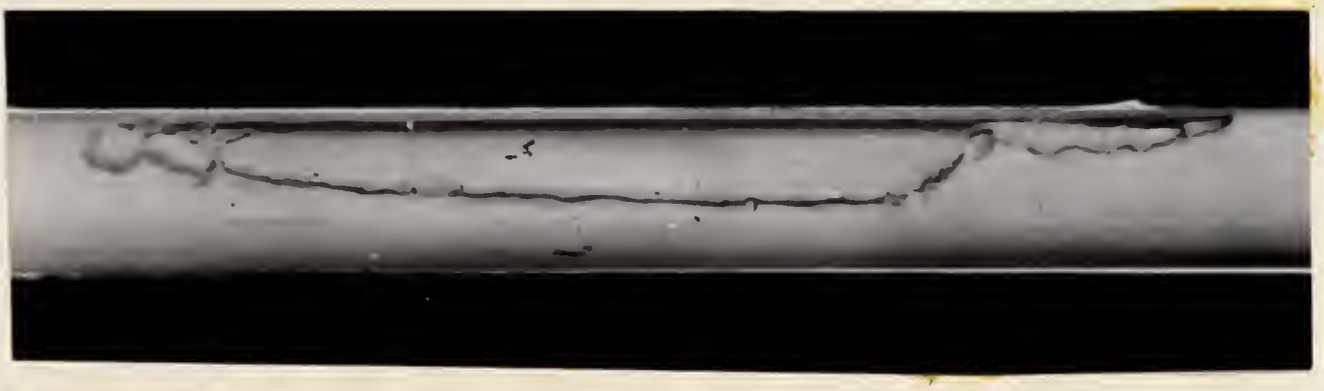

Plug Flow V_s = 2.00 ft. per sec.

Bubble Flow V_s = 0.14 ft. per sec.

Bubble Flow V_s = 0.14 ft. per sec.

PLATE VI

FLOW PATTERNS AT V_R = 3.02 ft. per sec.

than 1.0 ft. per sec. and second phase superficial velocities from 0.1 ft. per sec. to 1.0 ft. per sec.

Plug Flow: This type of flow was encountered at the same superficial velocities of reference phase as in the case of bubble flow but at higher superficial velocities of second phase i.e. from 2.0 ft. per sec to 10.0 ft. per sec.

Stratified Flow: Stratified flow generally occurred when the superficial velocities of the two phases were low. For the range of superficial velocities of reference phase from 0.01 ft. per sec. to 0.1 ft. per sec., stratified flow occurred when the second phase superficial velocity range was from 0.1 ft. per sec. to 5.0 ft. per sec. For superficial velocities of reference phase between 0.1 ft. per sec. and 1.0 ft. per sec., the maximum superficial velocity of second phase to cause stratified flow was 2.0 ft. per sec. At higher superficial velocities of reference phase, stratified flow was not encountered during the range of the second phase superficial velocities employed. Schneider (34) has found a similar behaviour.

Wave or Ripple Flow: Wave or Ripple flow occurred also at low superficial velocities of reference phase i.e. from 0.01 ft. per sec.to 0.5 ft. per sec. For superficial velocities of reference phase up to 0.1 ft. per sec. wave flow occurred when the superficial velocity of second phase was between 5 ft. per sec. and 10 ft. per sec. But for superficial velocities of reference phase between 0.1 ft. per sec. and 0.5 ft. per sec. superficial velocities of second phase between 5 ft. per sec and 20 ft. per sec. caused wave flow pattern. No wave flow pattern was observed for superficial velocities of reference phase greater than 0.5 ft. per sec.

at any of the superficial velocities of second phase.

Slug Flow: This type of flow pattern was observed only at superficial velocities of reference phase greater than 0.5 ft. per sec. and at superficial velocities of second phase greater than 6 ft. per sec. Slug flow did not exist for any superficial velocities of reference phase less than 0.5 ft. per sec. for any of the superficial velocities of second phase.

Film Flow: Film or Semiannular or annular flow occurred at low superficial velocities of reference phase i.e. between 0.01 ft. per sec. and 0.3 ft. per sec. and at superficial velocities of second phase greater than 10 ft. per sec. Film flow was not encountered for superficial velocities of reference phase greater than 0.3 ft. per sec. even at the maximum superficial velocity of second phase employed during the tests.

A chart indicating the occurrence of the various flow patterns is given in Figure 12. This chart has been prepared on the basis of the experiments and observations made in this investigation and is similar to one presented by Schneider (34) for the natural gas-kerosene system. The abscissa and the ordinate are the mass velocities (lbs. per hr. - sq. ft.) of water and air respectively. The calculated mass velocities of the two phases and the corresponding flow pattern are presented in Table II B of Appendix B. The solid lines indicate the regions developed on the basis of the present investigation. The dashed lines define the same regions as developed by Schneider (34). From a comparison between the two, it is evident that the shape of the regions is similar though not identical. The flow pattern regions developed on the basis of the present investigation are more extensive than the corresponding regions

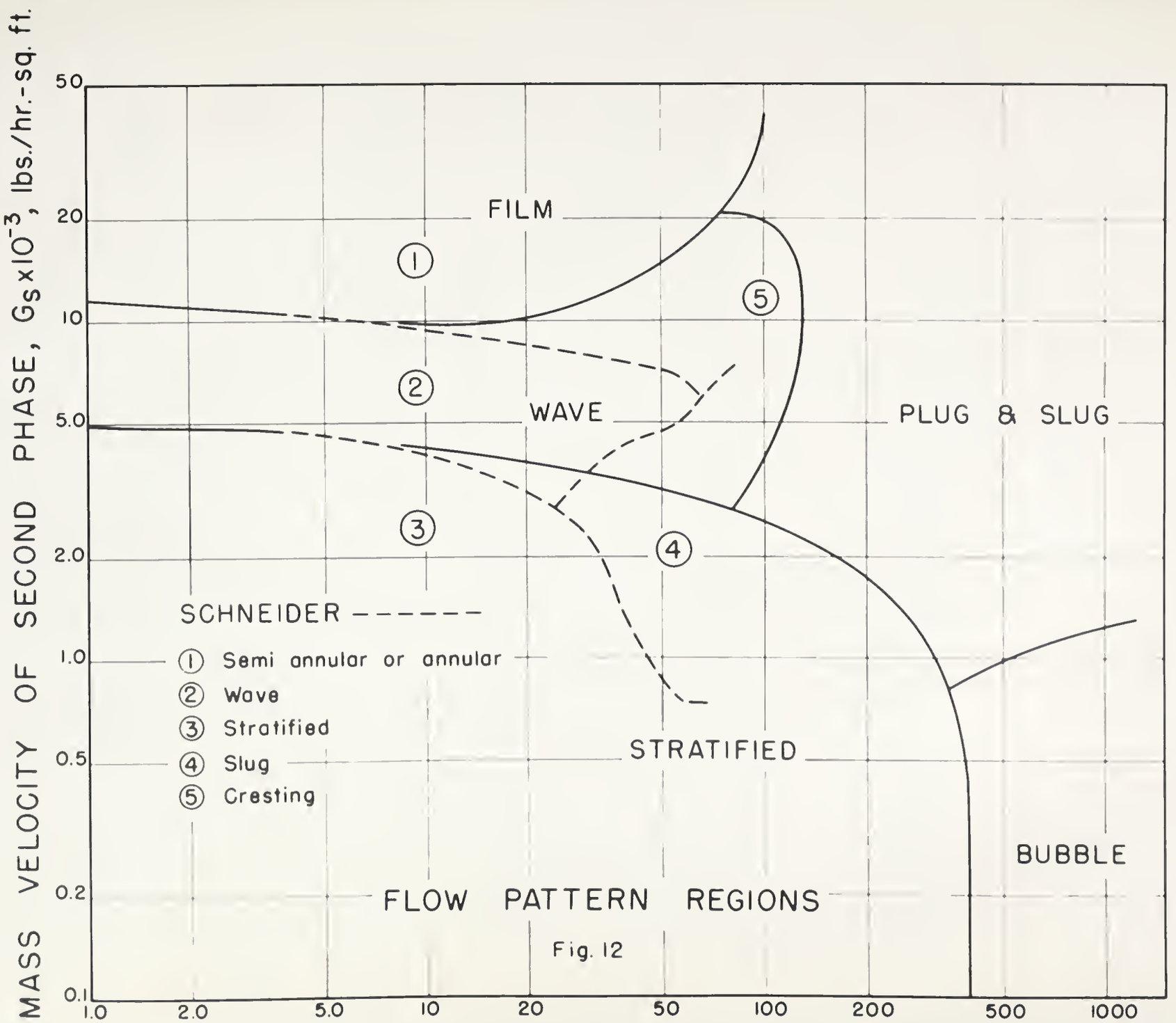
MASS VELOCITY OF SECOND PHASE, $G_S \times 10^{-3}$, lbs./hr.-sq. ft.
50
20
10
5.0
2.0
1.0
0.5
0.2
0.1
FILM
①
⑤
②
WAVE
PLUG & SLUG
③
④
SCHNEIDER ------
① Semi annular or annular
② Wave
③ Stratified
④ Slug
⑤ Cresting
STRATIFIED
BUBBLE
FLOW PATTERN REGIONS
Fig. 12
1.0
2.0
5.0
10
20
50
100
200
500
1000
MASS VELOCITY OF REFERENCE PHASE, $G_R \times 10^{-3}$, lbs./hr.-sq. ft.

indicated by Schneider (34). 'Cresting Flow', a type resembling annular flow but occurring at much higher liquid rates and mentioned by Schneider (34) in his plot was not encountered in the present study. At the same time Bubble Flow is not mentioned by Schneider (34) as his studies cover mainly wave, semiannular and annular flow.

Pressure Drop and Friction Factor

Two phase pressure drops were recorded for various superficial velocities of the second phase (air) at constant superficial velocities of the reference phase (water) of 0.01, 0.0303, 0.0697, 0.1, 0.3, 0.5, 0.7, 1.0, 3.02 and 5.03 ft. per sec. It was originally planned to go up to a reference phase superficial velocity of 10 ft. per sec. but it was not possible since beyond a superficial velocity of 5.0 ft. per sec. the controller could not maintain the mid-point pressure of 35-36 psia.

The experimental pressure drops are presented in Table II A of Appendix A. As can be seen from this table, whenever there were fluctuations in the manometer, which could not be avoided, the high, the low and the average values of the pressure drops are given. At the lower superficial velocities of reference phase, low second phase superficial velocities could not be employed since at those flow rates, the pressure drops were too small to be measured accurately with the equipment available.

The calculated superficial friction factor f_R using Eqn. (49) is tabulated in Table I B of Appendix B, along with other calculated values of the input air-water volume ratio R_V and the hold-up ratio, H_R. The superficial friction factor f_R is plotted against $(R_V + 1)$ in Figures 2 to 11, each at a different constant superficial velocity of the reference

phase. The addition of the constant 1, to the R_v values enabled the f_R vs (R_v + 1) curves to be extrapolated to the single phase friction factor where the value of the abscissa is one since this value of abscissa represents the reference phase flowing alone.

Figures 2 to 5 represent the f_R versus (R_v + 1) curves for superficial velocities of reference phase of 0.01, 0.0303, 0.0697 and 0.1 ft. per sec. At these low superficial velocities of reference phase the data give smooth curves. Figures 6 to 10 represent the same plots for superficial velocities of reference phase of 0.3, 0.5, 0.7, 1.0 and 3.02 ft. per sec. Here again the curves are smooth but exhibit a point of inflection. Figure 11, representing the same plot for a superficial velocity of reference phase of 5.03 ft. per sec. is almost a straight line. The only explanation for this dissimilarity is that at low superficial velocities of reference phase the flow patterns encountered were 'stratified', 'wave' and 'film' which are considered to be more stable in nature with no fluctuations in the pressure drops, thereby giving smooth curves. At higher superficial velocities of the reference phase, 'plug' and 'slug' type of flow were also observed though there were no instances of 'wave' flow. A change in the flow pattern, particularly from a stable one to an unstable one, might have caused a sudden change in the pressure drop. Moreover, a look at the plots at higher superficial velocities of reference phase shows that a change in the shape of the curve coincided invariably with a change in the flow pattern. This change in shape with a change in flow pattern is more pronounced in the hold-up ratio curves which are discussed later.

From data shown in Figures 2 to 11, values of the superficial

friction factor, f_R, were obtained for input air-water volume ratios of 1.0, 5.0, 10.0, 20.0, 50.0, 100 and 200. Figure 13 shows on logarithmic co-ordinates, the variation of the friction factor, f_R, with the Reynolds number calculated from the properties of the reference phase. In addition the single phase friction factor relation is also shown. In effect, Figure 13, is a correlation of the friction factor, f_R, as a function of the reference phase Reynolds number with the input air-water volume ratio as the parameter. The data of Figure 13 in the laminar region show that the friction factor, f_R, is inversely proportional to the reference phase Reynolds number up to an input volume ratio of 50 but is less dependent on the reference phase Reynolds number as the input volume ratio increases. The discontinuity present in the single phase line ($R_V = 0$) due to the transition from laminar to turbulent flow, is more pronounced for the two-phase lines up to an input volume ratio of 20.0. As the input volume ratio increases the discontinuity decreases. In the turbulent region the lines for the input volume ratio of 1.0 and 5.0 are very similar and almost parallel to the single phase line. At higher values of input volume ratio the slopes of the lines decrease. For an input volume ratio of 20.0 the line in the turbulent region is almost parallel to the abscissa. For higher values of input volume ratio i.e. 50.0, 100 and 200 the lines have a positive slope. The discontinuity, due to the transition from laminar to turbulent flow, in the two-phase friction factor versus Reynolds number curves has a wider range than in the case of single phase flow. Furthermore the transition region or the discontinuity appears to shift to the left gradually with increasing

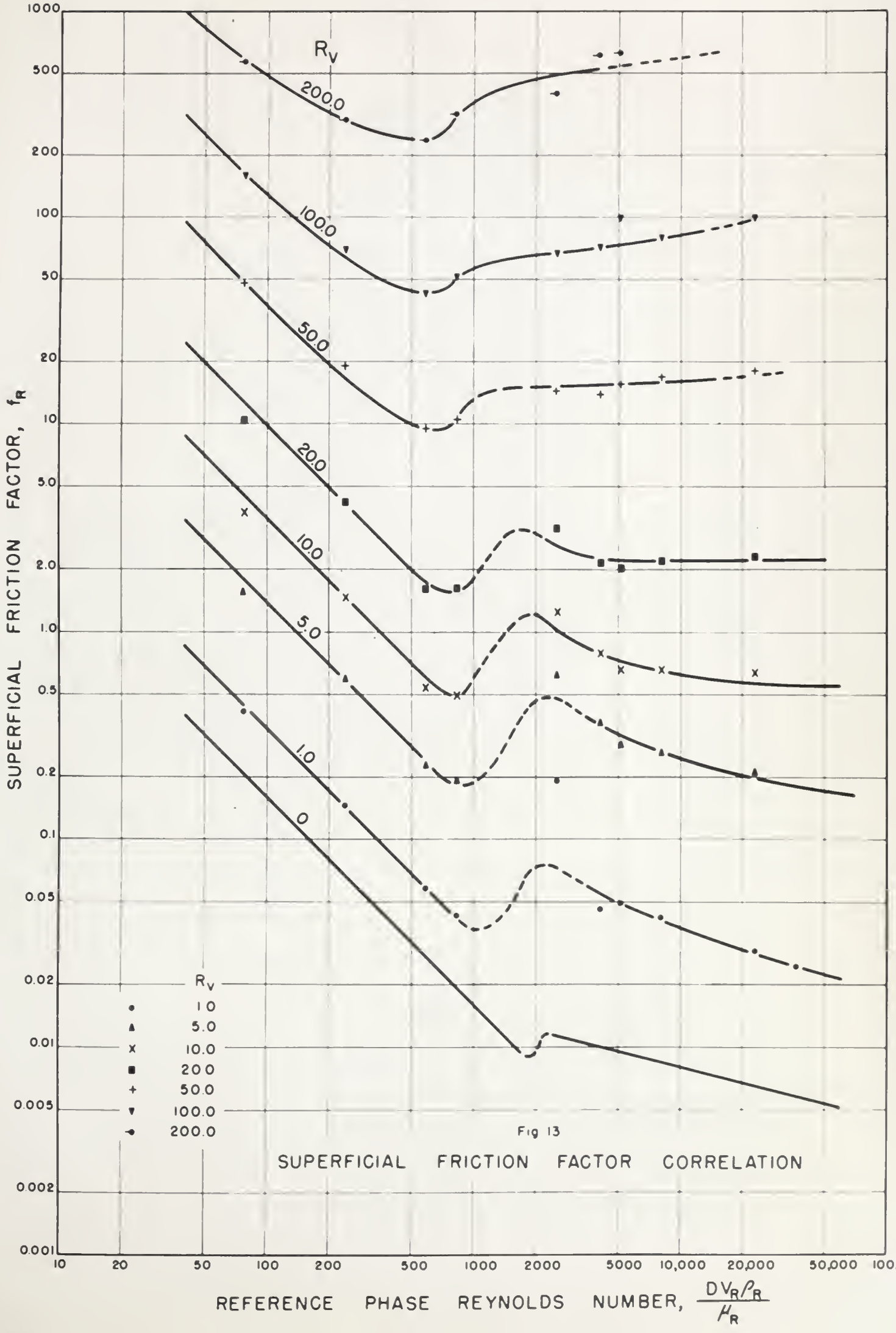

Fig 13

SUPERFICIAL FRICTION FACTOR CORRELATION

values of input volume ratio. No explanation is forwarded to justify the trend noticeable in Figure 13 though the trend seems to be very systematic.

A comparison of the data collected in the present investigation with the Lockhart and Martinelli (28) correlation is presented in Figures 14 to 17. Calculated values of the parameters X and ϕ necessary for these plots are tabulated in Table III of Appendix B. The comparison is very good (Figure 14) when both the phases are in turbulent motion. Figure 15 is for the water in turbulent and air in viscous motion. Here also the data compare favourably well with the Martinelli correlation. Figures 16 and 17 are for the viscous-turbulent and viscous-viscous mechanism respectively. Here the comparison is not very good, almost all of the points falling lower than the Lockhart and Martinelli curve. However, most of the points on these figures represent experimental data in the stratified region of flow for which Lockhart and Martinelli correlation is not valid (18).

Comparison of the superficial friction factor, f_R, versus reference phase Reynolds number curves for the present investigation with some data of Schneider (34), Thomsen (29) and Johnson and Abou-Sabe (23) is presented in Figure 18. The data of Schneider (34), Thomsen (29) and Johnson and Abou-Sabe (23) is evaluated on the basis of the calculations employed in the present investigation. No data is available in the laminar region. Schneider's (34) data though in the laminar region, corresponds to input volume ratio, R_v, values greater than 500. The dashed lines plotted in Figure 18, indicate interpolated data at lower R_v values comparable to those encountered in the present

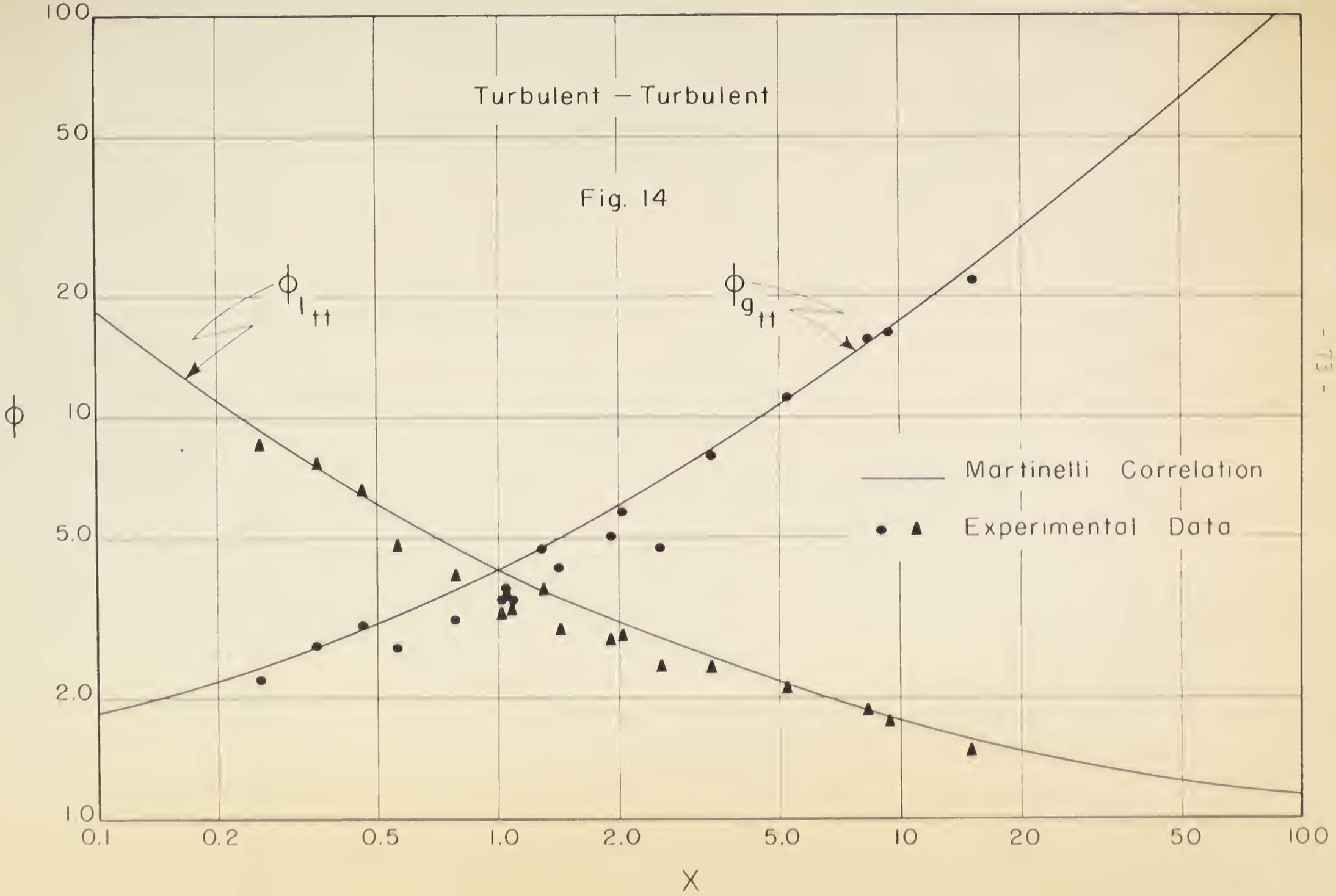
Turbulent — Turbulent
Fig. 14
$\phi_{l_{tt}}$
$\phi_{g_{tt}}$
Martinelli Correlation
Experimental Data
100
50
20
10
5.0
2.0
1.0
ϕ
0.1
0.2
0.5
1.0
2.0
5.0
10
20
50
100
X

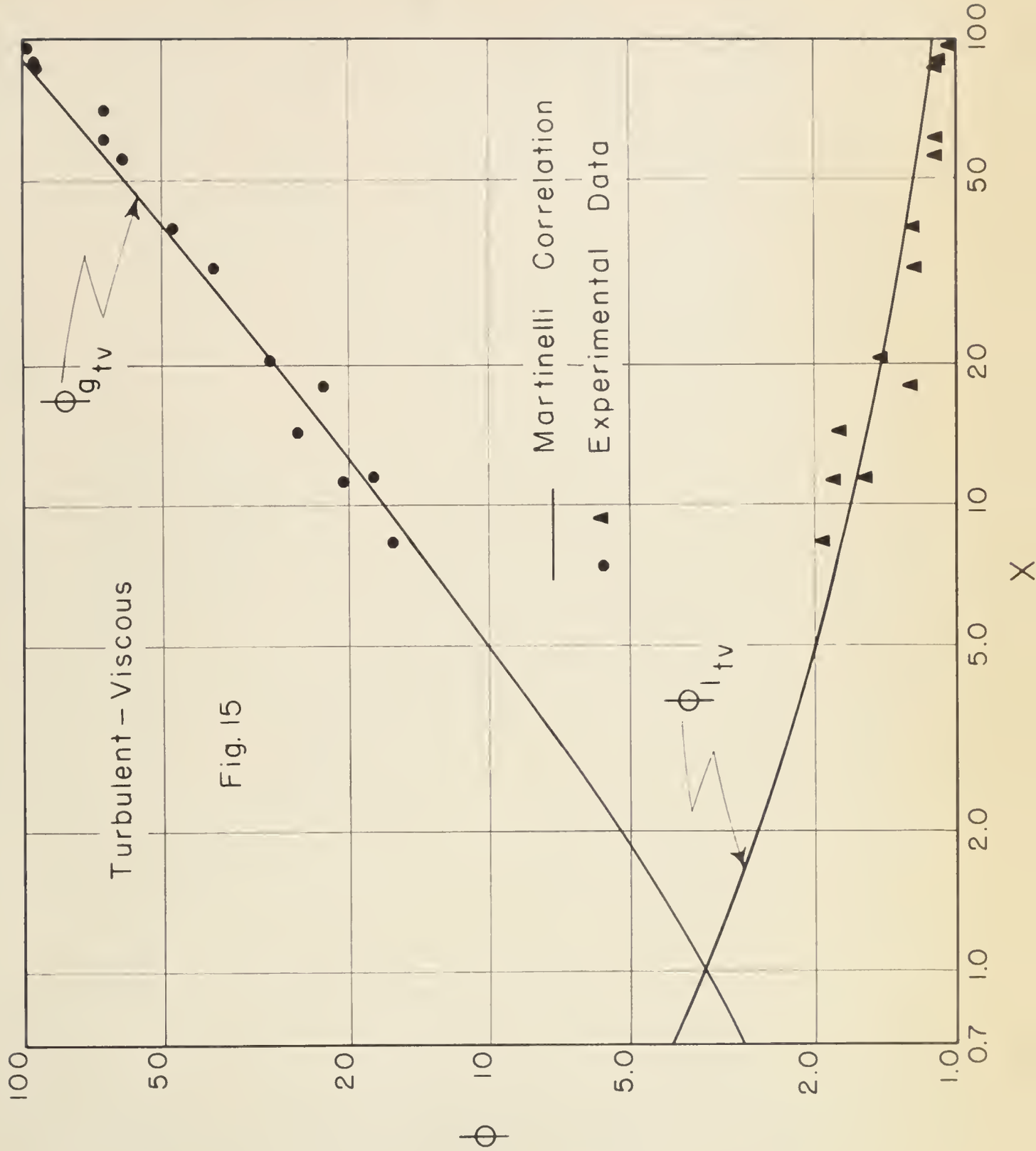
Turbulent – Viscous
Martinelli Correlation
Experimental Data
$\phi_{g_{tv}}$
$\phi_{l_{tv}}$
ϕ
X
100
50
20
10
5.0
2.0
1.0
0.7
1.0
2.0
5.0
10
20
50
100

Fig. 15

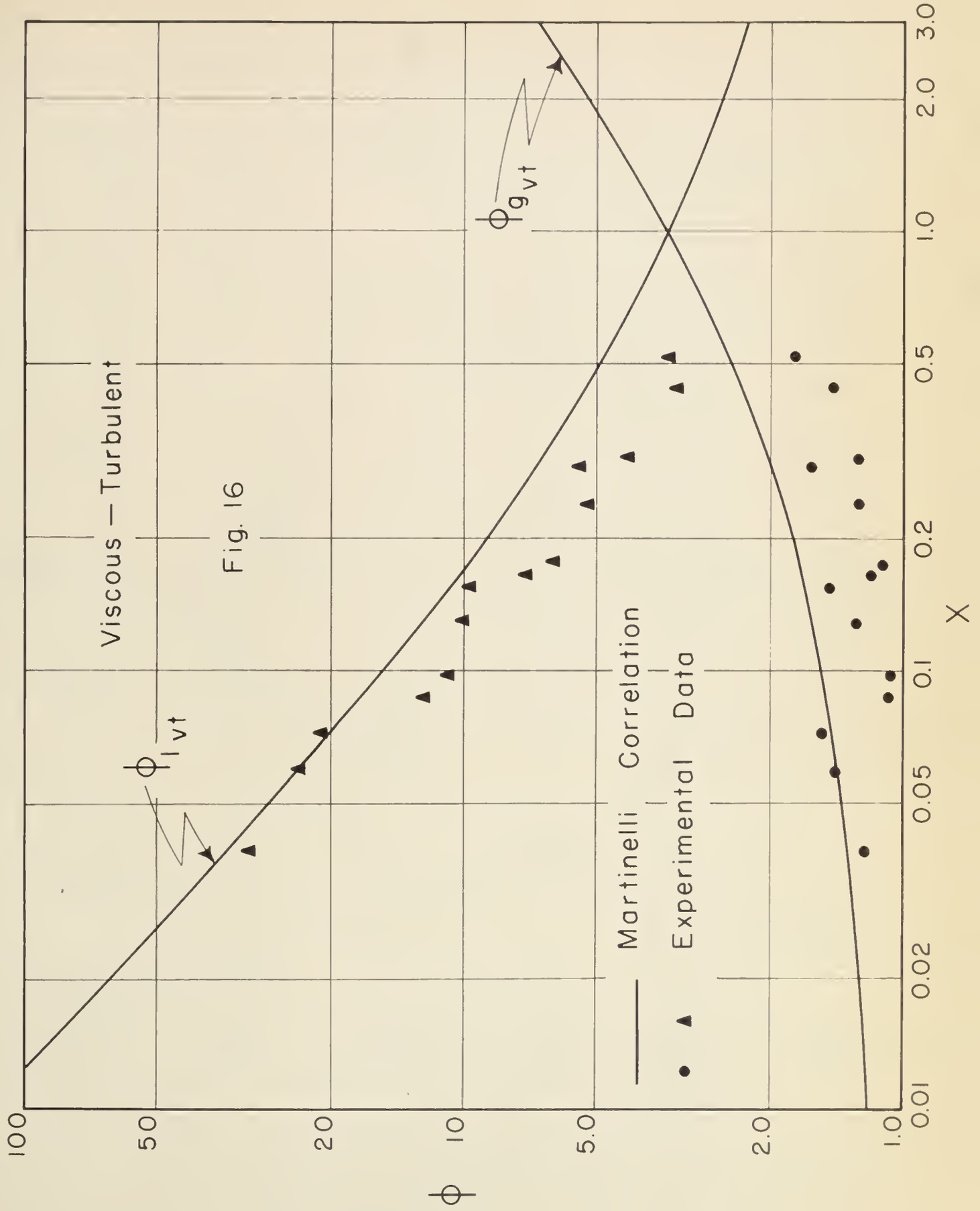
Viscous — Turbulent
Fig. 16
$\phi_{l\,vt}$
$\phi_{g\,vt}$
Martinelli Correlation
Experimental Data
ϕ
X
100
50
20
10
5.0
2.0
1.0
0.01
0.02
0.05
0.1
0.2
0.5
1.0
2.0
3.0

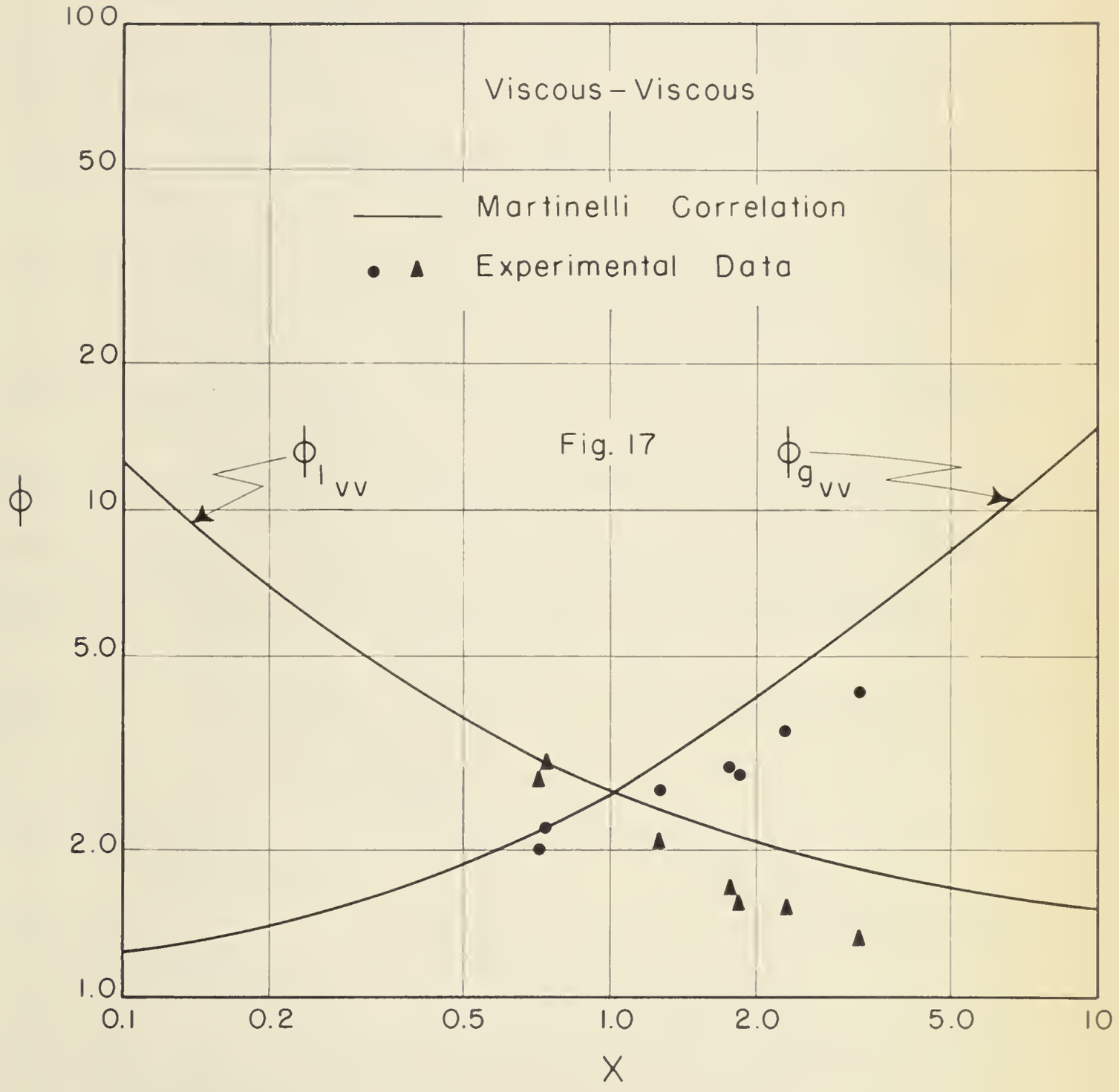
Viscous – Viscous
Martinelli Correlation
Experimental Data
$\phi_{l_{vv}}$
$\phi_{g_{vv}}$
ϕ
X
100
50
20
10
5.0
2.0
1.0
0.1
0.2
0.5
1.0
2.0
5.0
10

Fig. 17

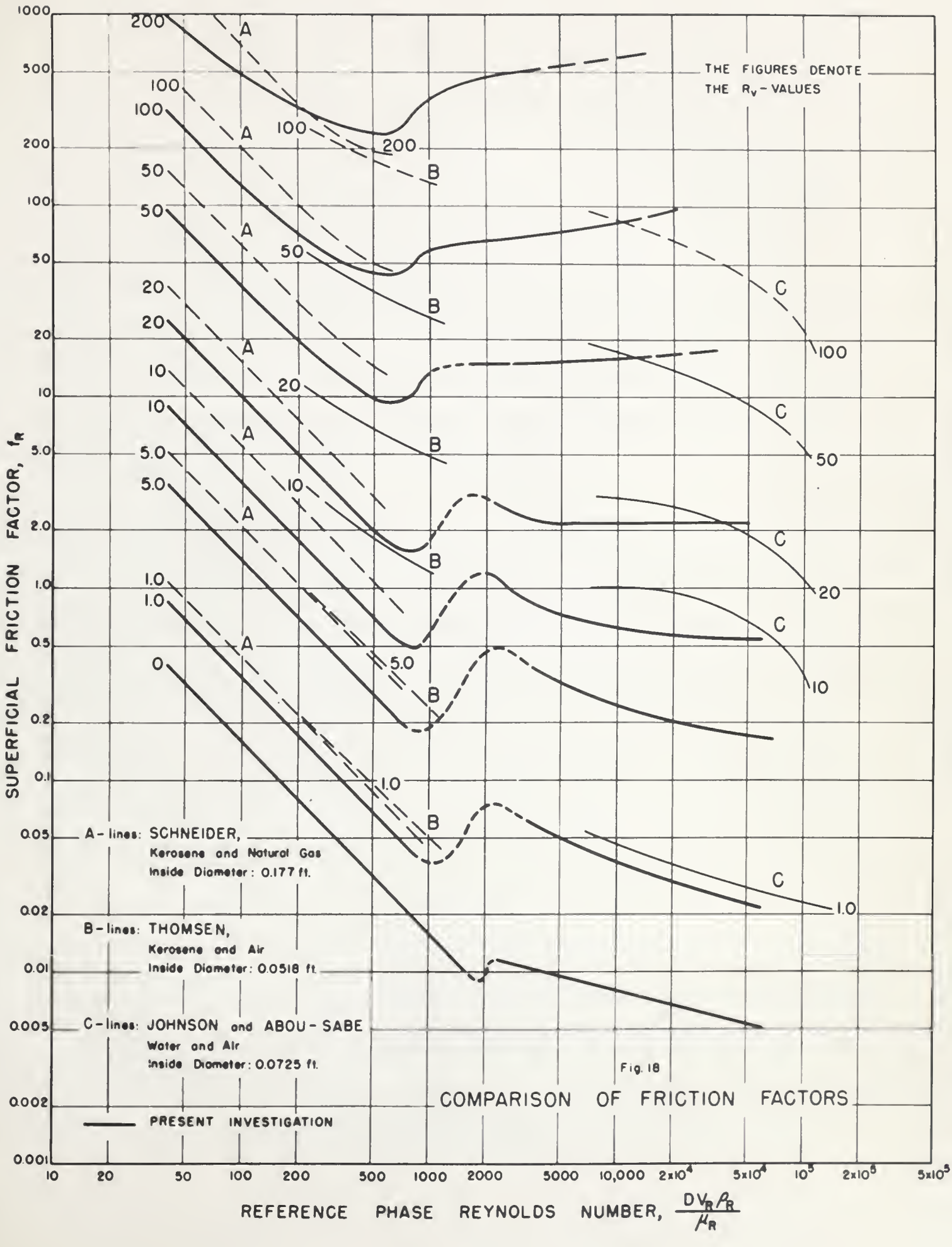

Fig. 18

COMPARISON OF FRICTION FACTORS

investigation. The influence of the gas phase (natural gas in Schneider's (34) work) is expected to be negligible and that of the liquid phase (kerosene in both Schneider (34) and Thomsen's (29) work) is taken into account by the abscissa of the plot. All these data, fall above that for the present investigation probably due to the different pipe diameters employed. The work of Johnson and Abou-Sabe (23) is the closest to the present investigation. They have employed the same components (water and air) and the pipe diameter (0.0725 ft.) is also very close to the one used in the present investigation. No explanation is forwarded, however, for the different trend exhibited by their data. On the whole the comparison is satisfactory.

Hold-up Ratio and Slip Velocity

As mentioned earlier, hold-up ratio and slip velocity are two measures of the same phenomenon which results in the development within the test section of a concentration of one of the phases greater than that in the supply mixture. Hold-up ratio, H_R, is shown as a function of air-water input volume ratio, R_v, in Figures 2 to 11, for different constant superficial velocities of reference phase. Up to a reference phase superficial velocity of 0.3 ft. per sec. the curves are smooth as shown in Figures 2 to 6. At reference phase superficial velocities greater than 0.3 ft. per sec. however these curves exhibit a discontinuity. This change which is shown in Figures 7 to 11 is more pronounced in these curves than in those for the superficial friction factor. At lower reference phase superficial velocities only ' stratified', 'wave', and 'film' flow were encountered while at higher superficial velocities of

the reference phase, 'plug' and 'slug' flow also were observed. Here again, a change in the shape of the curve has always coincided with a change in the flow pattern. This tends to show that the hold-up ratio or liquid hold-up is also a function of the flow pattern. A similar trend is noted by Levy (27). There is a strong tendency for all these curves to extend to a hold-up ratio of unity at zero input volume ratio. This can be expected since in the limiting condition of zero R_v or all liquid flow, the slip velocity is zero and by Eqn. (55) the hold-up ratio equals unity. The same trend was noted by Govier, Radford and Dunn (19) in their studies on the vertical upward flow of air-water mixtures.

A composite plot of hold-up ratio, H_R, versus R_v at different reference phase superficial velocities was first prepared but there was so much overlapping of the curves, that it is not included here. Figure 19 is a composite plot of H_R versus the second phase superficial velocity V_s with the superficial velocity of reference phase, V_R, as the parameter. The curves are separate and distinct, thereby emphasizing the importance of the parameter. Once again in the limiting condition when V_s is zero or all liquid flow, the curves approach a hold-up ratio of unity.

Slip velocity, V_{sl}, is calculated by using Eqn. (54). The calculated values are presented in Table IV B of Appendix B. The slip velocity, V_{sl}, is plotted in Figure 20 against air-water input volume ratio, R_v, with the superficial velocity of reference phase, V_R, as the parameter. At higher values of R_v most of these curves have a slope of

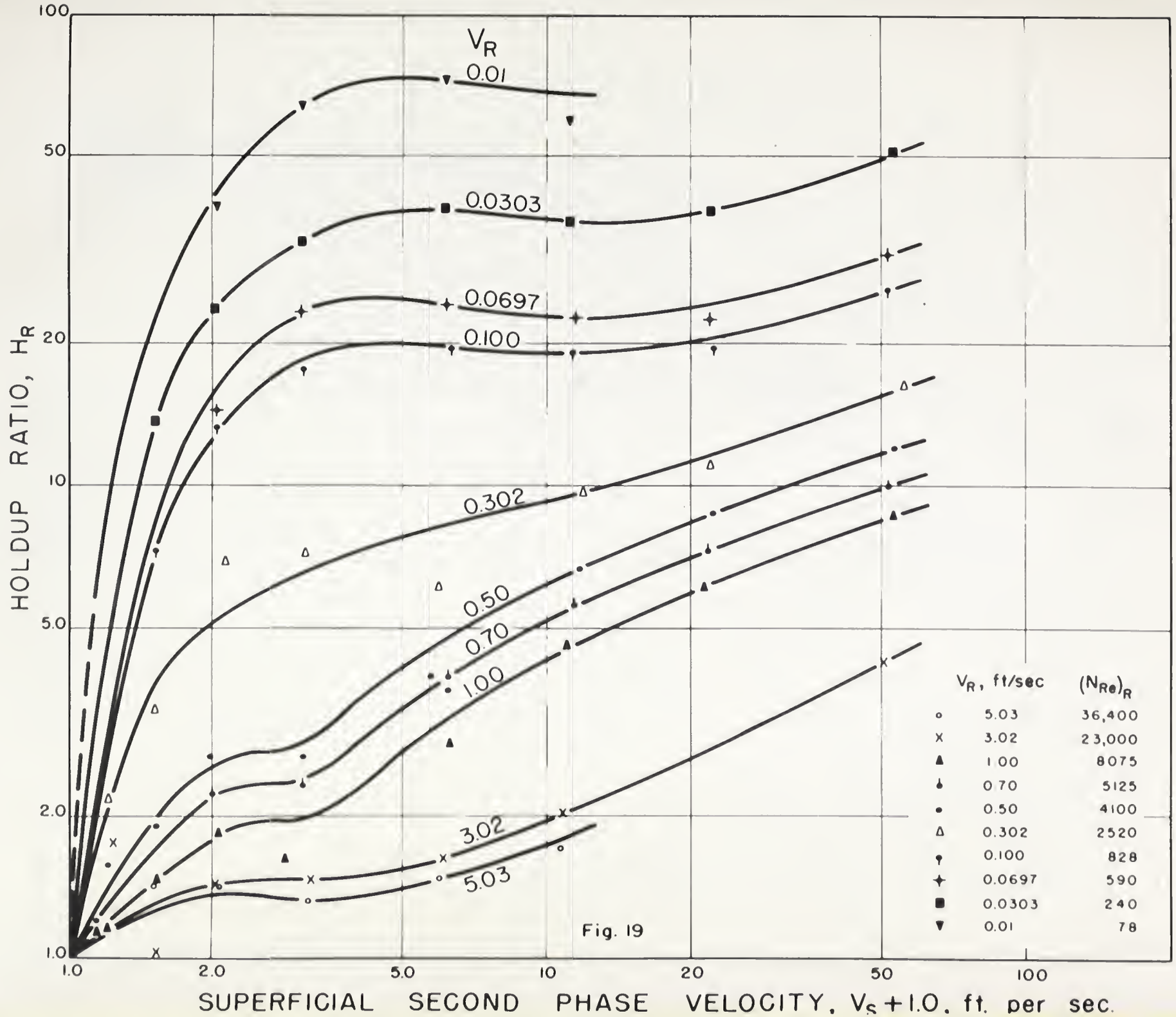
V_R
0.01
0.0303
0.0697
0.100
0.302
0.50
0.70
1.00
3.02
5.03
HOLDUP RATIO, H_R
SUPERFICIAL SECOND PHASE VELOCITY, $V_S + 1.0$, ft. per sec.
1.0
2.0
5.0
10
20
50
100
V_R, ft/sec
$(N_{Re})_R$
5.03 36,400
3.02 23,000
1.00 8075
0.70 5125
0.50 4100
0.302 2520
0.100 828
0.0697 590
0.0303 240
0.01 78

Fig. 19

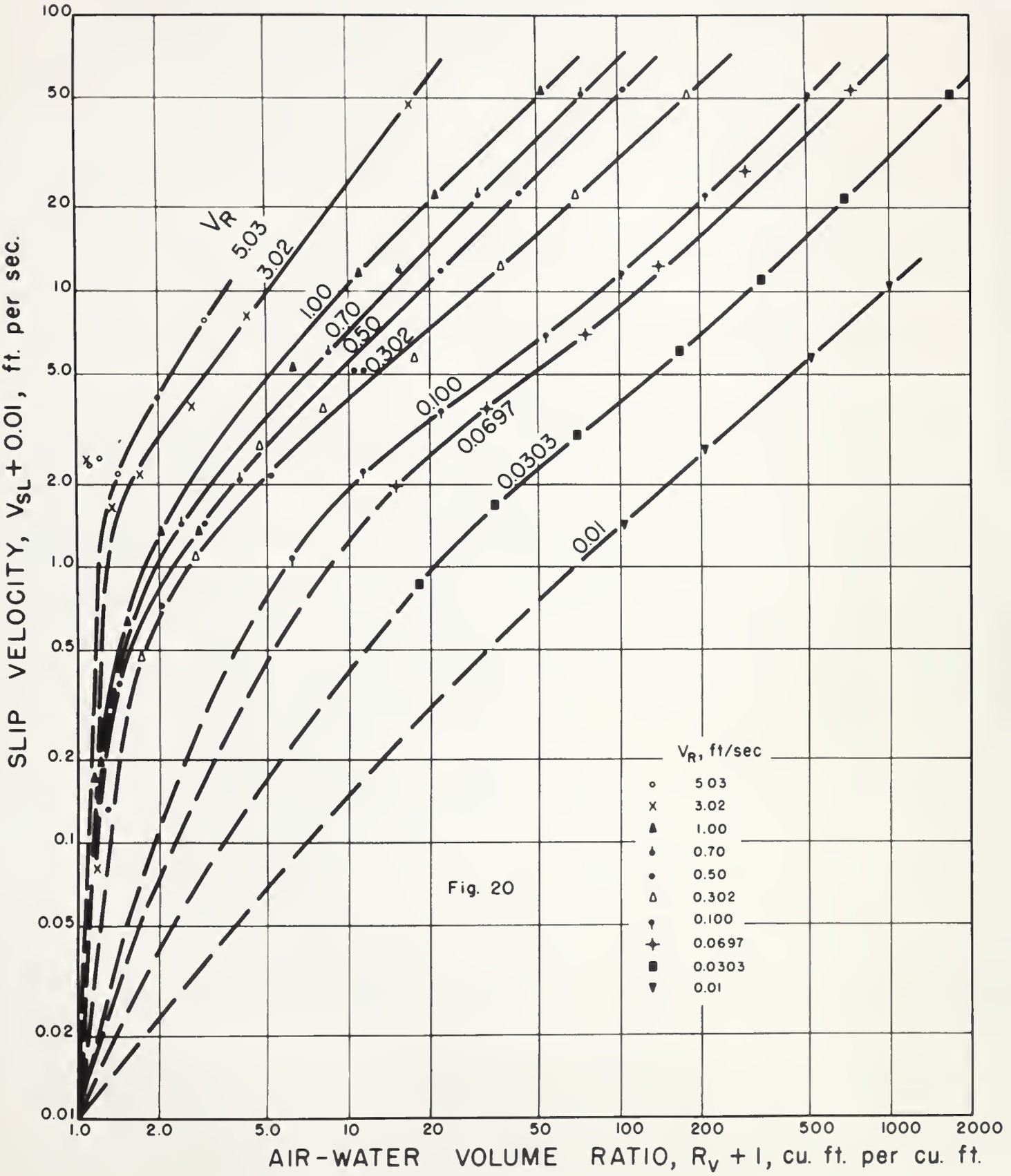
SLIP VELOCITY, V_{SL} + 0.01, ft. per sec.
AIR-WATER VOLUME RATIO, R_V + 1, cu. ft. per cu. ft.
100
50
20
10
5.0
2.0
1.0
0.5
0.2
0.1
0.05
0.02
0.01
1.0
2.0
5.0
10
20
50
100
200
500
1000
2000
V_R
5.03
3.02
1.00
0.70
0.50
0.302
0.100
0.0697
0.0303
0.01
V_R, ft/sec
5.03
3.02
1.00
0.70
0.50
0.302
0.100
0.0697
0.0303
0.01

Fig. 20

about unity. A general trend towards zero slip velocity at an input air-water volume ratio of zero is also noticeable from Figure 20. This is quite logical since at a R_v of zero, that is all liquid flow, the slip velocity is also zero.

CONCLUSIONS

1) Six types of flow pattern namely, bubble, plug, stratified, wave or ripple, slug and film (semiannular or annular) were noted. A tentative flow pattern chart is presented for air-water system. For such a combination of fluids, it allows the prediction of the type of flow which would exist under a given set of mass velocities of the two phases.

2) Pressure drop data for the horizontal flow of air-water mixtures have been obtained and correlated by plotting a superficial friction factor, based on the water properties against a superficial reference phase (water) Reynolds number. This correlation is limited to air-water systems, in a one inch smooth horizontal pipe at an average system pressure of 35-36 psia and temperature of 55°-75°F. The data compares quite favourably with the Lockhart and Martinelli correlation (28), although deviating somewhat in the viscous-turbulent and viscous-viscous mechanisms.

3) Hold-up ratio is plotted against second phase superficial velocity and the input volume ratio. In both cases, in the limiting conditions of the second phase superficial velocity or the input volume ratio being zero, the hold-up ratio approaches unity.

4) Slip velcoity is plotted against input volume ratio. In the limiting case of all liquid flow, the slip velocity approaches zero.

NOMENCLATURE*

A	Cross-sectional area of the pipe,	sq. ft.
C	Volume fraction of a component in the supply mixture at average flow conditions,	dimensionless
D	Inside diameter of pipe,	ft.
f	Friction factor in general,	dimensionless
g_c	Dimensional conversion constant,	$\frac{\text{lb.(mass)}}{\text{lb.(force)}} \frac{\text{ft.}}{\text{sec.}^2}$
G	Mass velocity of a component,	lbs.per sec. sq.ft.
H_R	Hold-up ratio, ratio of input volume ratio to insitu volume ratio, both volumes at average flow conditions,	dimensionless
ΔL	Length of pipe line,	ft.
N_{Re}	Reynolds number,	dimensionless
ΔP	Pressure drop,	lbs.per sq. ft.
$\frac{\Delta P}{\Delta L}$	Pressure drop per unit length,	lbs. per sq.ft. - ft.
Q	Volume rate of flow at average flow conditions,	cu. ft. per sec.
R	Fraction of pipe volume occupied by a component at average flow conditions,	dimensionless
R_M	Input gas-liquid mass ratio,	dimensionless
R_v	Input gas-liquid volume ratio, both volumes at average flow conditions,	dimensionless
v	Specific volume of the fluid at average flow conditions,	cu. ft. per lb.
V	Superficial velocity of fluid at average flow conditions based on total pipe cross-section,	ft. per sec.
V'	Actual average lineal velocity of fluid at average flow conditions,	ft. per sec.
V_{sl}	Actual average slip velocity = $V'_g - V'_l$,	ft. per sec.
W	Mass rate of flow,	lbs. per sec.
X	Lockhart and Martinelli parameter,	dimensionless

* Special terms have been defined in their proper context.

ϕ - Lockhart and Martinelli parameter, dimensionless

ρ - Density of fluid at average flow conditions, lbs. per cu. ft.

μ - Absolute viscosity of fluid at average flow conditions, lbs.per ft. sec.

ν - Kinematic viscosity of fluid at average flow conditions, sq. ft. per sec.

Subscripts:

g - Refers to the gas phase or values calculated by using the gas phase properties.

l - Refers to the liquid phase or values calculated by using the liquid phase properties.

m - Refers to the two-phase mixture or values calculated by using the properties of the mixture.

R - Denotes the reference phase (Water, in the present investigation) or values calculated by using the properties of the reference phase.

s - Denotes the second phase (Air, in the present investigation) or values calculated by using the properties of the second phase.

tp - Refers to two-phase in general.

tpg - Refers to two-phase but using the properties of the gas.

tpl - Refers to two-phase but using the properties of the liquid.

tpm - Refers to two-phase and using the properties of the mixture.

BIBLIOGRAPHY

1. Abramson, A.E., "Investigation of Annular Liquid Flow with Co-current Air Flow in Horizontal Tubes", Jour. App. Mech., Vol. 19, p. 267 - 274, Sept. 1952.

2. Alves, G.E., "Co-current Liquid and Gas Flow in Pipeline Contactor", Chem. Eng. Prog., Vol. 50, p. 449 - 456, 1954.

3. Baker, O., "Design of Pipelines for Multiphase Flow of Oil and Gas", The Oil and Gas Jour., Vol. 53, p. 185 - 195, July 26, 1954.

4. Baker, O., "Multiphase Flow in Pipelines", The Oil and Gas Jour., Vol. 56, p. 156 - 167, Nov. 10, 1958.

5. Baxendell, P.B., "Pipeline Flow of Oil and Gas Mixtures", Proceedings Fourth World Petroleum Congress, Sect. II/E, p. 343 - 351.

6. Bergelin, O.P. and Gazley, C. Jr., "Co-current Gas-liquid Flow-I, Flow in Horizontal Tubes", Heat Transfer and Fluid Mechanics Institute, Berkeley, Calif., 1949, (Published by Am. Soc. Mech. Engrs.) 5 - 18, 1949.

7. Bertuzzi, A.F., Tek, M.R. and Poettman, F.H., "Simultaneous Flow of Liquid and Gas Through Horizontal Pipe", AIME Trans., Jour. Pet. Tech., Vol. 8, p. 17 - 23, Jan. 1956.

8. Boelter, L.M.K. and Kepner, R.H., "Pressure Drop Accompanying Two-component Flow Through Pipe", Ind. Eng. Chem., Vol. 31, p. 426 - 434, 1939.

9. Brown, R.A.S., Sullivan, G.A. and Govier, G.W., "Upward Vertical Flow of Air-water Mixtures", Submitted for publication in Can. Jour. Chem. Eng.

10. Charles, M.E.,* "Horizontal Pipeline Flow of Equal Density Oil and Water Mixtures", M. Sc. Thesis in Chem. Eng., Univ. of Alberta, Sept. 1959.

11. Chenoweth, J.M. and Martin, M.W., "Pressure Drop Correlation for Turbulent Two-phase Flow of Gas-liquid Mixtures in Horizontal Pipe", Pet. Ref., Vol. 34, p. 151 - 155, Oct. 1955, Pet. Engr., Vol. 28, p. c42 - c45, April 1956.

12. Chisholm, D. and Laird, A.D.K., "Two-phase Flow in Rough Tubes", Trans. Am. Soc. Mech. Engrs., Vol. 80, p. 276 - 286, 1958.

13. Coulson, J.M. and Richardson, J.F., "Chemical Engineering", Vol. 1, p. 275, Pergaman Press, London, 1956.

14. Dunn, J.S.C., "Gas-liquid Flow in Vertical Pipes", M. Sc. Thesis in Chem. Eng., Univ. of Alberta, April 1952.

15. Freeman, H.A., "Technique in the Kirkuk Oil-field", Third World Petroleum Congress, The Hague, 1951, Production Sect. II, Drilling and Production.

16. Fried, L. "Pressure Drop and Heat Transfer for Two-phase, Two-component Flow", Chem. Eng. Prog. Symposium Series, No. 9, Vol. 50, "Heat Transfer - Research Studies for 1954", Publ. by Am. Inst. Chem. Engrs., Vol. 49, 1954.

17. Gazley, C. Jr., "Interfacial Shear and Stability", Ph. D. Thesis, Univ. of Delaware, Aug. 1948.

18. Gazley, C. Jr. and Bergelin, O.P., Discussion of paper "Proposed Correlation of Data for Iso-thermal Two-phase, Two-component Flow in Pipes", by Lockhart, R.W. and Martinelli, R.C., Chem. Eng. Prog., Vol. 45, p. 45 - 46, 1949.

19. Govier, G.W., Radford, B.A. and Dunn, J.S.C., "The Upward Vertical Flow of Air-water Mixtures, I. Effect of Air and Water Rates on Flow Pattern, Hold-up and Pressure Drop", Can. Jour. Chem. Eng., Vol. 35, p. 58 - 79, Aug. 1957.

20. Govier, G.W. and Short, W.L., "The Upward Vertical Flow of Air-water Mixtures, II. Effect of Tubing Diameter on Flow Pattern, Hold-up and Pressure Drop", Can. Jour. Chem. Engr., Vol. 36, p. 195 - 202, Oct. 1958.

21. Hoogendoorn, C.J., "Gas-liquid Flow in Horizontal Pipes", Chem. Eng. Sci., Great Britain, Vol. 9, p. 205 - 217, 1959.

22. Jenkins, R., "Two-phase, Two-component Flow of Water and Air", M. Ch. E. Thesis, Univ. of Delaware, 1948.

23. Johnson, H.A. and Abou-Sabe, A.H., "Heat Transfer and Pressure Drop for Turbulent Flow of Air-water Mixtures in a Horizontal Pipe", Trans. Am. Soc. Mech. Engrs., Vol. 74, p. 977, 1952.

24. Kosterin, S.I., "Hydraulic Resistance to Movement of Gas-liquid Mixtures", Bull. Akad. Sci. U.S.S.R., Classe. Sci. Tech. No. 11/12, p. 37 - 49, 1943.

25. Kosterin, S.I., "An Investigation of the Influence of the Diameter and Inclination of a Tube on the Hydraulic Resistance and Flow Structure of Gas-liquid Mixtures", Izvest. Akad. Nauk., U.S.S.R., Otdel. Tekh. Nauk., No. 12, p. 1824 - 1831, 1949.

26. Kosterin, S.I. and Rubanovich, M.N., "Effect of Surface Tension on the Hydraulic Resistance and the Structure of the Flow of Gas-liquid Mixtures in Pipes", Izvest, Akad. Nauk., U.S.S.R., Otdel. Tekh. Nauk., p. 1085 - 1093, 1949.

27. Levy, S., "Theory of Pressure Drop and Heat Transfer for Two-phase, Two-component Annular Flow in Pipes", M. S. Thesis, Univ. of California, Berkeley, 1951.

28. Lockhart, R.W. and Martinelli, R.C., "Proposed Correlation of Data for Iso-thermal, Two-phase, Two-component Flow in Pipes", Chem. Eng. Prog., Vol. 45, p. 39 - 48, 1949.

29. Martinelli, R.C., Boelter, L.M.K., Taylor, T.H.M., Thomsen, E.G. and Morrin, E.H., "Iso-thermal Pressure Drop for Two-phase, Two-component Flow in Horizontal Pipe", Trans. Am. Soc. Mech. Engrs., Vol. 66, p. 139 - 151, 1944.

30. Martinelli, R.C., Putman, J.A. and Lockhart, R.W., "Two-phase, Two-component Flow in the Viscous Region", Trans. Am. Inst. Chem. Eng., Vol. 42, p. 681 - 705, 1946.

31. Radford, B.A., "Gas-liquid Flow in Vertical Pipes", M.Sc. Thesis in Chem. Eng., Univ. of Alberta, Nov. 1949.

32. Reid, R.C., Reynolds, A.B., Diglio, A.J., Spiewak, I. and Klipstein, D.H., "Two-phase Pressure Drops in Large-diameter Pipes", A.I. Chem. Engr. Jour., Vol. 3, p. 321 - 324, Sept. 1957.

33. Russell, T.W.F.,* "Horizontal Pipeline Flows of Oil-water Mixtures", M. Sc. Thesis in Chem. Eng., Univ. of Alberta, Feb. 1958.

34. Schneider, F.N.,† "Some Aspects of Simultaneous Horizontal Two-phase Flow", M. Pet. Eng. Thesis, Univ. of Oklahoma, 1953.

35. Schueler, A.P., "Momentum Transfer in Two-phase Flow", M.Sc. Thesis, Univ. of Illinois, 1951.

36. Short, W.L., "The Upward Vertical Flow of Air-water Mixtures, Effect of Diameter on Flow Pattern, Hold-up and Pressure Drop", M. Sc. Thesis in Chem. Eng., Univ. of Alberta, Sept. 1957.

37. Smith, J.M. and Van Ness, H.C., "Introduction to Chemical Engineering Thermodynamics", Second Edition, p. 241, McGraw Hill, New York, 1959.

38. Sullivan, G.A., "The Upwards Vertical Flow of Air-water and Oil-water Mixtures, Effect of Second Phase Density on Pressure Drop, Flow Pattern and Hold-up," M. Sc. Thesis, Univ. of Alberta, 1958.

39. Teletov, S.G., "On the Coefficients of Resistance for the Movement of Two-phase Mixtures", Compt. Rend. Acad. Sci., U.S.S.R., Vol. 51, p. 579 - 582, 1946.

40. Van Wigen, N., "Pressure Drop for Oil-gas Mixtures in Horizontal Flow Lines", World Oil, Vol. 129, p. 156 - 158, Oct. 1949.

41. White, P.D. and Huntington, R.L., "Horizontal Co-current Two-phase Flow of Fluids in Pipelines", Pet. Engr., Vol. 27, p. 615, Aug. 1955.

42. Widell, T., "Pressure Losses in the Flow of Gas and Liquid Mixtures in Horizontal Pipes", Ingen. Vetensk. Akad. Forsk., Vol. 20, p. 60 - 74, 1949.

* The investigations relating to the theses of Russell (33) and Charles (10) were carried out at the Research Council of Alberta. Russell's (33) work was published as:

Russell, T.W.F., Hodgson, G.W. and Govier, G.W., "Horizontal Pipeline Flow of Mixtures of Oil and Water", Can. Jour. Chem. Eng., Vol. 37, p. 9-17, Feb. 1959.

Charles' (10) work as:

Charles, M.E., Govier, G.W. and Hodgson, G.W. is submitted to the Can. Jour. Chem. Eng. for publication.

In this connection also refer to :

Russell, T.W.F., and Charles, M.E., "The Effect of the Less Viscous Liquid in the Laminar Flow of Two Immiscible Liquids", Can. Jour. Chem. Eng., Vol. 37, p. 18-24, Feb. 1959.

\+ Also refer to:

Schneider, F.N., White, P.D. and Huntington, R.L., "Horizontal Two-Phase Oil and Gas Flow", Pipeline Industry, Vol. 1, p. 47-51, Oct. 1954.

APPENDIX A

(EXPERIMENTAL DATA)

Table I A gives general information about the pipeline test section.

Table II A gives the experimental data collected for the flow of air-water mixtures in a horizontal pipe.

For a particular experiment number the table gives:

The superficial velocities of water and air, ft. per sec.

the temperature of water, air and the mixture, ^{o}F.

the pressure drop over the test section of 30 feet, lbs. per sq.ft.

the mid-point pressure, lbs. per sq. in. abs.

the flow pattern, and

the weight of water trapped, in the test section, lbs.

TABLE I A

GENERAL DATA

Overall length of pipe line, 41.0 ft.

Test section length, i.e. distance over which the pressure drop was measured, 30.0 ft.

Inside diameter of pipe, 1.026 inch = 0.0855 ft.

Volume of pipe line for hold-up measurements, 0.2345 cu. ft.

TABLE II A

EXPERIMENTAL DATA

Length of test section 30.0 ft.
Inside Diameter of pipe 1.026 in.

1	2	3	4			5			6	7	8
Exp. No.	Superficial* Velocity of Ref. Phase (water) V_R ft./sec.	Superficial* Velocity of Second Phase (air) V_s ft./sec.	Temperature °F Water	Air	Mixture	Pressure drop $\frac{lb.}{ft.^2}$ over test section 1	2	Average	Mid-point Pressure psia	Flow Pattern	Water Collected lbs.
101	0.01	1.04	72	68	69	-	-	0.251	35.31	ST	4.01
102	0.01	1.072	79	74	76	-	-	0.274	35.48	ST	3.94
103	0.01	2.09	77	74	75	-	-	0.408	35.48	ST	3.46
104	0.01	5.05	61	51	54	1.022	1.198	1.110	35.45	ST	1.86
105	0.01	9.91	61	51	54	3.14	3.24	3.190	35.20	F	0.83
106	0.0303	0.519	72	69	70	-	-	0.226	35.43	ST	6.50
107	0.0303	1.018	73	68	69	-	-	0.349	35.36	ST	6.05
108	0.0303	2.08	72	69	71	-	-	0.610	35.41	ST	4.74
109	0.0303	5.08	75	70	72	-	-	1.420	35.43	ST	2.74
110	0.0303	9.95	65	57	61	-	-	4.120	35.60	W	1.32
111	0.0303	20.80	65	58	60	-	-	11.96	35.34	F	0.772
112	0.0303	51.60	65	58	60	-	-	76.90	35.44	F	0.43
113	0.0697	1.038	75	72	74	-	-	0.413	35.25	ST	7.00
114	0.0697	2.060	72	69	71	-	-	0.69	35.25	ST	6.27
115	0.0697	5.18	73	69	70	-	-	1.868	35.25	ST	3.40
116	0.0697	10.42	75	70	74	-	-	4.91	35.30	W	1.725
117	0.0697	20.80	75	68	73	-	-	15.85	35.40	F	0.820
118	0.0697	50.40	73	64	71	-	-	100.00	35.30	F	0.60

* At average flow conditions.

TABLE II A (Contd.)

1	2	3	4			5		6	7	8
119	0.1	0.519	72	69	70	-	-	0.45	35.43	ST	8.55⁴
120	0.1	1.028	72	68	70	0.57	0.63	0.60	35.48	ST	8.24
121	0.1	2.095	72	70	70	-	-	1.170	35.43	ST	6.71
122	0.1	5.30	75	71	71	-	-	2.99	35.23	ST	3.96
123	0.1	10.30	65	53	59	-	-	7.30	35.40	W	2.12
124	0.1	21.25	69	62	65	-	-	23.90	35.04	F	1.24
125	0.1	50.6	70	61	64	-	-	115.90	35.19	F	0.71
126	0.3	0.218	71	70	68	8.30	13.0	10.64	34.75	ST	10.96
127	0.3	0.514	73	70	71	-	-	14.55	35.80	ST	9.71
128	0.3	1.115	71	66	66	-	-	12.45	35.75	ST	9.53
129	0.3	2.12	71	70	69	-	-	14.55	35.40	ST	7.41
130	0.3	4.97	72	69	69	-	-	16.60	35.35	W	3.93
131	0.3	10.8	72	70	68	27.00	29.70	28.35	35.35	W	3.11
132	0.3	20.85	71	65	68	46.8	53.4	50.20	35.40	W	2.01
133	0.3	54.4	68	60	64	196.0	218.0	208.0	35.35	F	1.21
134	0.5	0.145	70	74	72	-	-	-	36.14	ST	11.99
135	0.5	0.212	72	73	72	4.16	6.24	5.20	35.64	ST	11.52
136	0.5	0.522	73	72	73	7.53	8.82	8.20	35.49	ST	9.46
137	0.5	0.976	74	72	73	12.0	13.50	12.75	34.94	ST	8.46
138	0.5	2.092	68	72	71	-	-	18.70	35.24	W	5.71
139	0.5	4.73	75	72	73	26.00	28.60	27.30	35.39	W	4.21
140	0.5	10.12	68	72	71	33.8	39.0	36.35	35.43	W	-
141	0.5	10.60	72	71	70	33.8	39.0	36.4	35.33	W	3.52
142	0.5	21.10	67	72	70	-	-	77.5	35.18	W	2.52
143	0.5	52.00	69	71	71	-	-	259.0	35.33	SL	1.52

TABLE II A (Contd.)

1	2	3		4		5			6	7	8
144	0.7	1.0	63	76	66	-	-	20.80	35.53	ST	8.93
145	0.7	2.085	63	73	65	28.00	32.20	30.10	35.53	ST	6.41
146	0.7	5.20	62	59	60	34.30	36.90	35.6	35.60	SL	5.09
147	0.7	10.38	59	63	61	46.9	62.40	54.6	35.60	SL	4.01
148	0.7	20.55	62	60	61	92.50	107.50	100.0	35.53	SL	2.91
149	0.7	50.80	63	58	61	361.00	375.0	368.0	35.38	SL	1.77
150	1.0	0.1468	68	71	69	10.40	12.45	11.40	35.5	ST	12.96
151	1.0	0.210	68	71	69	14.6	16.90	15.75	35.9	ST	12.37
152	1.0	0.520	68	71	69	21.30	23.40	22.35	35.00	ST	10.77
153	1.0	1.055	73	71	72	33.25	36.35	34.80	35.00	ST	9.31
154	1.0	1.825	72	73	72	36.40	39.4	37.90	35.00	ST	6.91
155	1.0	5.25	71	71	71	59.30	61.90	60.60	35.00	SL	5.15
156	1.0	10.00	73	70	72	81.30	83.70	82.50	35.63	SL	4.61
157	1.0	20.22	69	70	70	140.5	145.5	143.0	35.38	SL	3.40
158	1.0	51.50	70	70	70	438.0	494.0	466.0	35.33	SL	2.11
159	3.02	0.147	62	71	62	72.7	83.6	78.2	35.40	B	13.93
160	3.02	0.214	67	72	67	89.5	91.5	90.5	35.25	B	13.99
161	3.02	0.52	68	72	68	-	-	94.6	35.40	B	12.51
162	3.02	1.035	65	73	65	115.0	117.0	116.0	35.35	B	11.81
163	3.02	2.215	66	69	66	152.5	157.5	155.0	34.85	PL	9.74
164	3.02	5.04	67	71	67	212.0	254.0	233.0	35.75	PL	7.21
165	3.02	9.915	67	66	67	325.0	367.0	346.0	35.45	SL	5.65
166	3.02	49.00	66	65	65	990.0	1130.0	1060.0	35.45	SL	3.02

TABLE II A (Contd.)

1	2	3	4			5		6	7	8
167	5.03	0.511	58	63	59	-	-	219.0	35.30	B	13.65
168	5.03	1.052	68	73	69	-	-	233.0	35.35	B	12.77
169	5.03	2.16	64	71	66	-	-	276.0	35.35	PL	11.05
170	5.03	4.94	58	70	60	-	-	416.5	35.35	PL	8.81
171	5.03	9.78	59	68	59	671.0	707.0	689.0	35.30	PL	6.87

APPENDIX B

(CALCULATED DATA)

Appendix B gives all the calculated data under different tables. Each table is followed by a sample calculation as an illustration.

Table I B gives, besides the superficial velocities of water and air, the following calculated data:

Input volume ratio, $(R_v)_{input}$

Insitu volume ratio, $(R_v)_{insitu}$

Hold-up ratio, H_R

Density of the second phase,

i.e. air at average flow condition, ρ_s, lbs. per cu. ft.

The superficial friction factor, f_R

(These data are plotted in Figures 2 to 11 and 19.)

Table II B gives the mass velocities of the two phases and the flow pattern. (This data is employed in Figure 12.)

Table III B primarily gives the calculated values of the parameters ϕ_g, ϕ_l and X. It also tabulates the Reynolds numbers of the two phases, the pressure drop in lbs. per sq. ft. for the two phases flowing alone and the observed two-phase pressure drop in lbs. per sq. ft. (These data are used in presenting the comparisons in Figures 14 to 17.)

Table IV B gives the values of the slip velocity and the input volume ratio which are used in Figure 20.

TABLE I B

CALCULATED DATA

Length of test section 30.0 ft.
Inside diameter of pipe 1.026 ins.

1	2	3	4	5	6	7	8		
	Superficial* Velocity of Ref. Phase (water)	Superficial* Velocity of Second Phase (air)	Input* Volume Ratio $(R_v)_{input}$	Insitu* Volume Ratio $(R_v)_{insitu}$	Hold-up Ratio = $\frac{(R_v)_{input}}{(R_v)_{insitu}}$	Density of* Second Phase	Superficial Friction Factor f_R		
Exp. No.	V_R ft./sec.	V_s ft./sec.	$= V_s/V_R$			lbs./cu.ft.	1	2	Average
101	0.01	1.04	104.0	2.74	39.40	0.18070	-	-	194.4
102	0.01	1.072	107.2	2.68	40.00	0.1790	-	-	171.6
103	0.01	2.09	209.0	3.255	64.20	0.1795	-	-	630.0
104	0.01	5.05	505.0	6.87	73.50	0.1865	3,810	4,455	4,132.0
105	0.01	9.91	991.0	16.63	59.60	0.1860	22,950	23,650	23,300.0
106	0.0303	0.519	17.1	1.255	13.62	0.1805	-	-	3.28
107	0.0303	1.018	33.6	1.416	23.75	0.1810	-	-	9.7
108	0.0303	2.08	68.6	2.09	32.80	0.1810	-	-	34.1
109	0.0303	5.08	167.6	4.33	38.70	0.1805	-	-	192.2
110	0.0303	9.95	328.0	10.05	32.60	0.1870	-	-	1,085.0
111	0.0303	20.80	686.0	17.90	38.30	0.1840	-	-	6,585.0
112	0.0303	51.60	1,700.0	33.00	51.50	0.1840	-	-	104,500.0
113	0.0697	1.038	14.90	1.025	14.55	0.1790	-	-	0.99
114	0.0697	2.060	29.55	1.258	23.50	0.1800	-	-	3.192
115	0.0697	5.180	74.03	3.06	24.20	0.1795	-	-	21.410
116	0.0697	10.42	149.80	6.57	22.80	0.1795	-	-	112.30
117	0.0697	20.80	298.50	13.22	22.60	0.1805	-	-	720.00
118	0.0697	50.4	724.0	22.35	31.00	0.1810	-	-	10,960.00

* At average flow conditions.

TABLE I B (Contd.)

1	2	3	4	5	6	7	8		
119	0.1	0.519	5.19	0.714	7.28	0.1805	-	-	0.2045
120	0.1	1.028	10.28	0.773	13.30	0.1818	0.478	0.515	0.4965
121	0.1	2.095	20.95	1.183	17.70	0.1806	-	-	1.895
122	0.1	5.30	53.00	2.70	19.65	0.1800	-	-	11.90
123	0.1	10.30	103.00	5.90	17.50	0.1850	-	-	59.67
124	0.1	21.25	212.50	10.80	19.68	0.1815	-	-	380.40
125	0.1	50.60	506.00	19.65	25.90	0.1822	-	-	4,324.00
126	0.3	0.218	0.727	0.335	2.175	0.1780	0.1172	0.1832	0.1502
127	0.3	0.514	1.715	0.506	3.39	0.1825	-	-	0.323
128	0.3	1.115	3.72	0.535	6.95	0.1818	-	-	0.4815
129	0.3	2.12	7.06	0.975	7.25	0.1807	-	-	0.96
130	0.3	4.97	16.55	2.72	6.08	0.1810	-	-	2.35
131	0.3	10.80	36.00	3.70	9.74	0.1808	8.15	8.95	8.55
132	0.3	20.85	69.50	6.27	11.08	0.1830	27.30	31.30	29.30
133	0.3	54.40	181.00	11.1	16.30	0.1830	295.00	325.0	310.00
134	0.5	0.145	0.290	0.242	1.200	0.1835	-	-	-
135	0.5	0.212	0.424	0.2675	1.585	0.1811	0.0176	0.0264	0.022
136	0.5	0.522	1.044	0.545	1.918	0.1805	0.0453	0.053	0.049
137	0.5	0.976	1.952	0.729	2.68	0.1780	0.1032	0.1170	0.1101
138	0.5	2.092	4.184	1.56	2.68	0.1795	-	-	0.2855
139	0.5	4.730	9.460	2.38	3.98	0.1800	0.80	0.88	0.84
140	0.5	10.12	20.240	-	-	0.1805	2.11	2.43	2.27
141	0.5	10.60	21.200	3.15	6.72	0.1805	2.21	2.55	2.38
142	0.5	21.10	42.150	4.8	8.775	0.1795	-	-	9.80
143	0.5	52.00	104.00	8.62	12.08	0.1805	-	-	80.00

TABLE I B (Contd.)

1	2	3	4	5	6	7	8		
144	0.7	1.0	1.43	0.639	2.24	0.1790	-	-	0.076
145	0.7	2.085	2.98	1.285	2.32	0.1800	0.1675	0.1925	0.18
146	0.7	5.20	7.43	1.875	3.965	0.1850	0.434	0.465	0.45
147	0.7	10.38	14.82	2.650	5.600	0.1840	1.112	1.482	1.300
148	0.7	20.55	29.40	4.025	7.310	0.1845	4.160	4.850	4.50
149	0.7	50.80	72.60	7.260	10.00	0.1840	39.80	41.45	40.60
150	1.0	0.1468	0.1468	0.128	1.142	0.1815	0.00875	0.0105	0.0096
151	1.0	0.210	0.210	0.1815	1.158	0.183	0.01205	0.01505	0.014
152	1.0	0.520	0.520	0.358	1.452	0.181	0.0238	0.0262	0.025
153	1.0	1.055	1.055	0.57	1.85	0.1785	0.0428	0.0468	0.0448
154	1.0	1.825	1.825	1.116	1.635	0.1782	0.0757	0.0825	0.0790
155	1.0	5.25	5.25	1.835	2.860	0.1775	0.2720	0.2840	0.278
156	1.0	10.00	10.00	2.17	4.615	0.1815	0.655	0.697	0.670
157	1.0	20.22	20.22	3.30	6.13	0.1805	2.19	2.27	2.23
158	1.0	51.50	51.50	5.92	8.70	0.1800	16.10	19.10	17.60
159	3.02	0.147	0.0486	0.0469	1.037	0.1815	0.0064	0.00682	0.00661
160	3.02	0.214	0.079	0.0445	1.774	0.1802	0.0078	0.00798	0.00787
161	3.02	0.52	0.173	0.1695	1.02	0.1810	-	-	0.00896
162	3.02	1.035	0.343	0.239	1.435	0.1808	0.01248	0.0127	0.01258
163	3.02	2.215	0.734	0.50	1.467	0.1790	0.01795	0.02545	0.02170
164	3.02	5.04	1.668	1.03	1.62	0.1820	0.0456	0.0547	0.05
165	3.02	9.915	3.24	1.59	2.04	0.1820	0.1112	0.1258	0.1185
166	3.02	49.00	16.25	3.84	4.235	0.1830	1.372	1.570	1.470

TABLE I B (Contd.)

1	2	3	4	5	6	7	8		
167	5.03	0.511	0.1018	0.0708	1.438	0.1835	-	-	0.007025
168	5.03	1.052	0.210	0.1465	1.432	0.1805	-	-	0.008208
169	5.03	2.160	0.430	0.323	1.332	0.1810	-	-	0.01148
170	5.03	4.94	0.982	0.659	1.49	0.1830	-	-	0.02404
171	5.03	9.78	1.945	1.125	1.73	0.1830	0.0575	0.0605	0.059

SAMPLE CALCULATION

Experiment No. 112

$$\text{Input volume ratio } R_v = \frac{Q_s}{Q_R} = \frac{V_s}{V_R} = \frac{51.6}{0.0303} = 1700$$

Weight of water collected (from Table I A) = 0.43 lbs.

$$\text{Volume of water collected} = \frac{0.43}{62.4} = 0.0069 \text{ cu. ft.}$$

Volume of pipe occupied by gas = 0.2345 - 0.0069 = 0.2276 cu. ft.

$$\text{Insitu volume ratio} = \frac{0.2276}{0.0069} = 33.00$$

$$\text{Hold-up ratio} = \frac{(R_v)_{input}}{(R_v)_{insitu}} = \frac{1700}{33} = 51.5$$

Density of the second phase at average flow conditions $= (0.0808)\ \frac{(492)}{(519)}\ \frac{(3544)}{(147)} = 0.184$ lbs. per cu. ft.

Superficial friction factor f_R

By using Eqn.(49)

$$f_R = \frac{\Delta P_{tp}}{\Delta L}\ \frac{g_c}{2}\ \frac{D}{V_R^2}\ \frac{(R_v + 1)}{\rho_R}$$

ΔP_{tp} = 76.90 lbs. per sq. ft. from Table II A

ΔL = 30.0 ft.

D = 0.0855 ft.

ρ_R = 62.4 lbs. per cu. ft.

Substituting the values in Eqn. (49) we have

$$f_R = \frac{76.90}{30}\ \frac{32.17}{2}\ \frac{0.0855}{(0.0303)^2}\ \frac{1701}{62.4} = 104{,}500$$

TABLE II B

FLOW PATTERN

1 Expt. No.	2 Superficial* velocity of reference phase V_R ft./sec.	3 Mass Velocity of reference phase $G_R \times 10^{-3}$ lb./ft.^{2} hr.	4 Superficial* velocity of second phase V_s ft./sec.	5 Density of* second phase ρ_s lb./ft.^{3}	6 Mass Velocity of second phase $G_s \times 10^{-3}$ lb./ft.^{2} hr.	7 Flow Pattern
101	0.01	2.245	1.04	0.1807	0.676	ST
102	0.01	2.245	1.072	0.1790	0.691	ST
103	0.01	2.245	2.09	0.1795	1.350	ST
104	0.01	2.245	5.05	0.1865	3.39	ST
105	0.01	2.245	9.91	0.1860	6.630	F
106	0.0303	6.8	0.519	0.1805	0.338	ST
107	0.0303	6.8	1.018	0.1810	0.668	ST
108	0.0303	6.8	2.08	0.1810	1.355	ST
109	0.0303	6.8	5.08	0.1805	3.30	ST
110	0.0303	6.8	9.95	0.1870	6.70	W
111	0.0303	6.8	20.8	0.1840	13.78	F
112	0.0303	6.8	51.6	0.1840	34.2	F
113	0.0697	15.66	1.038	0.1790	0.668	ST
114	0.0697	15.66	2.06	0.1800	1.335	ST
115	0.0697	15.66	5.18	0.1795	3.345	ST
116	0.0697	15.66	10.42	0.1795	6.45	W
117	0.0697	15.66	20.8	0.1805	13.52	F
118	0.0697	15.66	50.4	0.1810	32.80	F
119	0.1	22.4	0.519	0.1805	0.338	ST
120	0.1	22.4	1.028	0.1818	0.673	ST
121	0.1	22.4	2.095	0.1806	1.36	ST
122	0.1	22.4	5.30	0.1800	3.54	ST

* At average flow condi tions.

TABLE II B (Cont'd.)

1	2	3	4	5	6	7
123	0.1	22.4	10.3	0.1850	6.85	W
124	0.1	22.4	21.25	0.1815	13.9	F
125	0.1	22.4	50.6	0.1822	33.2	F
126	0.3	67.35	0.218	0.1780	0.1395	ST
127	0.3	67.35	0.514	0.1825	0.338	ST
128	0.3	67.35	1.115	0.1818	0.73	ST
129	0.3	67.35	2.12	0.1807	1.38	ST
130	0.3	67.35	4.97	0.1810	3.24	W
131	0.3	67.35	10.8	0.1808	7.03	W
132	0.3	67.35	20.85	0.1830	13.75	W
133	0.3	67.35	54.4	0.1830	35.8	F
134	0.5	112.25	0.145	0.1835	0.0956	ST
135	0.5	112.25	0.212	0.1811	0.138	ST
136	0.5	112.25	0.522	0.1805	0.339	ST
137	0.5	112.25	0.976	0.1780	0.626	ST
138	0.5	112.25	2.092	0.1795	1.35	W
139	0.5	112.25	4.73	0.1800	3.06	W
140	0.5	112.25	10.12	0.1805	6.58	W
141	0.5	112.25	10.60	0.1805	6.88	W
142	0.5	112.25	21.10	0.1795	13.64	W
143	0.5	112.25	52.00	0.1805	33.8	SL
144	0.7	157.2	1.0	0.179	0.645	ST
145	0.7	157.2	2.085	0.1800	1.35	ST
146	0.7	157.2	5.20	0.1850	3.46	SL
147	0.7	157.2	10.38	0.1840	6.86	SL
148	0.7	157.2	20.55	0.1845	13.65	SL
149	0.7	157.2	50.80	0.1840	33.60	SL
150	1.0	225.0	0.1468	0.1815	0.096	ST
151	1.0	225.0	0.210	0.1830	0.138	ST

TABLE II B (Cont'd.)

1	2	3	4	5	6	7
152	1.0	225.0	0.520	0.1810	0.339	ST
153	1.0	225.0	1.055	0.1785	0.678	ST
154	1.0	225.0	1.825	0.1782	1.17	ST
155	1.0	225.0	5.25	0.1775	3.35	SL
156	1.0	225.0	10.00	0.1815	6.54	SL
157	1.0	225.0	20.22	0.1805	13.15	SL
158	1.0	225.0	51.50	0.1800	33.35	SL
159	3.02	678.0	0.147	0.1815	0.096	B
160	3.02	678.0	0.214	0.1802	0.139	B
161	3.02	678.0	0.52	0.1810	0.339	B
162	3.02	678.0	1.035	0.1808	0.674	B
163	3.02	678.0	2.215	0.1790	1.428	PL
164	3.02	678.0	5.04	0.1820	3.30	PL
165	3.02	678.0	9.915	0.1820	6.48	SL
166	3.02	678.0	49.00	0.1830	32.30	SL
167	5.03	1,130.0	0.511	0.1835	0.338	B
168	5.03	1,130.0	1.052	0.1805	0.684	B
169	5.03	1,130.0	2.16	0.1810	1.41	PL
170	5.03	1,130.0	4.94	0.1830	3.25	PL
171	5.03	1,130.0	9.78	0.1830	6.45	PL

SAMPLE CALCULATION

Experiment No. 112

$$G_R = \rho_R V_R = (62.4)(0.0303)(3600)$$

$$= 6800 \text{ lbs. per hr. sq. ft.}$$

$$G_R \times 10^{-3} = 6.80 \text{ lbs. per hr. sq. ft.}$$

$$G_s = \rho_s V_s = (0.184)(51.6)(3600)$$

$$= 34{,}200 \text{ lbs. per hr. sq. ft.}$$

$$G_s \times 10^{-3} = 34.2 \text{ lbs. per hr. sq. ft.}$$

TABLE III B

CALCULATED VALUES OF MARTINELLI PARAMETERS

Length of test section 30.0 ft.
Inside diameter of pipe 1.026 ins.

1 Superficial* Velocity of Ref. Phase V_R ft./sec.	2 Reynolds No. of Ref.Phase $(N_{Re})_R$	3 Pressure drop for Ref.Phase $(\Delta P)_R$ lbs./ft.^{2}	4 Superficial* Velocity of Second Phase V_s ft./sec.	5 Reynolds No. of Second Phase $(N_{Re})_s$	6 Pressure drop for Second Phase $(\Delta P)_s$ lbs./ft.^{2}	7 Flow Mechanism	8 Two Phase Pressure drop $(\Delta P)_{tp}$ lbs./ft.^{2}	9 $\phi_g = \left[\frac{\Delta P_{tp}/\Delta L}{\Delta P_s/\Delta L}\right]^{1/2}$	10 $\phi_l = \left[\frac{\Delta P_{tp}/\Delta L}{\Delta P_R/\Delta L}\right]^{1/2}$	11 $X = \left[\frac{\Delta P_R/\Delta L}{\Delta P_s/\Delta L}\right]^{1/2}$
5.03	36,400	196.8	9.78	12,920	2.82	tt	689.0	15.62	1.87	8.34
5.03	36,400	196.8	4.94	6,515	0.8655	tt	416.5	21.90	1.45	15.08
3.02	23,000	79.0	49.00	64,100	47.50	tt	1,060.0	4.70	3.70	1.29
3.02	23,000	79.0	9.915	13,320	2.865	tt	346.0	11.00	2.09	5.29
3.02	23,000	79.0	5.04	6,520	0.895	tt	233.0	16.10	1.71	9.39
1.0	8,075	10.9	51.5	65,500	51.30	tt	466.0	3.01	6.54	0.46
1.0	8,075	10.9	20.22	25,800	10.05	tt	143.0	3.77	3.62	1.04
1.0	8,075	10.9	10.00	12,830	2.935	tt	82.5	5.01	2.75	1.92
1.0	8,075	10.9	5.25	6,590	0.944	tt	60.6	8.01	2.35	3.40
0.7	5,125	6.311	50.8	67,970	50.63	tt	368.0	2.69	7.64	0.353
0.7	5,125	6.311	20.55	27,500	10.40	tt	100.0	3.10	3.98	0.7785
0.7	5,125	6.311	10.38	13,880	3.10	tt	54.6	4.2	2.94	1.42
0.7	5,125	6.311	5.20	7,000	0.968	tt	35.6	6.06	2.37	2.55
0.5	4,100	3.4	52.0	66,200	52.50	tt	259.0	2.22	8.50	0.254
0.5	4,100	3.4	21.1	26,900	10.85	tt	77.5	2.67	4.77	0.56

* At average flow conditions.

TABLE III B (Contd.)

1	2	3	4	5	6	7	8	9	10	11
0.5	4,100	3.4	10.6	13,520	3.24	tt	36.4	3.5	3.20	1.024
0.5	4,100	3.4	10.12	12,930	2.955	tt	36.35	3.5	3.27	1.07
0.5	4,100	3.4	4.73	6,000	0.803	tt	27.3	5.83	2.83	2.06
5.03	36,400	196.8	1.052	1,342	0.052	tv	233.0	67.0	1.08	61.5
5.03	36,400	196.8	0.511	681	0.02455	tv	219.0	94.5	1.05	89.6
3.02	23,000	79.0	1.035	1,330	0.0507	tv	116.0	47.8	1.21	39.4
3.02	23,000	79.0	0.52	670	0.0255	tv	94.6	60.9	1.09	55.6
3.02	23,000	79.0	0.214	274	0.0105	tv	90.5	92.8	1.07	86.7
3.02	23,000	79.0	0.147	192	0.00853	tv	78.2	97.5	1.00	96.2
1.0	8,075	10.9	1.055	1,330	0.052	tv	34.8	25.8	1.78	14.5
1.0	8,075	10.9	0.52	665	0.0257	tv	22.35	29.5	1.43	20.6
1.0	8,075	10.9	0.21	272	0.0104	tv	15.75	38.9	1.20	32.4
0.7	5,125	6.311	1.0	1,280	0.0488	tv	20.8	20.6	1.8	11.3
0.5	4,100	3.4	0.976	1,220	0.0485	tv	12.75	16.2	1.93	8.37
0.5	4,100	3.4	0.522	662	0.02592	tv	8.20	17.8	1.55	11.40
0.5	4,100	3.4	0.212	270	0.0105	tv	5.20	22.2	1.23	18.00
0.1	828	0.263	50.6	66,600	50.1	vt	115.9	1.52	21.00	0.072
0.1	828	0.263	21.25	27,700	10.95	vt	23.9	1.47	9.53	0.155
0.1	828	0.263	10.3	13,200	3.06	vt	7.3	1.6	5.4	0.29
0.1	828	0.263	5.30	6,740	0.966	vt	2.99	1.76	3.37	0.52

TABLE III B (Contd.)

1	2	3	4	5	6	7	8	9	10	11
0.0697	590	0.1784	50.4	66,000	50.1	vt	100	1.41	23.6	0.0597
0.0697	590	0.1784	20.8	27,850	10.72	vt	15.85	1.21	9.4	0.129
0.0697	590	0.1784	10.42	13,600	3.10	vt	4.91	1.25	5.20	0.24
0.0697	590	0.1784	5.18	6,475	0.912	vt	1.868	1.43	3.23	0.44
0.0303	240	0.08175	51.6	69,000	52.05	vt	76.9	1.21	30.70	0.039
0.0303	240	0.08175	20.8	27,820	10.60	vt	11.96	1.06	12.10	0.087
0.0303	240	0.08175	9.95	12,900	2.94	vt	4.12	1.18	7.10	0.166
0.0303	240	0.08175	5.08	6,460	0.894	vt	1.42	1.26	4.16	0.302
0.01	78	0.02788	9.91	12,500	2.90	vt	3.19	1.049	10.70	0.098
0.01	78	0.02788	5.05	6,450	0.894	vt	1.11	1.11	6.20	0.177
0.1	828	0.263	1.028	1,336	0.04925	vv	0.60	3.50	1.50	2.31
0.1	828	0.263	0.519	682	0.0249	vv	0.45	4.20	1.3	3.25
0.0697	590	0.1784	1.038	1,305	0.0515	vv	0.413	2.83	1.52	1.86
0.0303	240	0.08175	1.018	1,310	0.050	vv	0.349	2.645	2.07	1.28
0.0303	240	0.08175	0.519	662	0.0257	vv	0.226	2.98	1.67	1.78
0.01	78	0.02788	1.04	1,329	0.0513	vv	0.251	2.215	3.027	0.737
0.01	78	0.02788	1.072	1,345	0.0535	vv	0.2155	2.0	2.78	0.72

SAMPLE CALCULATION

Reynolds number of the reference phase

$$(N_{Re})_R = \frac{D\ V_R\ \rho_R}{\mu_R}$$

$$= \frac{(0.0855)\ (0.0303)\ (62.4)}{(1)\ \ (0.000672)} = 240$$

Pressure drop for water flowing alone

$$(\Delta P_R) = \frac{2\ f\ \Delta L\ V_R^2\ \rho_R}{g_c\ \ D}$$

$$f \text{ at } (N_{Re})_R \text{ of } 240 = \frac{16}{(N_{Re})_R} = \frac{16}{240} = 0.066$$

$$\Delta P_R = \frac{(2)\ (0.066)\ (30)\ (0.0303)^2\ \ (62.4)}{(32.17)\ \ (0.0855)}$$

$$= 0.08175 \text{ lbs. per sq. ft.}$$

Reynolds number of the second phase

$$(N_{Re})_s = \frac{D\ V_s\ \rho_s}{\mu_s}$$

$$= \frac{(0.0855)\ \ (51.6)\ \ (0.184)}{(0.0175)\ \ (0.000672)} = 69{,}000$$

At $(N_{Re})_s$ of 69,000 friction factor from Blasius eqn.

$$f = \frac{0.079}{(69{,}000)^{0.25}} = 0.004874$$

$$\Delta P_s = \frac{(2)\ (0.004874)\ (30)\ (51.6)^2\ \ (0.184)}{(32.17)\ \ (0.0855)} = 52.05\ \frac{\text{lbs.}}{\text{ft.}^2}$$

$$\phi_g = \left[\frac{\Delta P_{tp}/\Delta L}{\Delta P_s/\Delta L}\right]^{1/2} = \left[\frac{76.9/30}{52.05/30}\right]^{1/2} = 1.21$$

$$\phi_l = \left[\frac{\Delta P_{tp}/\Delta L}{\Delta P_R/\Delta L}\right]^{1/2} = \left[\frac{76.9/30}{0.08175/30}\right]^{1/2} = 30.70$$

$$X = \left[\frac{\Delta P_R/\Delta L}{\Delta P_s/\Delta L}\right]^{1/2} = \left[\frac{0.08175/30}{52.05/30}\right]^{1/2} = 0.039$$

TABLE IV B

SLIP VELOCITY

1	2	3	4	5	6
Expt. No.	Superficial* velocity of reference phase V_R ft./sec.	Hold-up ratio H_R	Volume* fraction of pipe occupied by second phase R_s	Slip* velocity V_{sl} ft./sec.	Input volume ratio R_v
101	0.01	39.4	0.726	1.40	104
102	0.01	40.0	0.731	1.43	107.2
103	0.01	64.2	0.764	2.68	209.0
104	0.01	73.5	0.873	5.71	505.0
105	0.01	59.6	0.944	10.64	991.0
106	0.0303	13.62	0.556	0.862	17.1
107	0.0303	23.75	0.586	1.662	33.6
108	0.0303	32.80	0.676	2.975	68.6
109	0.0303	38.70	0.8127	6.10	167.6
110	0.0303	32.60	0.908	10.40	328.0
111	0.0303	38.3	0.9473	21.42	686.0
112	0.0303	51.5	0.9706	52.00	1,700.0
113	0.0697	14.55	0.522	1.975	14.9
114	0.0697	23.50	0.572	3.50	29.55
115	0.0697	24.20	0.7675	6.95	74.03
116	0.0697	22.80	0.884	13.10	149.80
117	0.0697	22.60	0.943	26.4	298.50
118	0.0697	31.00	0.961	53.6	724.0
119	0.1	7.28	0.415	1.073	5.19
120	0.1	13.30	0.437	2.19	10.28
121	0.1	17.70	0.5415	3.64	20.95
122	0.1	19.65	0.7292	6.89	53.00
123	0.1	17.50	0.855	11.40	103.00
124	0.1	19.68	0.9153	22.02	212.50
125	0.1	25.90	0.9515	51.4	506.0
126	0.3	2.175	0.2515	0.461	0.727
127	0.3	3.39	0.336	1.081	1.715
128	0.3	6.95	0.349	2.742	3.72
129	0.3	7.25	0.4945	3.715	7.06
130	0.3	6.08	0.7315	5.67	16.55
131	0.3	9.74	0.7875	12.32	36.00
132	0.3	11.08	0.8627	22.02	69.50
133	0.3	16.30	0.9173	55.5	181.00

* At average flow conditions

TABLE IV B (Cont'd.)

1	2	3	4	5	6
134	0.5	1.20	0.181	0.1221	0.29
135	0.5	1.585	0.212	0.371	0.424
136	0.5	1.918	0.3545	0.711	1.044
137	0.5	2.68	0.421	1.45	1.952
138	0.5	2.68	0.6092	2.15	4.184
139	0.5	3.98	0.7125	5.18	9.460
140	0.5	-	-	-	20.24
141	0.5	6.72	0.7592	11.88	21.20
142	0.5	8.775	0.8277	22.60	42.15
143	0.5	12.08	0.8962	53.40	104.00
144	0.7	2.24	0.39	1.422	1.43
145	0.7	2.32	0.562	2.082	2.98
146	0.7	3.965	0.652	5.96	7.43
147	0.7	5.60	0.726	11.75	14.82
148	0.7	7.310	0.801	22.2	29.40
149	0.7	10.00	0.879	52.05	72.60
150	1.0	1.42	0.115	0.1605	0.1468
151	1.0	1.158	0.155	0.187	0.210
152	1.0	1.452	0.265	0.615	0.520
153	1.0	1.85	0.3645	1.338	1.055
154	1.0	1.635	0.5282	1.345	1.825
155	1.0	2.860	0.6480	5.285	5.25
156	1.0	4.615	0.6850	11.46	10.00
157	1.0	6.13	0.7680	22.10	20.22
158	1.0	8.70	0.8560	53.50	51.50
159	3.02	1.037	0.0448	0.117	0.0486
160	3.02	1.774	0.044	2.442	0.079
161	3.02	1.02	0.145	0.0707	0.173
162	3.02	1.435	0.1925	1.628	0.343
163	3.02	1.467	0.335	2.122	0.734
164	3.02	1.62	0.508	3.805	1.668
165	3.02	2.04	0.614	8.15	3.24
166	3.02	4.235	0.7935	47.25	16.25
167	5.03	1.438	0.067	2.36	0.1018
168	5.03	1.432	0.128	2.49	0.210
169	5.03	1.332	0.24	2.195	0.430
170	5.03	1.49	0.3985	4.10	0.982
171	5.03	1.73	0.530	7.81	1.945

SAMPLE CALCULATIONS

Experiment No. 112

From calculations following Table I B, we have

Hold-up ratio = 51.5 and

volume of pipe occupied by gas = 0.2276 cu. ft.

volume fraction of pipe occupied by gas $R_s = \frac{0.2276}{0.2345} = 0.9706$

From Eqn. (54)

$$\text{Slip velocity, } V_{sl} = \frac{V_R \ (H_R - 1)}{(1 - R_s)}$$

$$= \frac{(0.0303) \ (51.5 - 1)}{(1 - 0.9706)}$$

Slip velocity V_{sl} = 52.00 ft. per sec.

APPENDIX C

(CALIBRATION DATA)

Calibration of Rotameters and Orifices

The rotameter and orifice plates for air up to 0.125 inch in diameter were calibrated by using a gas-holder. The orifice plates for air from 0.188 inch to 0.66 inch in diameter were calibrated by using a critical flow prover. The original calibration data are tabulated in the research note-book. The calibration curve for the rotameter is given in Figure 1c, in which the air flow Q_g in cu. ft. per min. (at 60°F and 14.4 psia) and the flow rate divided by the rotameter reading is plotted against the rotameter reading as the abscissa. The calibration curves for air orifice plates is given in Figure 2c, in which the flow rate Q_g in cu. ft. per min. (at 60°F and 14.4 psia) is plotted against $\frac{P\Delta h}{T_a}$ on logarithmic co-ordinates where,

P is the static pressure, upstream of the orifice, psia

Δh is the pressure drop across the orifice, inches of water

T_a temperature of flowing air, °R

The rotameter and the orifice plates for water were calibrated by weight-time measurements. The original data is tabulated in the research note-book. The calibration curve for the rotameter appears in Figure 3c in which the flow rate in cu. ft. per sec. divided by the rotameter reading is plotted against the rotameter reading. The calibration curves for the orifices appear in Figure 4c as a plot of rate of flow of water in cu.ft. per sec. versus the pressure drop across the orifice in inches of mercury on logarithmic co-ordinates.

Pipe Diameter

The internal diameter of the pipe was determined by inside calipers. A large number of readings were averaged to give an inside pipe diameter of 1.026 inches.

Pipe Volume for Hold-up Measurements

The total volume between the two plug valves A and B was found to be 0.2345 cu. ft. A number of single phase runs with water were conducted and the water trapped was collected and weighed. The difference between the theoretical and the average of a number of amounts of water collected was 0.21 lbs. or 1.435% of the theoretical value. The loss was attributed to the water sticking to the pipe walls and the valves. This value (0.21 lbs.) was added to the weight of water collected in each of the two phase flow experiments to measure the hold-up.

Pipe-line Calibration

The calibration of the flow meters, the pipe-line diameter and the operation of the pressure drop measuring equipment was checked by conducting single phase runs with air and water flowing alone. The pressure drop and the calculated friction factors are tabulated in the research note-book. They are presented graphically in Figures 5c and 6c together with the curve $f = \frac{16}{N_{Re}}$ for the laminar region of flow and the Blasius equation for the turbulent region. Good agreement is evident between the experimental data and accepted curves.

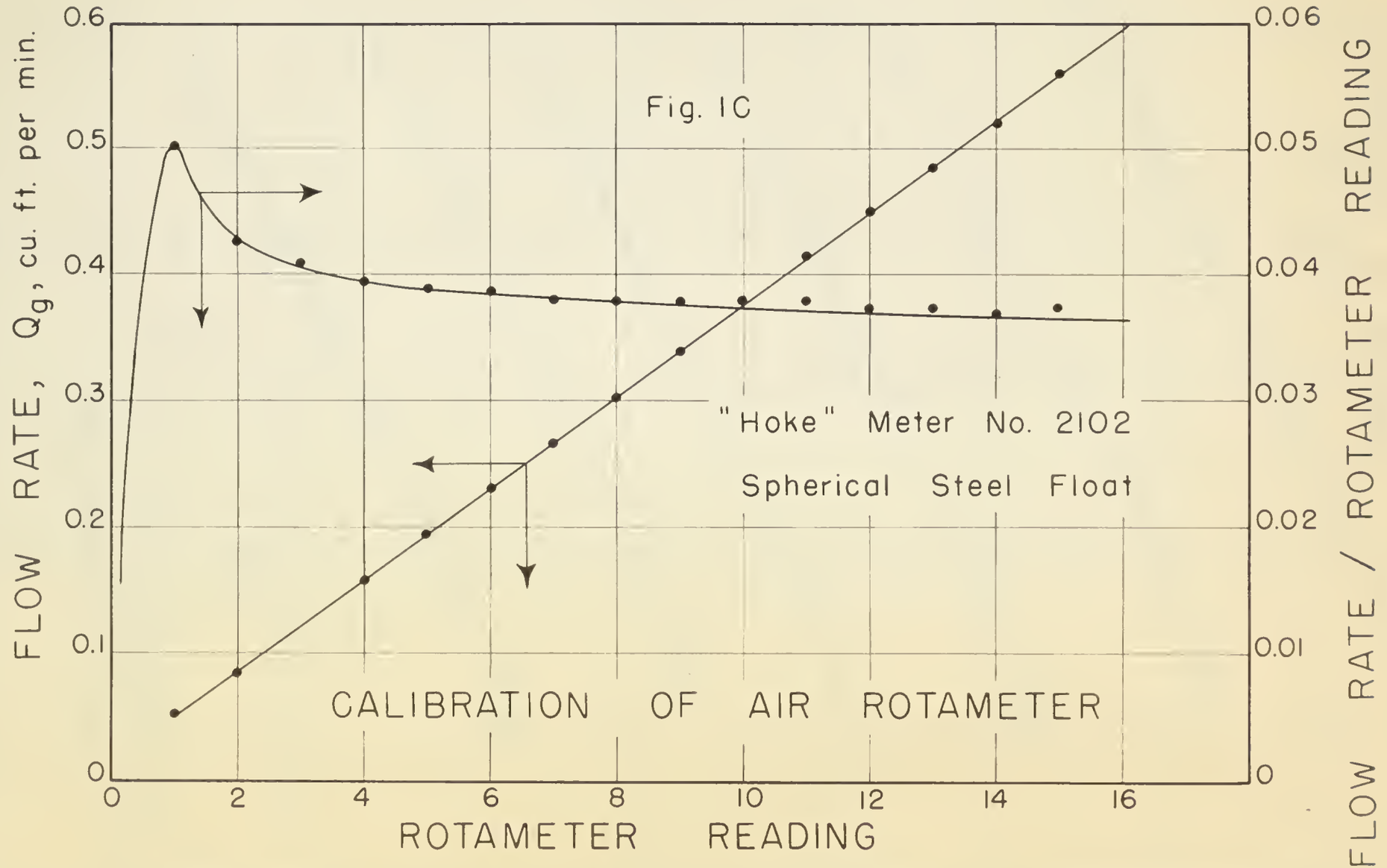
Fig. 1C
"Hoke" Meter No. 2102
Spherical Steel Float
CALIBRATION OF AIR ROTAMETER
FLOW RATE, Q_g, cu. ft. per min.
FLOW RATE / ROTAMETER READING
ROTAMETER READING
0
0.1
0.2
0.3
0.4
0.5
0.6
0.01
0.02
0.03
0.04
0.05
0.06
2
4
6
8
10
12
14
16

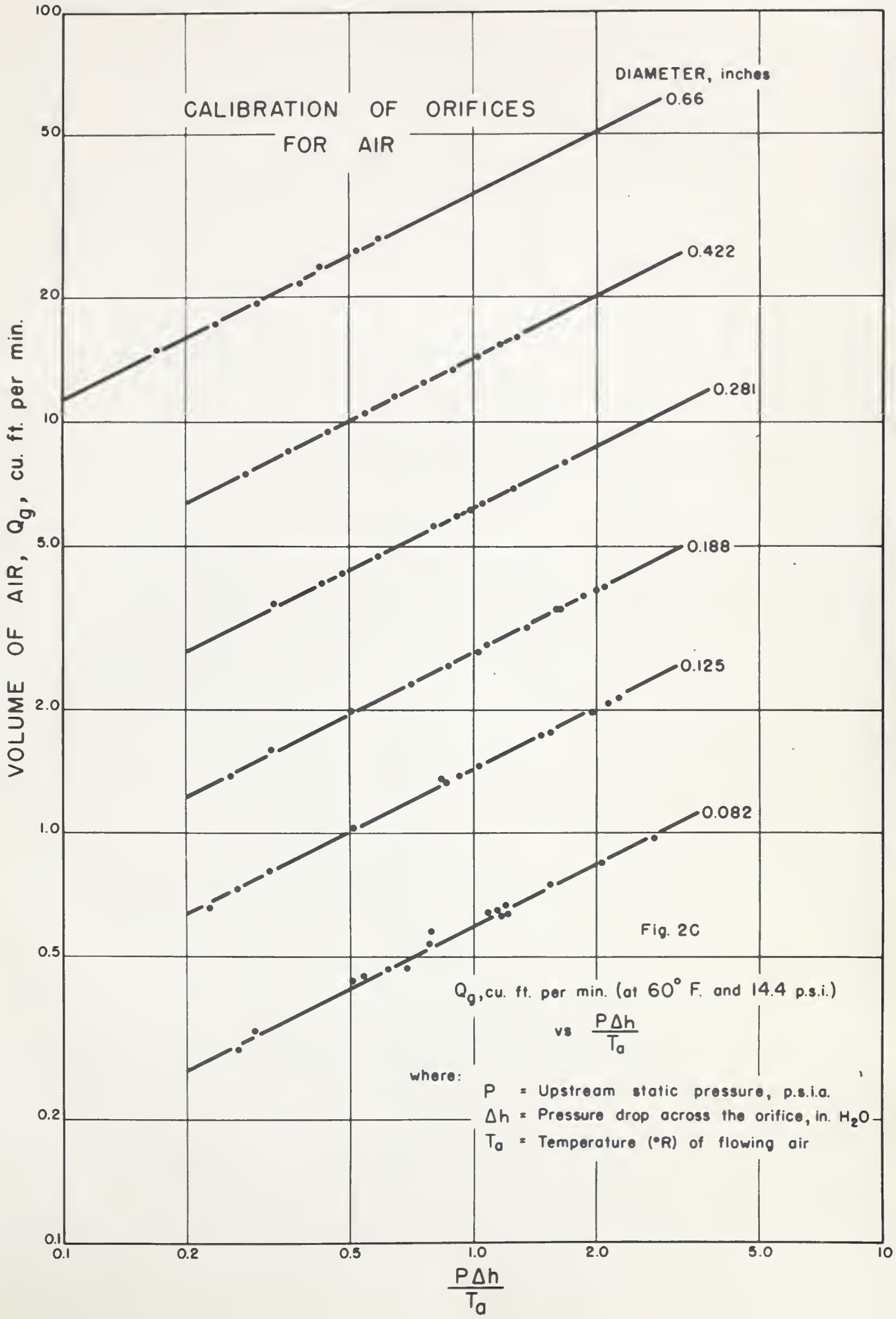
CALIBRATION OF ORIFICES FOR AIR
DIAMETER, inches
0.66
0.422
0.281
0.188
0.125
0.082
VOLUME OF AIR, Q_g, cu. ft. per min.
100
50
20
10
5.0
2.0
1.0
0.5
0.2
0.1
0.1
0.2
0.5
1.0
2.0
5.0
10
$\frac{P\Delta h}{T_a}$
Fig. 2C
Q_g, cu. ft. per min. (at 60° F. and 14.4 p.s.i.)
vs $\frac{P\Delta h}{T_a}$
where:
P = Upstream static pressure, p.s.i.a.
Δh = Pressure drop across the orifice, in. H_2O
T_a = Temperature (°R) of flowing air

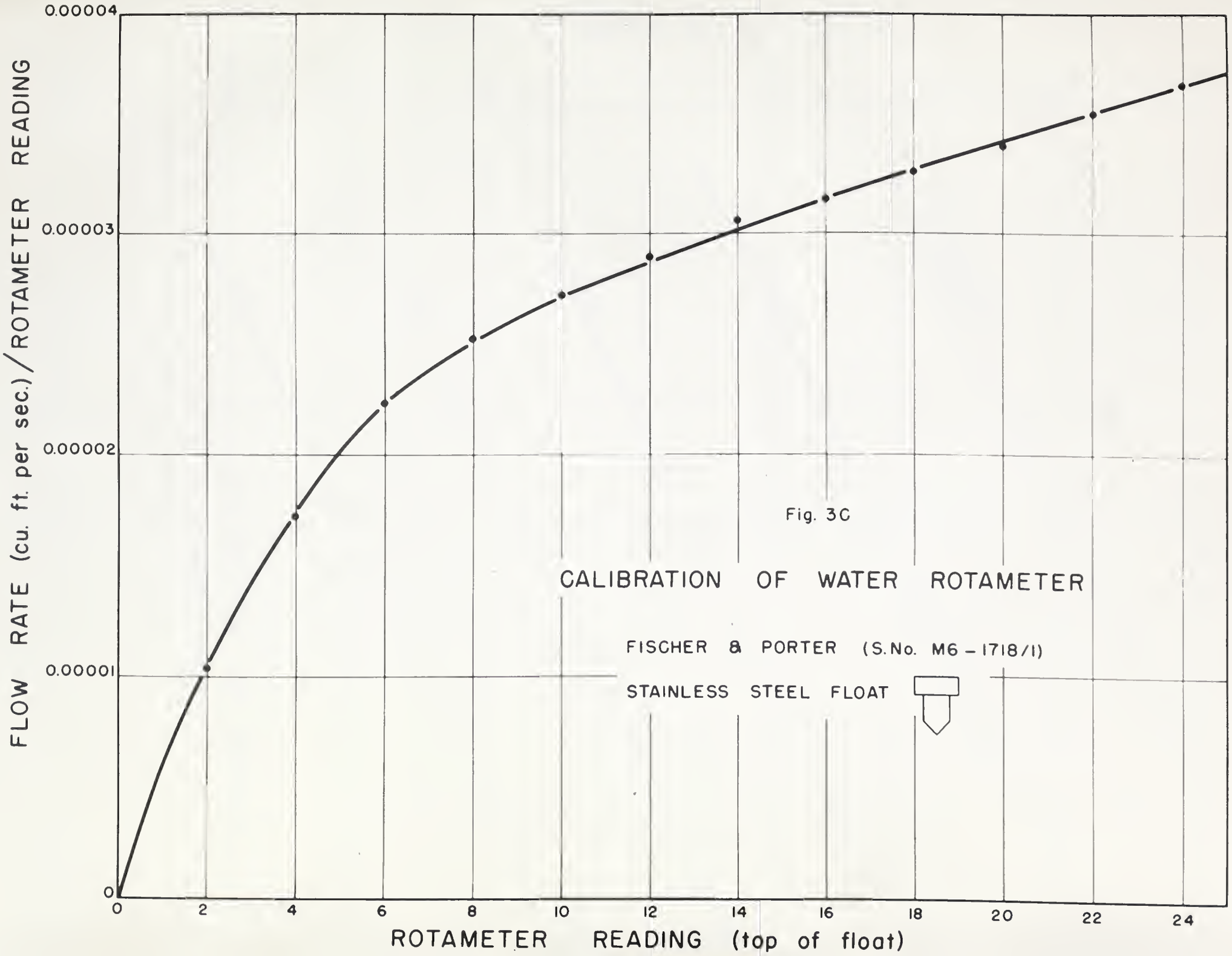
0.00004
0.00003
0.00002
0.00001
0
FLOW RATE (cu. ft. per sec.) / ROTAMETER READING
0
2
4
6
8
10
12
14
16
18
20
22
24
ROTAMETER READING (top of float)
Fig. 3C
CALIBRATION OF WATER ROTAMETER
FISCHER & PORTER (S.No. M6 – 1718/1)
STAINLESS STEEL FLOAT

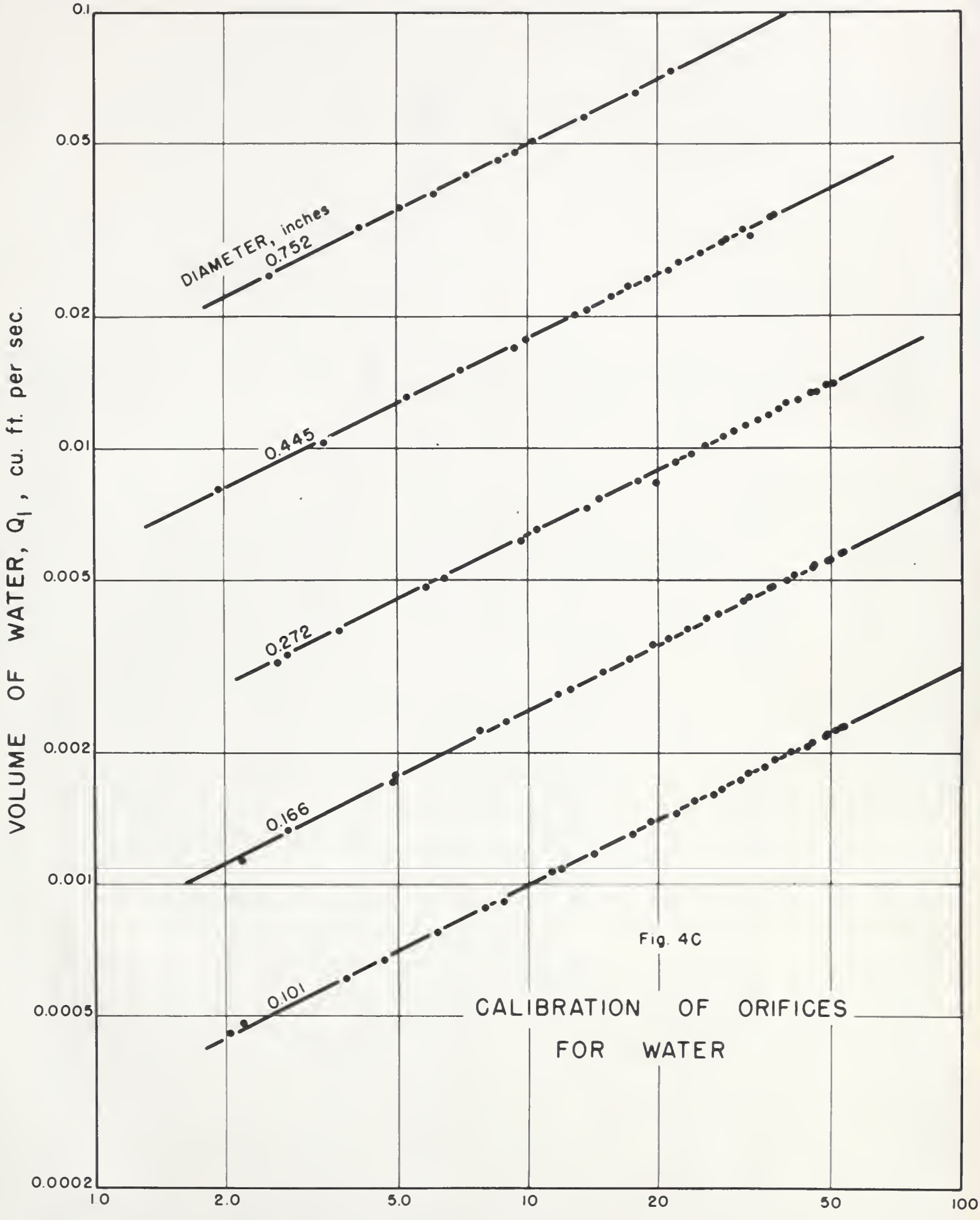

Fig. 4C

CALIBRATION OF ORIFICES FOR WATER

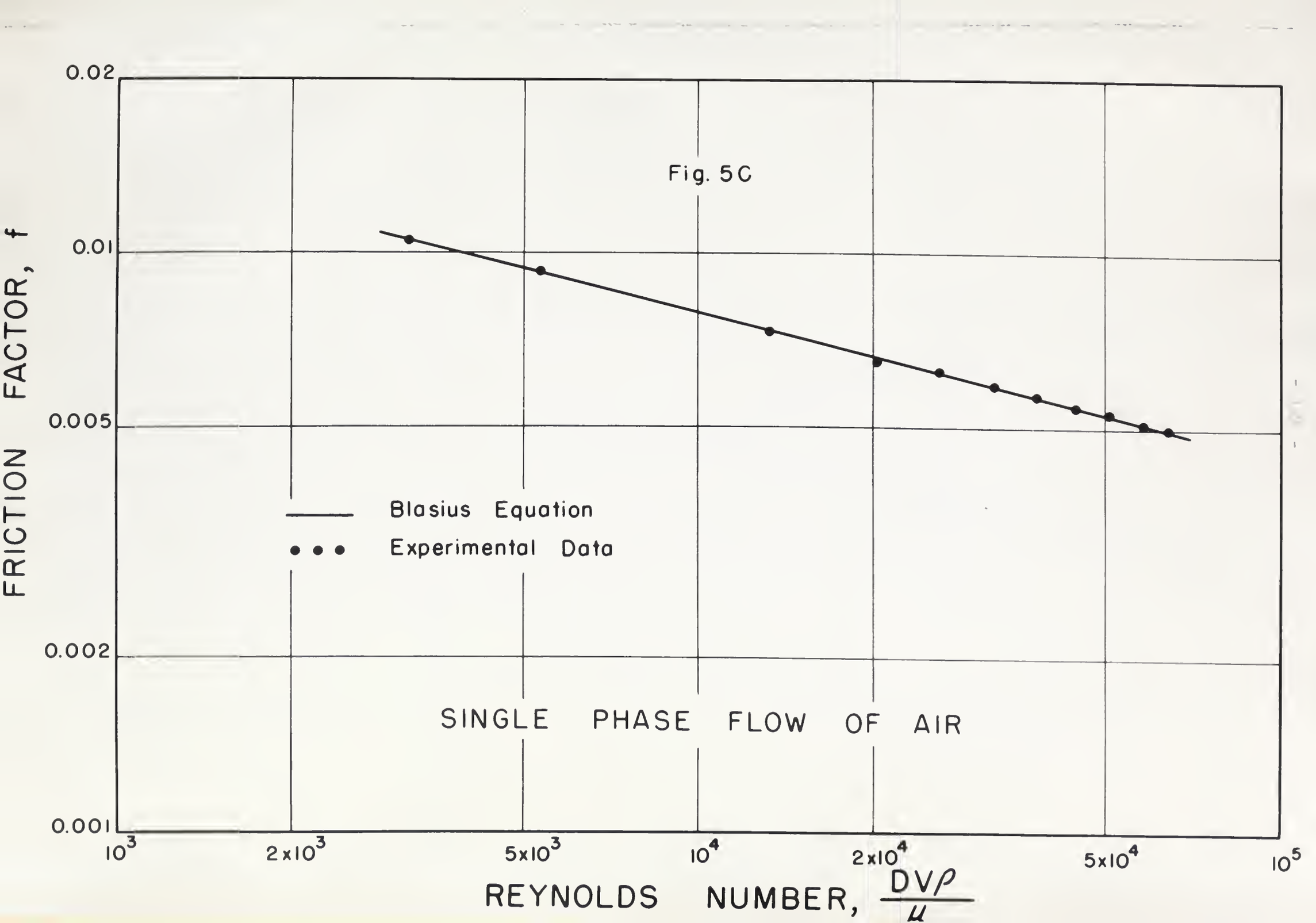
Fig. 5C
0.02
0.01
0.005
0.002
0.001
FRICTION FACTOR, f
Blasius Equation
Experimental Data
SINGLE PHASE FLOW OF AIR
10^3
2×10^3
5×10^3
10^4
2×10^4
5×10^4
10^5
REYNOLDS NUMBER, $\frac{DV\rho}{\mu}$

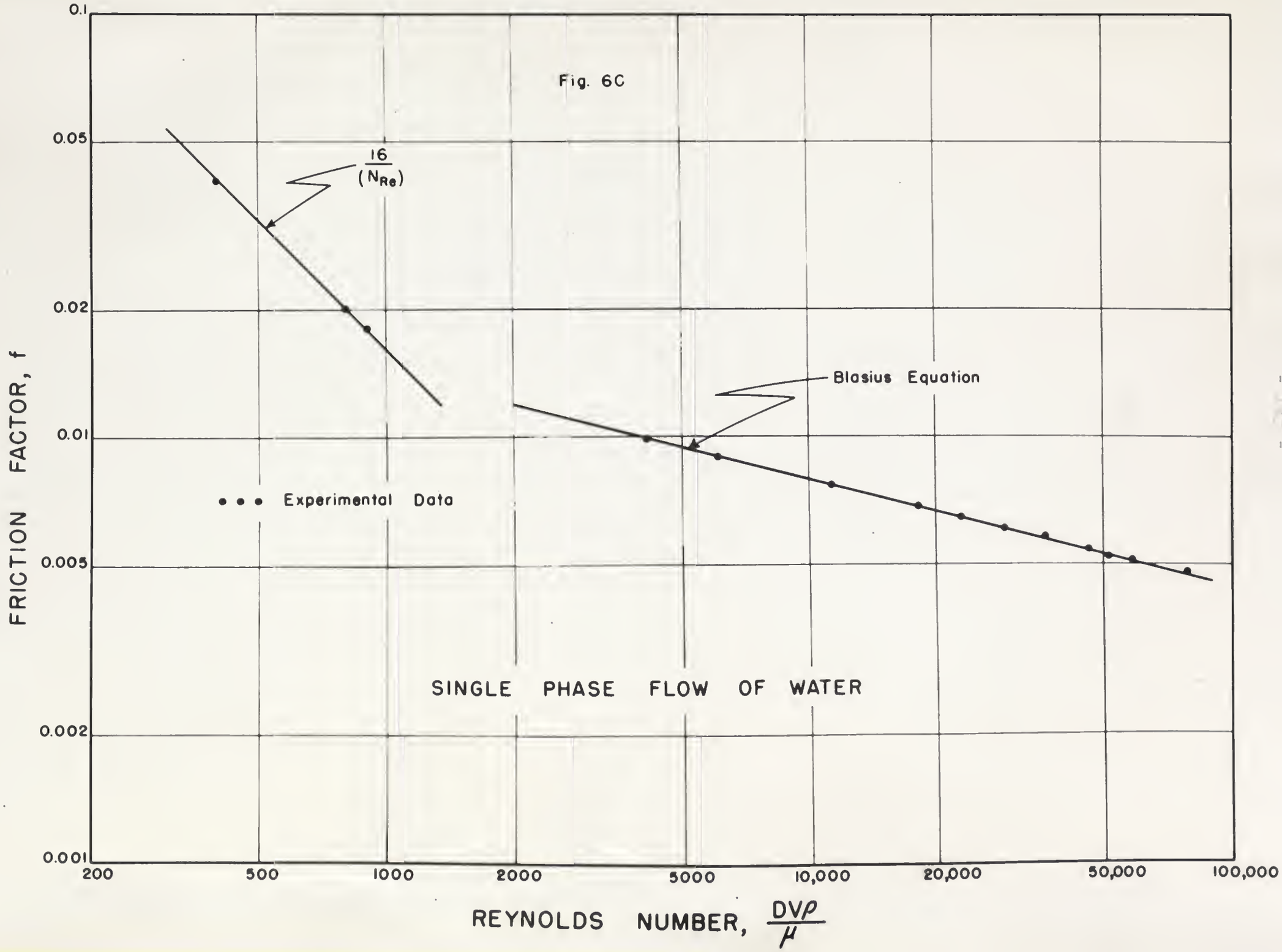
Fig. 6C
0.1
0.05
0.02
0.01
0.005
0.002
0.001
FRICTION FACTOR, f
16/(N_Re)
Blasius Equation
• • • Experimental Data
SINGLE PHASE FLOW OF WATER
200
500
1000
2000
5000
10,000
20,000
50,000
100,000
REYNOLDS NUMBER, DVρ/μ